Engineering the Extra Domain A of fibronectin as a vaccine adjuvant and study of its role in tissue regeneration.

PAR

Ziad JULIER

acceptée sur proposition du jury:

Prof. A. Radenovic, présidente du jury
Prof. J. A. Hubbell, directeur de thèse
Prof. D. Mooney, rapporteur
Prof. J. Spatz, rapporteur
Prof. B. Correia, rapporteur

EPFL

ÉCOLE POLYTECHNIQUE
FÉDÉRALE DE LAUSANNE

Suisse
2016

Acknowledgements

I would like to thank the following people who helped me towards the completion of my PhD,

My thesis advisor, Prof. Jeffrey Hubbell, for his supervision, giving me the opportunity to do my PhD in a stimulating research environment and giving me the independence to develop my own ideas.

The members of my thesis committee, Prof. David Mooney, Prof. Joachim Spatz, Prof. Bruno Correia and Prof. Aleksandra Radenovic, for taking time to review my thesis.

Prof. Mikaël Martino, for his precious advices and directions before and during my PhD, and for giving me the opportunity to continue my scientific career with him after my PhD.

Dr. Alexandre de Titta, Alizée Grimm and Priscilla Briquez for being the most amazing labmates and friends I could have wished for.

Xavier Quaglia-Thermes, Giacomo Diaceri and Yassin Ben Saida for technical support and for being never short on jokes.

Dr. Federico Tortelli, Dr. Eleonora Simeoni and Carol Bonzon for advices and administrative support throughout this thesis.

My parents and my girlfriend Laurice for their unconditional support and my brother Waleed for being a fantastic role model.

Abstract

The extracellular matrix (ECM) protein fibronectin (FN) is a remarkably multifaceted molecule, including numerous fibronectin type III (FNIII) repeats carrying out different functions, which despite being extensively studied for over thirty years still presents certain functions that remain incompletely elucidated. The alternatively spliced FN variant containing the extra domain A (FNIII EDA), located between FNIII 11 and FNIII 12, is expressed in sites of injury, chronic inflammation, and solid tumors. Although its function is not well understood, FNIII EDA is known to agonize Toll-like receptor 4 (TLR4) and appears to be involved in the progression of different skin diseases while studies also suggest that FNIII EDA is involved in tissue repair. The aim of this thesis is thus to better understand some of the immunological and regenerative functions of FNIII EDA and to translate these findings to develop new vaccination strategies based on endogenous proteins.

One important task in vaccinology is to develop delivery strategies by which to present antigen, along TLR agonists, so as to induce a desirable adaptive immune response. The use of TLR agonists is associated with sometimes severe constraints and concerns about safety, causing inflammatory responses. Thus, the development of safe and effective vaccines with fewer side effects is a strong need and requires the development of new adjuvants with a correct balance between a strong activation of the immune system and a low toxicity for the patient.

Here, by producing various FN fragments containing FNIII EDA, we show that the immunological activity of FNIII EDA depends on its local intramolecular context within

the FN chain. N-terminal extension of the isolated FNIII EDA with its neighboring FNIII repeats enhanced its activity in agonizing TLR4, while C-terminal extension abrogated it. In addition, we reveal that an elastase 2 cleavage site is present between FNIII EDA and FNIII 12. Moreover, as FNIII EDA is naturally present within the ECM, we incorporated FNIII EDA bound in a fibrin matrix to mimic the *in vivo* situation and create an adjuvant-rich microenvironment. Such matrices were shown to induce functional cytotoxic CD8$^+$ T cell responses in two murine cancer models.

Furthermore, combinations of specific TLR-agonists have the ability to synergize to induce immune responses that are greater than the sum of their individual effect. Hence, we demonstrate that combination of the TLR9 agonist CpG with FNIII EDA synergizes to induce an efficient immune response while keeping the dose of the toxic CpG at a minimum. Here, the combination of both adjuvants induced a potent immune response sufficient to slow down tumor growth in a murine tumor model as well as to break immune tolerance to eradicate circulating hepatitis B virus (HBV) in a transgenic HBV mouse model.

Finally, in the last part of this thesis we revealed that FNIII EDA is a growth factor binding domain of FN, with a strong affinity for the platelet-derived growth factor-AA (PDGF-AA). We also demonstrated that FNIII EDA and PDGF-AA have together the ability to enhance fibroblasts proliferation and differentiation into myofibroblasts. In addition, we explored the effects of fibrin matrices functionalized with variants of FNIII EDA on wound closure.

Résumé

La Fibronectine (FN) est une protéine multifonctionnelle de la matrice extracellulaire (ECM), incluant de nombreux domaines de type III (FNIII) occupants des fonctions différentes. Bien qu'ayant été étudiée depuis plus de trente ans, la FN présente encore des fonctions qui restent incomplètement élucidées. L'épissage alternatif de la FN contenant l'extra domain A (FNIII EDA), placé entre FNIII 11 et FNIII 12, est exprimé sur les sites de blessures, d'inflammations chroniques et dans les tumeurs solides. Bien que ces fonctions ne soient pas bien comprises, FNIII EDA est connu comme étant un activateur du Toll-like receptor 4 (TLR4) et semble être impliqué dans la progression de diverses maladies de la peau, tandis que d'autres études suggèrent également une implication dans la réparation tissulaire. Ainsi, le but de cette thèse est de mieux comprendre certaines des fonctions immunologiques et régénératives de FNIII EDA et d'appliquer ces résultats dans le développement de nouvelles stratégies de vaccination basées sur des protéines endogènes.

Une tâche importante en vaccinologie est le développement de stratégies d'administration présentant l'antigène, ainsi qu'un activateur de TLR, de façon à obtenir la réponse immunitaire adaptive désirée. L'utilisation d'activateurs de TLR est associée à des contraintes et des soucis parfois sévères liés à la sécurité, causant d'indésirables réponses inflammatoires. Ainsi, le développement de vaccins sûrs et efficaces avec de faibles effets secondaires est nécessaire et requiert le développement de nouveaux adjuvants présentant le bon équilibre entre une forte activation du système immunitaire et une faible toxicité pour le patient.

Ici, en produisant divers fragments de FN contenant FNIII EDA, nous montrons que l'activité immunologique de FNIII EDA dépend de son contexte intramoléculaire au sein de la chaîne de FN. L'extension N-terminale d'un fragment isolé de FNIII EDA par ses domaines adjacents a amplifié son activité activatrice de TLR4, tandis qu'une extension C-terminale l'a abrogé. De plus, nous révélons qu'un site de clivage de l'elastase 2 est présent entre FNIII EDA et FNIII 12. Comme FNIII EDA est naturellement présent dans l'ECM, nous l'avons incorporé dans une matrice de fibrine afin de mimer sa situation *in vivo* et de créer un microenvironnement riche en adjuvant. L'utilisation de ces matrices a permis d'induire une réponse fonctionnelle de cellules T CD8+ cytotoxiques dans deux modèles de cancer murins.

En outre, différents activateurs de TLR ont la capacité de synergiser afin d'induire une réponse immunitaire plus grande que la somme de leurs effets individuels. Ainsi, nous avons démontré que la combinaison de l'activateur de TLR9 CpG avec FNIII EDA synergise et induit une réponse immunitaire efficace tout en gardant la dose de CpG a un minimum, ce dernier étant potentiellement toxique. Ici la combinaison des deux adjuvants a induit une puissante réponse immunitaire suffisante pour ralentir la croissance de tumeurs dans un modèle de tumeurs murin ainsi que de casser la tolérance immunitaire pour éradiquer le virus de l'hépatite B dans un modèle de souris HBV transgéniques.

Finalement dans la dernière partie de cette thèse nous révélons que FNIII EDA est un domaine de liaison de facteurs de croissance, avec une forte affinité pour PDGF-AA. Nous démontrons également que FNIII EDA et PDGF-AA ont ensemble la capacité d'amplifier la prolifération de fibroblastes ainsi que leur différentiation en

myofibroblasts. De plus, nous avons exploré les effets d'une matrice de fibrine fonctionnalisée avec des variantes de FNIII EDA sur la ré-épithélisation de blessures.

Mots clés : matrice extracellulaire, fibronectine, FNIII EDA, récepteur de reconnaissance de motifs moléculaire, récepteur de type Toll, adjuvant, immunité adaptive, vaccins anti-cancereux, HBV, CpG, médecine régénérative, microenvironnement, protéines recombinantes, facteurs de croissance, matrice de fibrine

Table of Contents

Chapter 1

Overview of the thesis

1.1 Motivation and aim

The extracellular matrix (ECM) protein fibronectin (FN) is a remarkably multifaceted molecule which despite being extensively studied for over thirty years still presents certain functions that remain incompletely elucidated. Some of these functions are carried out by the alternatively spliced type III repeat extra domain A (FNIII EDA) which presence is crucial during embryogenesis[1]. Although the type III repeat extra domain B (FNIII EDB) is often expressed simultaneously with FNIII EDA during cancer-related biological processes and embryogenesis[1], its expression within tumor is not as consistent as the one observed for FNIII EDA. Perhaps the most intriguing function of FNIII EDA is its ability to stimulate the immune system through agonization of Toll-like receptor 4 (TLR4) which appears to be involved in the progression of different skin diseases[2,3] whereas FNIII EDB did not show similar ability. Thus, given the unexpected nature of the presence of an endogenous TLR agonist within the ECM and the potential for further vaccine applications, this thesis will focus on FNIII EDA.

One of the aims of this thesis is to understand how the surrounding FN type III domains of FNIII EDA modulates its immunological activities, addressing the roles of its N-terminal and C-terminal extensions. We also sought to understand the physiological mechanism allowing the modulation of the immunological activity of FNIII EDA by its neighboring domains to take place. We then translated these findings to develop new vaccination strategies based on endogenous proteins. Indeed, one important task in vaccinology is to develop delivery strategies by which to present antigen, along with TLR agonists, so as to induce a desirable adaptive immune

response. The use of TLR agonists as adjuvants is associated with sometimes-severe constraints and concerns about safety, causing undesirable inflammatory responses. FNIII EDA as already been the subject of adjuvant research[4–9], inducing modest CD8 T cell responses when injected as a soluble adjuvant. As FNIII EDA is naturally present within the ECM, we incorporated FNIII EDA bound in matrix to mimic the *in vivo* situation and create an adjuvant-rich-cell-trafficking environment. In addition, matrix-based vaccines have already proved to be an interesting option for immunotherapies[10,11].

Some combinations of TLR-agonists are known to synergize and induce responses that are greater than the sum of their individual effect[12–14]. The strength, and most importantly the quality of the response induced by combined TLRs agonists are increased[15]. Thus, the ability of FNIII EDA to synergize with other TLR agonists was also explored with the objective to develop potent vaccine formulations able to break immune tolerance while keeping the amount of adjuvant to a safe level.

Finally, we intended to better understand the role of FNIII EDA in tissue repair. Interactions between the ECM and growth factors (GF) and cytokines being crucial to wound healing[16], the interactions between FNIII EDA and numerous signaling molecules was also explored. Furthermore, we tried to determine whether the TLR4-agonization ability of FNIII EDA is involved in the wound re-epithelization process.

1.2 Background

1.2.1 Fibronectin

Fibronectin (FN) is a multifunctional glycoprotein which is a component of the extracellular matrix (ECM) and the blood plasma that is involved in essential biological functions such as cell migration, adhesion, growth and differentiation[17]. In vertebrates, FN can be either found as soluble plasma FN (pFN) in the blood or as insoluble cellular FN (cFN) in the ECM. The structure of FN is composed of three types of repeating units, or domains, and forms dimers of two 220-250kDa monomers[17]. From the single gene that encodes FN, alternative splicing of its mRNA can produce as many as 20 different splicing variants in humans[18,19]. The three types of fibronectin are generally referred to as type I, II or III. The repartition of the different FN types and their domains is illustrated in Fig. 1 with indication of their most common interaction and integrin binding sites.

FN is crucial for embryogenesis, as shown by FN gene inactivation leading to major embryonic defects and lethality[20]. It is also essential in wound healing[21,22], helping restore the ECM and re-epithelization. During the healing process FN expression is upregulated, and cFN is one of the main constituent of the granulation tissue replacing the provisional matrix[21].

Although the role of FN in embryogenesis and wound healing has already been described[20–22], its interaction with the immune system is still not fully understood. Nevertheless some studies show that such an interaction exists[23] as developed in the next paragraph.
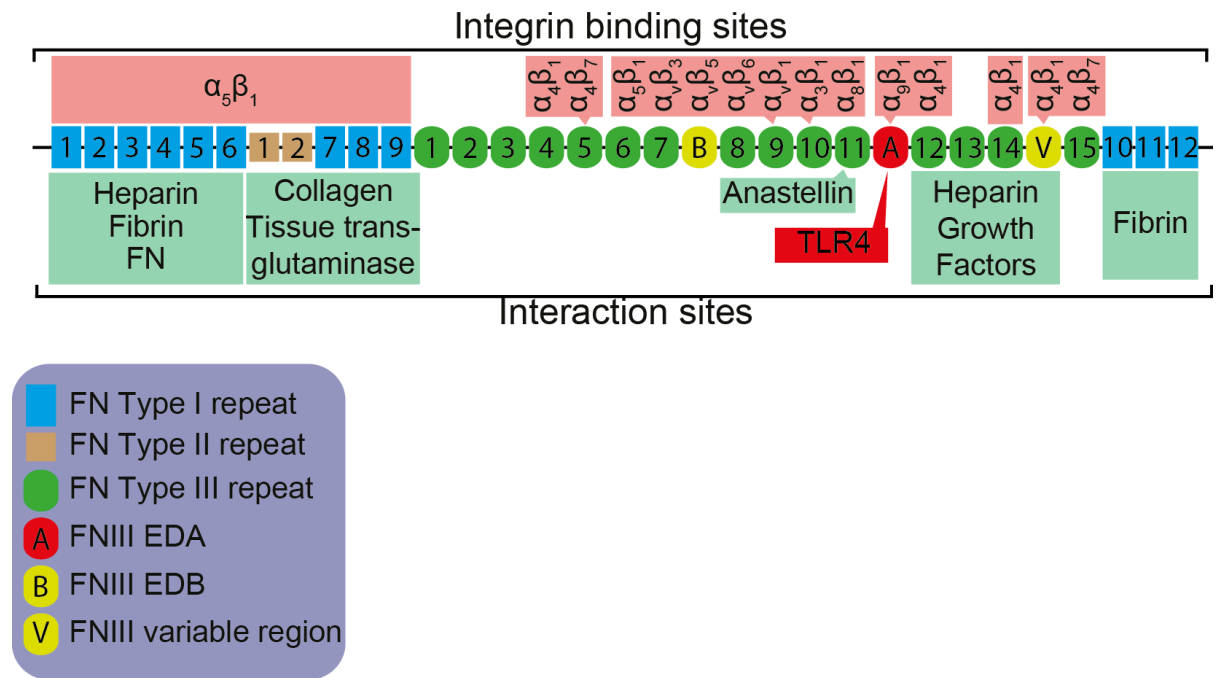
Fig. 1. Fibronectin structure. Full length FN with its major interaction sites displayed

1.2.2 FNIII EDA

One splicing variant of Fibronectin containing the type III repeat extra domain A (FNIII EDA) is normally expressed in the vicinity of developing vessels during embryogenesis[18,24] and later in particular cases such as after tissue injury[25–27], within tumors[28–30], and at sites of chronic inflammation such as psoriatic lesions[3,31,32]. FNIII EDA has the ability to induce inflammatory cytokines and activate matrix metalloproteinases (MMPs) and has been observed to trigger similar reactions to the TLR4 ligand lipopolysacchardide (LPS)[23]. This observation led to the discovery that FNIII EDA binds to the TLR4 receptor and activates its signaling pathway leading to the activation of NF-κB. However, the physiological consequences of the tight regulation of FNIII EDA-containing FN during inflammation and its ability to bind TLR4 are still not

fully understood. Furthermore, this activity has been shown to be highly dependent on the presence or absence of the neighboring domains of FNIII EDA[33].

Based on the observation that FN III EDA ligates and activates TLR4, one research group has explored the use of FNIII EDA as an adjuvant damage-associated molecular patterns (DAMP) in subunit vaccines, generating the fusion protein FNIII EDA-antigen[8]. This strategy successfully induced an antigen-specific cytotoxic T-cell response although vaccinations have failed to show therapeutic effects in animal models without additional adjuvants. However, in spite of a modest effect of FNIII EDA in recombinant subunit vaccines, the adjuvancy of FNIII EDA has not been adequate to confer protection in viral challenge models in the mouse. As such, it would seem that FNIII EDA has the potential to compose a multiple adjuvant vaccine, but insufficiently potent to be used on its own.

1.2.3 Functionalized fibrin matrices

Fibrin, a biopolymer approved by the FDA for use as an adhesive glue, is involved in the coagulation cascade. Fibrin matrices form spontaneously in tissue repair upon polymerization of fibrinogen, a circulating hexamer glycoprotein clinically obtained by cryoprecipitation of human blood plasma. The polymerization process is initiated by thrombin, releasing fibrinopeptide A and B from fibrinogen[34], resulting in fibrinogen monomers. The monomers are then cross-linked by factor XIIIa to form a fibrin network[35]. During its polymerization, fibrin can be functionalized with peptides or recombinant proteins modified to contain a transglutaminase substrate sequence

derived from α2-plasmin inhibitor (NQEQVSPL) at the N-terminus[36]. Functionalized

fibrin matrices have already proved to be an efficient approach towards wound

healing, serving as an ingenious way to deliver GFs[37] in an ECM-like environment.

However their use in vaccinology remains unexplored. Similarly, FNIII EDA-containing

FN fragments can be incorporated in fibrin gels in order to mimic its natural *in vivo*

context, while creating a microenvironment rich in both adjuvant and antigen.

1.2.4 Dendritic cells and T cells activation

As an antigen cannot be directly recognized by T cells, it needs to be processed

and presented by antigen presenting cells (APCs). The immune cells most frequently

targeted in vaccines include B cells, macrophages, and dendritic cells (DCs), which are

all effective antigen-presenting cells (APCs). DCs are typically considered the most

"professional" since they present antigen to their cognate naïve T cell partners and

instruct them as to how to respond to that antigen. DCs remain in an immature state

while sampling antigens in their environment to present them to T cells. Upon

phagocytosis by DCs the antigen will be processed and loaded on major

histocompatibility complex of class I (MHC-I) or class II (MHC-II) in order to be

presented. Along with co-stimulatory molecules (CD80, CD86, CD40) and pro-

inflammatory cytokines, presentation on MHC-I will activate naïve $CD8^+$ T cells to

cytotoxic T lymphocytes (Fig. 2) while presentation on MHC-II will activate naïve $CD4^+$

T helper cells (Fig. 2), which can be characterized mainly either by a T helper 1 (Th1) or

2 (Th2) polarization. Th1 cells promoting a $CD8^+$ T cell response and Th2 cells

promoting a humoral response through help to B cells.
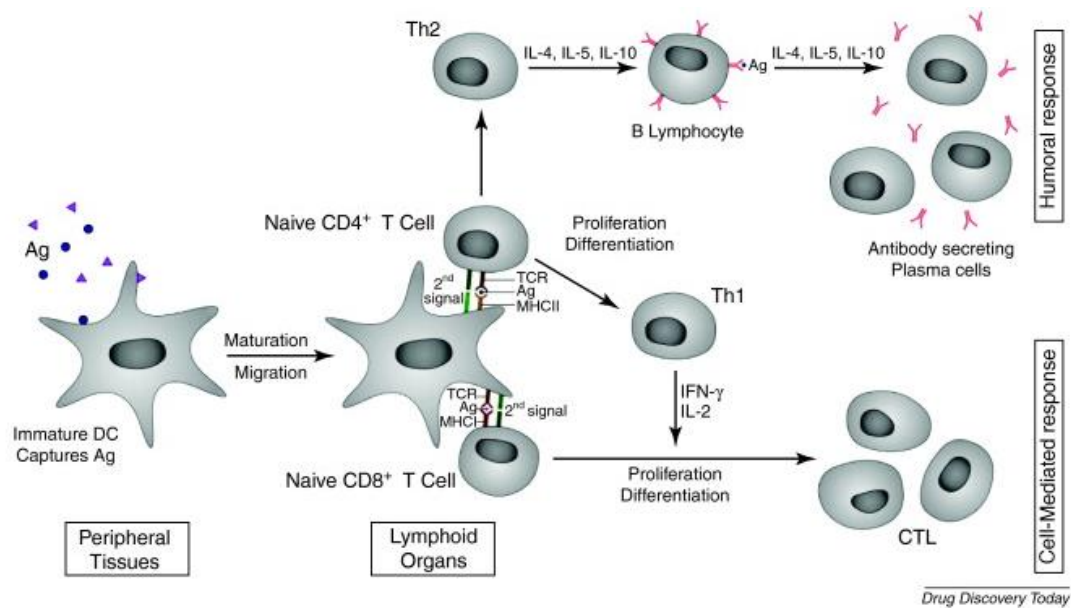
Fig. 2. Schematic overview of antigen presentation. Ag presentation by DCs via MHC class I and class II molecules accompanied by a second signal leads to activation, proliferation and differentiation of respectively Ag-specific CD4$^+$ and CD8$^+$ T cells. Th1 cells provide help to CD8$^+$ T cells, while Th2 cells provide help to B cells. Figure and legend adapted from a review by De Temmermann M.-L. et al.[38]

In addition to their ability to present antigens, DCs can recognize pathogen associated molecular patterns (PAMPs) from foreign agents such as bacteria and virus through pattern recognition receptors (PRR), a type of receptors which include TLRs. In addition, many endogenous molecules can also trigger DCs activation; such molecules known as DAMPs are typically associated with tissue damage or distress.

Activating ligands have been identified for most of the 13 human TLRs, with most of these ligands stemming from bacterial or viral origins. Common pathogenic ligands include LPS for TLR4, flagellin for TLR5 and CpG DNA for TLR9; however, endogenous ligands have also been identified. Signaling downstream of TLRs will mature the DCs, leading to immunity towards the antigen, whereas the absence of TLR signaling might keep the DCs from maturing after taking up the antigen and lead to the opposite effect

24

known as tolerance[39]. The response that a DC elicits depends on many factors, including the state of maturation of the DC, how the antigen was taken up and processed by the cell, and even the tissue in which the DC was activated. Importantly, the cytokine environment in which both DC activation and DC-T cell communication occurs can control the response and should be considered when choosing tissue targets. These cytokines can be secreted by DCs upon activation or inactivation, by the activated T cells themselves, by recruited neutrophils and macrophages to the inflammatory site, and finally, by stromal cells that can become activated during inflammation. Because the cytokine profile present during contact with the DC can determine T cell fate, engineering approaches that manipulate or utilize the cytokine environment are important design considerations.

1.2.5 Cancer immunotherapies

Existing cancer therapies include surgery, radio therapy, chemotherapy and more recently immunotherapy. Immunotherapies present the advantage over older types of treatments to be more efficient as they are designed to specifically target cancerous cells, thus limiting the damage to non-tumoral cells. Although various cancer immunotherapy strategies exist, cellular immunotherapies, also called cancer vaccines, will be the one of interest here.

Multiple characteristics need to be met for a cancer vaccine to be effective. Cancer vaccines need to be targeted to an antigen specific to the tumor in order to avoid harming healthy cells. Hence antigen identification still presents a challenge and

for these reasons the research presented in this thesis will use tumor models with known antigens. As tumor cells derive from endogenous cells their antigens are hardly targeted by the immune system and a proper danger signal need to be provided to mount an immune response against them. However many challenges are present when trying to mount an effective anti-tumoral immune response. Not only tumor antigens are not recognized as foreign by the immune system but they are also both centrally and peripherally tolerized[40], thus requiring an immune response sufficiently strong to break immune tolerance to self-neo-antigen. Furthermore tumor cells are able to create an immunosuppressive microenvironment, attracting high levels of Myeloid-derived suppressor cells (MDSC) and/or regulatory T-cells (Tregs)[41], which the T cells need to resist[42,43]. Thus formulations with the ability to modulate tumor immune suppression by controlling the population of MDSCs or Tregs are more suited to make effective therapeutic cancer vaccines[44].

Selection of the appropriate adjuvant, molecules that activate APCs to stimulate immune responses, is required. At the present time aluminum-based salts and a squalene-oil-water emulsion are approved for clinical use although they present limitations. The effective vaccine also should trigger the innate immune system to stimulate the production of Th1-polarizing cytokine to promote the efficiency of T cell priming[45]. It should also should seek to provide long-term memory to prevent tumor recurrence.

1.3 Accomplishments

In this work we explore and further characterize both the immunological and regenerative functions of FNIII EDA. In chapter 2, we explore the importance of the molecular context of FNIII EDA in its ability to activate TLR4. Here we reveal that the TLR4 agonizing potential of FNIII EDA is cryptic, becoming exposed by cleavage between FNIII EDA and FNIII 12 by elastase 2. Upon proteolysis, TLR4 agonization was increased up to 5 fold. We demonstrate using two tumor models that induction of CTL responses to a xeno- and an auto-antigen by FNIII EDA activity is enhanced when the domain is bound to an ECM analog. Thus we show that delivering ECM-bound FNIII EDA fragments in combination with antigens could be an attractive option for anti-tumoral immunotherapies.

In chapter 3, using a tumor model and a chronic hepatitis B transgenic mouse model expressing an HBV transgene we show that the TLR9 agonist unmethylated CpG oligodeoxynucleotide and FNIII 11-EDA have the ability to synergize to break T cell tolerance and induce an enhanced antigen specific response. It is important that these improved effects were obtained while lowering the total dose of foreign agent (CpG), opening the door to the development of potent immunotherapies with fewer side effects and improved safety.

Finally, in chapter 4 we show that FNIII EDA is yet another GF binding domain of FN, with an especially strong affinity for PDGF-AA. Our results here suggest that FNIII 11-EDA and PDGF-AA have together the ability to enhance fibroblasts proliferation and differentiation into myofibroblasts although additional experiments are still required to further investigate a potential synergy between these proteins. We show that fibrin

matrices functionalized with variants of FNIII 11-EDA surprisingly delay wound closure, however here again more experiment will be required to precisely characterize how FNIII EDA affects tissue repair.

1.4 References

1.   Astrof, S., Crowley, D. & Hynes, R. O. Multiple cardiovascular defects caused by the absence of alternatively spliced segments of fibronectin. *Dev. Biol.* **311,** 11–24 (2007).

2.   Bhattacharyya, S. *et al.* FibronectinEDA promotes chronic cutaneous fibrosis through Toll-like receptor signaling. *Sci. Transl. Med.* **6,** 232ra50 (2014).

3.   McFadden, J. P., Baker, B. S., Powles, A. V. & Fry, L. Psoriasis and streptococci: postscript regarding extra domain A fibronectin. *Br. J. Dermatol.* **161,** 706–7 (2009).

4.   Arribillaga, L. *et al.* A fusion protein between streptavidin and the endogenous TLR4 ligand EDA targets biotinylated antigens to dendritic cells and induces T cell responses in vivo. *Biomed Res. Int.* **2013,** 864720 (2013).

5.   Mansilla, C. *et al.* Immunization against hepatitis C virus with a fusion protein containing the extra domain A from fibronectin and the hepatitis C virus NS3 protein. *J. Hepatol.* **51,** 520–7 (2009).

6.   Mansilla, C. *et al.* Eradication of large tumors expressing human papillomavirus E7 protein by therapeutic vaccination with E7 fused to the extra domain a from fibronectin. *Int. J. Cancer* **131,** 641–51 (2012).

7.   San Román, B. *et al.* The extradomain A of fibronectin (EDA) combined with poly(I:C) enhances the immune response to HIV-1 p24 protein and the protection against recombinant Listeria monocytogenes-Gag infection in the mouse model. *Vaccine* **30,** 2564–9 (2012).

8.   Lasarte, J. J. *et al.* The extra domain A from fibronectin targets antigens to TLR4-expressing cells and induces cytotoxic T cell responses in vivo. *J. Immunol.* **178,** 748–56 (2007).

9.   Rudilla, F. *et al.* Combination of a TLR4 ligand and anaphylatoxin C5a for the induction of antigen-specific cytotoxic T cell responses. *Vaccine* **30,** 2848–58 (2012).

10.   Ali, O. A, Emerich, D., Dranoff, G. & Mooney, D. J. In situ regulation of DC subsets and T cells mediates tumor regression in mice. *Sci. Transl. Med.* **1,** 8ra19 (2009).

11.   Ali, O. A., Huebsch, N., Cao, L., Dranoff, G. & Mooney, D. J. Infection-mimicking materials to program dendritic cells in situ. *Nat. Mater.* **8,** 151–158 (2009).

12.   Zhu, Q. *et al.* Toll-like receptor ligands synergize through distinct dendritic cell pathways to induce T cell responses: implications for vaccines. *Proc. Natl. Acad. Sci. U. S. A.* **105,** 16260–16265 (2008).

13.   Bagchi, A. *et al.* MyD88-dependent and MyD88-independent pathways in synergy, priming, and tolerance between TLR agonists. *J. Immunol.* **178,** 1164–1171 (2007).

14.   Napolitani, G., Rinaldi, A., Bertoni, F., Sallusto, F. & Lanzavecchia, A. Selected Toll-like receptor agonist combinations synergistically trigger a T helper type 1-polarizing program in dendritic cells. *Nat. Immunol.* **6,** 769–76 (2005).

15.   Zhu, Q. *et al.* Using 3 TLR ligands as a combination adjuvant induces qualitative changes in T cell responses needed for antiviral protection in mice. *J. Clin. Invest.* **120,** 607–616 (2010).

16.   Barrientos, S., Stojadinovic, O., Golinko, M. S., Brem, H. & Tomic-Canic, M. Growth factors and cytokines in wound healing. *Wound Repair Regen.* **16,** 585–601 (2008).

17.   Pankov, R. & Yamada, K. M. Fibronectin at a glance. *J. Cell Sci.* **115,** 3861–3863 (2002).

18.   ffrench-Constant, C. Alternative splicing of fibronectin--many different proteins but few different functions. *Exp. Cell Res.* **221,** 261–71 (1995).

19.   White, E. S., Baralle, F. E. & Muro, A. F. New insights into form and function of fibronectin splice variants. *J. Pathol.* **216,** 1–14 (2008).

20.   George, E. L., Georges-Labouesse, E. N., Patel-King, R. S., Rayburn, H. & Hynes, R. O. Defects in mesoderm, neural tube and vascular development in mouse embryos lacking fibronectin. *Development* **119,** 1079–91 (1993).

21.   Valenick, L. V., Hsia, H. C. & Schwarzbauer, J. E. Fibronectin fragmentation promotes alpha4beta1 integrin-mediated contraction of a fibrin-fibronectin provisional matrix. *Exp. Cell Res.* **309,** 48–55 (2005).

22. Lenselink, E. A. Role of fibronectin in normal wound healing. *Int. Wound J.* 313–316 (2013). doi:10.1111/iwj.12109

23. Okamura, Y. *et al.* The extra domain A of fibronectin activates Toll-like receptor 4. *J. Biol. Chem.* **276,** 10229–33 (2001).

24. ffrench-Constant, C. & Hynes, R. O. Alternative splicing of fibronectin is temporally and spatially regulated in the chicken embryo. *Development* **106,** 375–88 (1989).

25. Jarnagin, W. R., Rockey, D. C., Koteliansky, V. E., Wang, S. S. & Bissell, D. M. Expression of variant fibronectins in wound healing: cellular source and biological activity of the EIIIA segment in rat hepatic fibrogenesis. *J. Cell Biol.* **127,** 2037–48 (1994).

26. Liao, Y. F., Gotwals, P. J., Koteliansky, V. E., Sheppard, D. & Van De Water, L. The EIIIA segment of fibronectin is a ligand for integrins alpha 9beta 1 and alpha 4beta 1 providing a novel mechanism for regulating cell adhesion by alternative splicing. *J. Biol. Chem.* **277,** 14467–74 (2002).

27. ffrench-Constant, C., Van de Water, L., Dvorak, H. F. & Hynes, R. O. Reappearance of an embryonic pattern of fibronectin splicing during wound healing in the adult rat. *J. Cell Biol.* **109,** 903–14 (1989).

28. Rybak, J. N., Roesli, C., Kaspar, M., Villa, A. & Neri, D. The extra-domain A of fibronectin is a vascular marker of solid tumors and metastases. *Cancer Res.* **67,** 10948–57 (2007).

29. Villa, A. *et al.* A high-affinity human monoclonal antibody specific to the alternatively spliced EDA domain of fibronectin efficiently targets tumor neo-vasculature in vivo. *Int. J. Cancer* **122,** 2405–13 (2008).

30. Borsi, L., Castellani, P., Allemanni, G., Neri, D. & Zardi, L. Preparation of phage antibodies to the ED-A domain of human fibronectin. *Exp. Cell Res.* **240,** 244–51 (1998).

31. McFadden, J. P., Baker, B. S., Powles, A. V. & Fry, L. Psoriasis and extra domain A fibronectin loops. *Br. J. Dermatol.* **163,** 5–11 (2010).

32. McFadden, J., Fry, L., Powles, A. V. & Kimber, I. Concepts in psoriasis: psoriasis and the extracellular matrix. *Br. J. Dermatol.* **167,** 980–6 (2012).

33. Saito, S. *et al.* The fibronectin extra domain A activates matrix metalloproteinase gene expression by an interleukin-1-dependent mechanism. *J. Biol. Chem.* **274,** 30756–63 (1999).

34. Blombäck, B., Hessel, B., Hogg, D. & Therkildsen, L. A two-step fibrinogen--fibrin transition in blood coagulation. *Nature* **275,** 501–505 (1978).

35.   Barry, E. L. & Mosher, D. F. Factor XIII cross-linking of fibronectin at cellular matrix assembly sites. *J. Biol. Chem.* **263,** 10464–9 (1988).

36.   Schense, J. C., Bloch, J., Aebischer, P. & Hubbell, J. A. Enzymatic incorporation of bioactive peptides into fibrin matrices enhances neurite extension. *Nat. Biotechnol.* **18,** 415–9 (2000).

37.   Patterson, J., Martino, M. M. & Hubbell, J. a. Biomimetic materials in tissue engineering. *Mater. Today* **13,** 14–22 (2010).

38.   De Temmerman, M. L. *et al.* Particulate vaccines: On the quest for optimal delivery and immune response. *Drug Discov. Today* **16,** 569–582 (2011).

39.   Bonifaz, L. *et al.* Efficient Targeting of Protein Antigen to the Dendritic Cell Receptor DEC-205 in the Steady State Leads to Antigen Presentation on Major Histocompatibility Complex Class I Products and Peripheral CD8+ T Cell Tolerance. *J. Exp. Med.* **196,** 1627–1638 (2002).

40.   Makkouk, A. & Weiner, G. J. Cancer Immunotherapy and Breaking Immune Tolerance: New Approaches to an Old Challenge. *Cancer Res.* **75,** 5–10 (2015).

41.   Melero, I. *et al.* Therapeutic vaccines for cancer: an overview of clinical trials. *Nat. Rev. Clin. Oncol.* **11,** 509–524 (2014).

42.   Gabrilovich, D. I. & Nagaraj, S. Myeloid-derived suppressor cells as regulators of the immune system. *Nat. Rev. Immunol.* **9,** 162–74 (2009).

43.   Dolcetti, L. *et al.* Myeloid-derived suppressor cell role in tumor-related inflammation. *Cancer Lett.* **267,** 216–25 (2008).

44.   Jeanbart, L. *et al.* Enhancing efficacy of anticancer vaccines by targeted delivery to tumor-draining lymph nodes. *Cancer Immunol. Res.* **2,** 436–47 (2014).

45.   Dubensky, T. W. & Reed, S. G. Adjuvants for cancer vaccines. *Semin. Immunol.* **22,** 155–161 (2010).

Chapter 2

The TLR4 Agonist Fibronectin Extra Domain A is Cryptic, Exposed by Elastase-2; use in a fibrin matrix cancer vaccine

2.1 Abstract

Fibronectin (FN) is an extracellular matrix (ECM) protein including numerous fibronectin type III (FNIII) repeats with different functions. The alternatively spliced FN variant containing the extra domain A (FNIII EDA), located between FNIII 11 and FNIII 12, is expressed in sites of injury, chronic inflammation, and solid tumors. Although its function is not well understood, FNIII EDA is known to agonize Toll-like receptor 4 (TLR4). Here, by producing various FN fragments containing FNIII EDA, we found that FNIII EDA's immunological activity depends upon its local intramolecular context within the FN chain. N-terminal extension of the isolated FNIII EDA with its neighboring FNIII repeats (FNIII 9-10-11) enhanced its activity in agonizing TLR4, while C-terminal extension with the native FNIII 12-13-14 heparin-binding domain abrogated it. In addition, we reveal that an elastase 2 cleavage site is present between FNIII EDA and FNIII 12. Activity of the C-terminally extended FNIII EDA could be restored after cleavage of the FNIII 12-13-14 domain by elastase 2. FN being naturally bound to the ECM, we immobilized FNIII EDA-containing FN fragments within a fibrin matrix model along with antigenic peptides. Such matrices were shown to stimulate cytotoxic CD8^{+} T cell responses in two murine cancer models.

2.2 Introduction

Fibronectin (FN) is a ubiquitous multidomain extracellular matrix (ECM) component and is critically important in numerous ECM-dependent processes such as cell adhesion, migration, growth, and differentiation[1]. Notably, certain functions of FN depend on the presence of the alternatively spliced type III repeats extra domains A (FNIII EDA) and B (FNIII EDB). These extra domains are expressed in the vicinity of developing vessels during embryogenesis[2,3] and later in particular cases such as after tissue injury[4–6], within tumors[7–9], and at sites of chronic inflammation such as psoriatic lesions[10–12]. Although expression of FNIII EDA and FNIII EDB is crucial for embryonic development[13], their postnatal functions remain incompletely elucidated.

One of the most interesting functions of FNIII EDA is its ability to act as an endogenous ligand for the pattern recognition receptor Toll-like receptor 4 (TLR4)[14] and activate its signaling pathway, which leads to the activation of NF-κB. Importantly, this TLR4-agonizing activity has been shown to contribute to disease progression, specifically in driving fibrosis in scleroderma[15] and stimulating the inflammatory cascade in psoriatic lesions[10].

Here, we sought to explore the importance of the local molecular context of FNIII EDA in its immunological activities, as the domain resides in the vicinity of other active FNIII repeats in the natural sequence FNIII 9-10-11-EDA-12-13-14 (Fig. 1a). FNIII 10 contains the well-studied RGD sequence that binds integrins such as $\alpha_v\beta_3$[16] and FNIII 9 contains the synergy site PHSRN that is critical for $\alpha_5\beta_1$ integrin activation[17]. FNIII 11 has been shown to bind anastellin[18], a small FN type I fragment, increasing its

thermolytic digestion. The FNIII 12-13-14 domain is one of the major heparin-binding sites of FN[19] and has been shown to promiscuously bind growth factors[20,21]. In some of FN's biological activities, this molecular context has been shown to be important; for example, the proximal location of the integrin-binding domain and the growth factor binding domain has been shown to lead to synergistic signaling between the ligated integrin and the ligated growth factor receptor, potentiating growth factor signaling[21–23]. Based on these recent findings, we were motivated to investigate the potential importance of the molecular context of FNIII EDA's placement within the FN chain upon its activity in inducing immune responses.

Moreover, FNIII EDA is known to induce the expression of inflammatory cytokines and matrix metalloproteinases (MMPs)[24], and these activities have been shown to be dependent on the presence of the neighboring domains FNIII11 and FNIII12[24]. For such exposure to occur *in vivo,* it would require FN to be cleaved by a protease, but only the bacterial protease thermolysin from *Bacillus thermoproteolyticus* has been shown to cleave FN close to the C-terminus of FNIII EDA[25]. Because no mammalian protease had been shown to carry out the same function, we were thus also motivated to search for mammalian proteases that might modulate the activity of FNIII EDA by inducing such cleavage.

Finally, because FNIII EDA can induce cellular immune responses including activation of CD8^{+} T cell responses[26–31], the domain has also been explored as a cancer vaccine adjuvant in mouse models[28,30,31]. However, FNIII EDA showed potency mostly in combination with other TLR agonists[28,31]. Here, because FNIII EDA is naturally displayed bound to the ECM, we hypothesized that its relatively weak adjuvancy could

be related to the fact that the domain was delivered as a soluble protein. Therefore, we also explored whether FNIII EDA variants could have better adjuvant potency when bound to the ECM.

2.3 Results

2.3.1 Production of FN fragments

To investigate the importance of the biomolecular context of FNIII EDA's activity as a TLR4 agonist, we expressed various FN fragments containing FNIII EDA (Fig. 1a). As the simplest construct, FNIII EDA was produced as a single FNIII repeat. Extending N-terminally, FNIII 11 was incorporated to produce FNIII 11-EDA. To further explore N-terminal extensions, FNIII 9-10-EDA and FNIII 9-10-11-EDA were expressed, thus comprising the cell-binding domain with the synergy site[1]. To explore C-terminal extensions, FNIII 9-10-EDA-12-13-14 and FNIII 9-10-11-EDA-12-13-14 were expressed, thus comprising the FNIII 12-13-14 domain, which binds heparin[1] and growth factors[20]. All FN fragments were successfully produced, and endotoxin levels were verified as being under 0.2 EU/μg using a limulus amebocyte lysate assay. Purity of the FN fragments is shown by SDS-PAGE in Fig. S1a.

2.3.2 The immunostimulatory activity of FNIII EDA can be modulated by addition or deletion of neighboring domains

To explore the dependence of TLR4 agonization upon the presence of various neighboring domains in the FN protein chain, we characterized TLR agonization using THP1-Blue cells (derived from the human monocytic THP1 cell line and modified to contain a reporter of agonization of several TLRs) and HEK-Blue TLR4 cells (derived from the human embryonic kidney 293 cell line and modified to contain a reporter of agonization of TLR4) as well as cytokine expression in dendritic cells (DCs). As expected, FNIII EDA agonized TLR4 in THP1-Blue cells in a dose-dependent manner (Fig. 1b). Interestingly, addition of FNIII 11 at the N-terminus, i.e. FNIII 11-EDA, agonized TLR4 up to 4-fold more potently (P<0.001) in THP1-Blue cells and up to 5-fold more potently (P<0.001) in HEK-Blue TLR4 cells, compared to FNIII EDA (Fig. 1b, c). To explore if this gain of activity derived from intrinsic activity within FNIII 11 or from an effect of N-terminal extension, which could for example influence the stability of the FNIII EDA domain, we produced the alternative construct FNIII 9-10-EDA, i.e. containing a neighboring N-terminal extension with FN's cell-binding domain and synergy site yet not the N-terminal FNIII 11 domain. Surprisingly, FNIII 9-10-EDA agonized TLR4 to the same extent as FNIII 11-EDA in both cell lines. Moreover, the complete N-terminal construct, FNIII 9-10-11-EDA, showed statistically equivalent behavior (Fig. 1b, c). We further explored the impact of neighboring FNIII repeats by extending FNIII EDA to the C-terminus with the native structure FNIII 9-10-11-EDA-12-13-14, as well as FNIII 9-10-EDA-12-13-14. Unexpectedly, in both THP1-Blue and HEK-Blue TLR4 cells, C-terminal extension with the FNIII 12-13-14 domain abrogated TLR4 agonization (Fig.1b, c). We

then tested the ability of the different FNIII EDA-containing constructs to stimulate the production of inflammatory cytokines in DCs, which are key monitors of innate immune signals such as TLR4 agonists. DC expression of TNF-α and IL-12p70 closely paralleled the TLR4 agonization that was observed in THP1-Blue and HEK-Blue TLR4 cells. The N-terminal extension of FNIII EDA strongly enhanced cytokine response, while C-terminal extension with FNIII 12-13-14 strongly decreased it (Fig.1d, e).
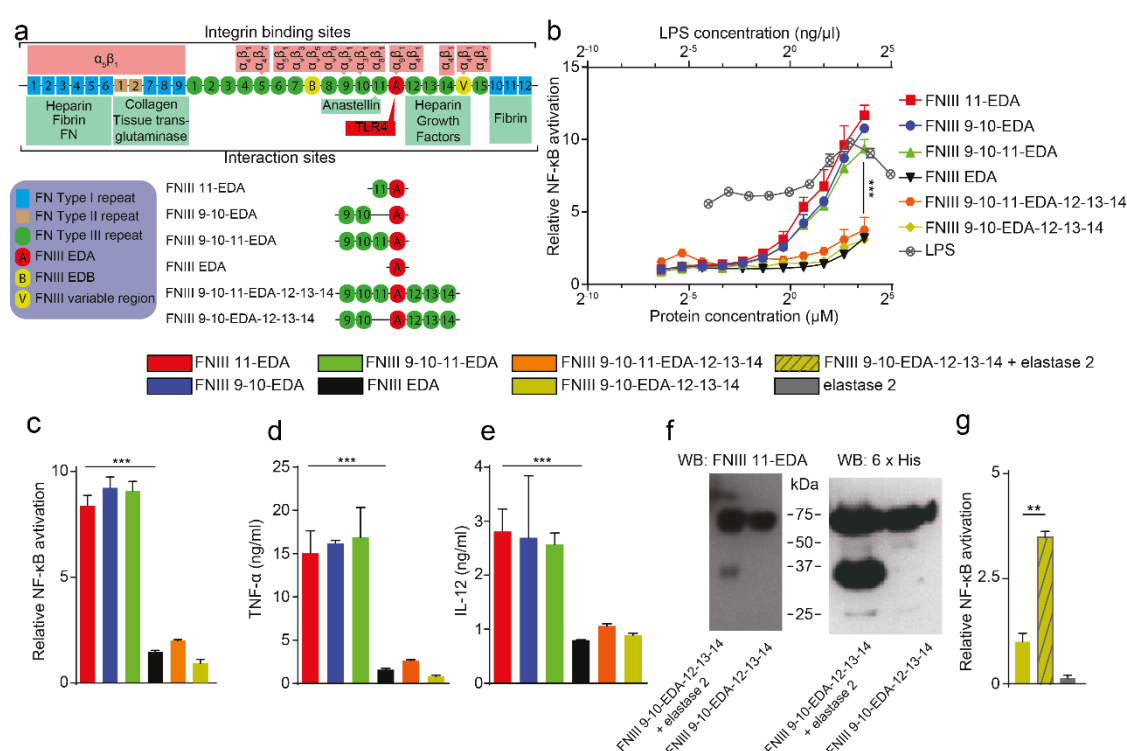
Fig. 1. TLR4 activation by FNIII EDA is modulated by the context of its neighboring FNIII domains. (a) FNIII EDA-containing FN fragments produced and of full length FN with some of its interaction sites displayed. (b) Activation of NF-κB in THP1-Blue cells as an indication of TLR agonization in response to various FNIII EDA-containing FN fragments, compared to LPS. The presence of a domain N-terminal to the FNIII EDA domain enhances activation, and the neighboring C-terminal domain abrogates activation. In the absence of the FNIII 12-13-14 domain, activation is comparable to that achieved by LPS. (c) Activation of NF-κB in HEK-Blue TLR4 cells as a cellular bioassay of TLR4 agonization. The presence of a domain N-terminal to the FNIII EDA domain enhances TLR4 agonization, and the neighboring C-terminal domain abrogates TLR4 agonization. In the absence of the FNIII 12-13-14 domain, TLR4 agonization is strong. (d, e) Production of TNF-α (d) or IL-12p70 (e) from murine bone marrow-derived DCs upon stimulation with various FNIII EDA-containing FN

39

fragments. In DCs, the same pattern of activation was observed as with the previous cell lines: the presence of a domain N-terminal to the FNIII EDA domain enhances activation, and the neighboring FNIII 12-13-14 domain abrogates activation. (f) Western blots of the digestion product of FNIII 9-10-EDA-12-13-14 by elastase 2 and undigested control, blotted against the FNIII EDA domain (N-terminal to a predicted elastase 2 cleavage site) and a 6xHis tag (C-terminal). Cleavage was observed to yield two fragments of similar molecular weight, consistent with the presence of elastase 2 cleavage site at position 87 of the 94 amino acid-long FNIII EDA domain. (g) Activation of HEK-Blue TLR4 cells with the digested and undigested FNIII 9-10-EDA-12-13-14. Digestion of FNIII 9-10-EDA-12-13-14 with elastase 2 recovers activation, consistent with elastase 2-dependent cryptic agonization of TLR4. Cellular experiments in c, d, e and f were done in the presence of 10 µg/ml polymixin B, to avoid any influence of potentially contaminating LPS. In c, d, e and f, bars and curves represent mean ± SEM of triplicate cultures from two independent experiments. **P < 0.01; ***P < 0.001.

2.3.3 The immunostimulatory activity of FNIII EDA is cryptic and dependent upon elastase 2 cleavage

We sought to understand the biological significance of the profound diminution of FNIII EDA activity through C-terminal extension with the FNIII 12-13-14 domain, hypothesizing that the FNIII EDA repeat is cryptic in its TLR4 agonizing activity. Using bioinformatics analytical tools[32], we suspected the presence of an elastase 2 (a serine protease, also referred to as neutrophil elastase) substrate between FNIII EDA and FNIII 12, after ile$_{87}$ in the 94 amino acid-long FNIII EDA domain. We verified the presence of such a cleavage site by incubating FNIII 9-10-EDA-12-14 with elastase 2. The digestion products were analyzed using Western blotting, detecting FNIII EDA or the 6xHis tag that is located at the C-terminus of the FN fragment. Therefore, the expected digestion products of the 67 kDa FNIII 9-10-EDA-12-14 protein are a 33 kDa FNIII EDA-positive fragment and a 34 kDa 6xHis tag-positive fragment. Western blotting confirmed the presence of the cleavage site, since both digestion products were detected (Fig.1f).

To assess if the biological activity of FNIII 9-10-EDA-12-14 could be recovered after digestion by elastase 2, we characterized TLR4 agonization in the HEK-Blue TLR4 cells. Proteolytic enhancement of TLR4 agonization was observed (Fig. 1g), consistent with activity obtained with the recombinant fragments lacking FNIII12-14 although not as high. The elastase 2 enzyme itself did not activate TLR4 in this assay (Fig. 1g). Other proteases tested (MMP-2, MMP-3, MMP-9, thrombin and plasmin) did not show cleavage of the protein as indicated by SDS-PAGE analysis (Fig. S1b).
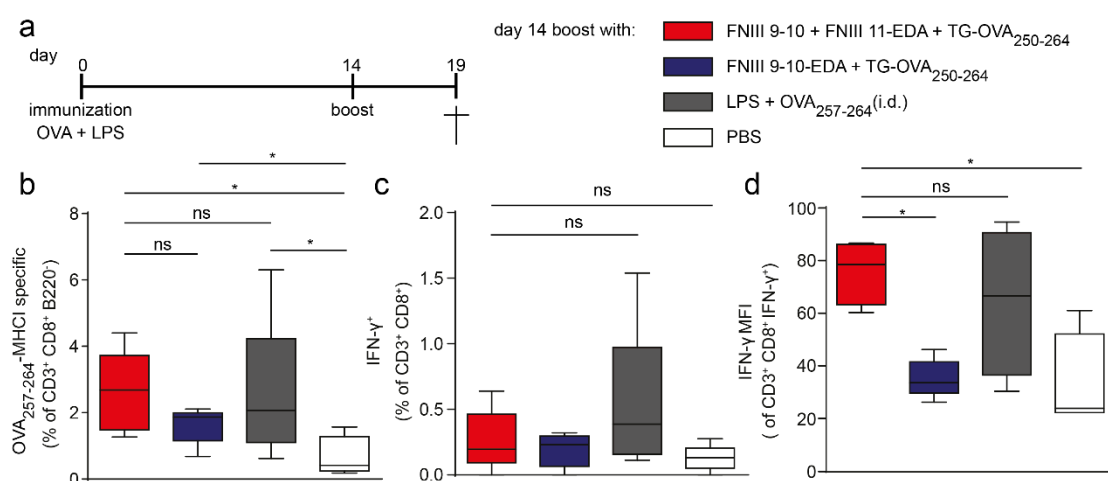
Fig. 2. Fibrin matrices functionalized with FNIII 9-10 + FNIII 11-EDA stimulate an antigen-specific CD8$^+$ T cell response. (a) Immunization schedule. C57BL/6J mice were immunized with 50 µg OVA and 20 µg LPS on day 0. The ability of FNIII EDA-containing fibrin-binding FN fragments to boost a CD8$^+$ T cell response was tested on day 14 by implanting s.c. fibrin matrices functionalized with 5 nmol of TG-OVA$_{250-264}$ (comprising the MHC-I binding immunodominant peptide of ovalbumin, OVA$_{257-264}$) + 5 nmol of FNIII 11-EDA or FNIII 9-10-EDA (each with an N-terminal TG domain); alternatively mice were injected i.d. with 5 nmol of soluble OVA$_{257-264}$ + 50 µg of LPS or with PBS only. On day 19, mice were sacrificed and the spleen was harvested. (b) Fibrin gels functionalized with fibrin-binding FNIII 9-10 + FNIII 11-EDA (each with an N-terminal TG domain) + TG-OVA$_{250-264}$ induced levels of OVA$_{257-264}$-MHC-I-specific CD8$^+$ T cells in the spleen comparable to that induced by i.d. injections of LPS + OVA$_{257-264}$. (c, d) IFN-γ production from splenocytes restimulated for 6 h *ex vivo* with OVA$_{257-264}$ were evaluated by flow cytometry. The proportion of IFN-γ producing CD8$^+$ T cell was similar among the different groups. However, the production of IFN-γ by CD8$^+$ T cells was greater, as shown by the mean fluorescence intensity (MFI) of IFN-γ intracellular staining, in mice that were boosted with fibrin matrices functionalized with FNIII 9-10 + FNIII 11-EDA (each with an N-terminal TG domain) + TG-OVA$_{250-264}$ or with LPS and

OVA$_{257-264}$; the group boosted with FNIII 11-EDA yielded statistically similar responses as the group boosted with LPS. Box plots represent median ± 95% confidence interval (n = 5). *P < 0.05; ns, not significant.

2.3.4 Fibrin matrices functionalized with FNIII 9-10 + FNIII 11-EDA mediate CD8$^+$ T cell expansion and effector phenotype

Since FNIII 11-EDA showed potent TLR4 activation *in vitro*, we evaluated its immunological activity *in vivo*. We selected a model based on the xenoantigen ovalbumin (OVA), in which vaccine-induced weak CD8$^+$ T cell responses could potentially be further boosted (Fig. 2a). To evaluate boosting the CD8$^+$ T cell responses, we co-delivered FNIII 11-EDA and the H2k^b MHC I immunodominant peptide OVA$_{257-264}$[33]. Because FNIII EDA is naturally present within FN in the ECM, we decided to incorporate the FN fragments bound in matrix to mimic the *in vivo* situation. Moreover, this strategy allows creating an adjuvant-rich microenvironment, which has proved to be successful for cancer vaccination in other studies[34]. Here, as a matrix model, we used a fibrin hydrogel resembling a fibrin clot, with a volume of 150 µL and a concentration of 8 mg/mL of fibrinogen. To be incorporated in the matrix, the FN fragments were designed to contain a transglutaminase substrate sequence derived from α$_2$-plasmin inhibitor (NQEQVSPL, denoted herein TG) at the N-terminus. Therefore, the FN fragments could be covalently incorporated in the matrix through the transglutaminase activity of factor XIIIa, which naturally crosslinks fibrin[35]. In addition, the OVA$_{257-264}$ peptide was designed to be incorporated in fibrin. The TG sequence was fused to a longer sequence of OVA, namely OVA$_{250-264}$, so as to comprise the protease substrate site SGLEQLE within the OVA chain that allows processing by APC antigen proteolysis

machinery and liberation of the OVA$_{257-264}$ epitope from TG-OVA$_{250-264}$ for cross-presentation on MHC I[36] . Furthermore, because cell migration within fibrin is enhanced by integrin binding, we incorporated the major integrin-binding domain of FN, FNIII 9-10[37]. Two fibrin matrix compositions were tested: fibrin functionalized with FNIII 9-10 plus FNIII 11-EDA and fibrin functionalized with FNIII 9-10-EDA.

First, we gave an intradermal (i.d.) vaccine prime dose of soluble OVA adjuvanted with lipopolysaccaride (LPS), which resulted in strong CD4$^+$ but modest CD8$^+$ T cell responses, as indicated by OVA$_{257-264}$:H2k^b p:MHC I pentamer binding (Fig. 2b). FNIII EDA being rarely the initiator of the inflammatory response *in vivo*, priming with this formulation to better study FNIII EDA in its ability to sustain a pre-established inflammatory response. Boosting with the soluble MHC I epitope OVA$_{257-264}$ + LPS increased the frequency of antigen-specific CD8$^+$ T cells (P<0.05). Boosting was also achieved by implanting fibrin matrices functionalized with FNIII 9-10 + FNIII 11-EDA + TG-OVA$_{250-264}$ (P<0.05) and with FNIII 9-10-EDA + TG-OVA$_{250-264}$ (P<0.05), although the boosting was marginally improved with the former (Fig. 2b). As an indication of the effector phenotype of these cells, we performed *ex vivo* restimulation of splenocytes with OVA$_{257-264}$: although the frequency of IFN-γ-expressing CD8$^+$ T cells was not enhanced by the FNIII EDA-containing proteins (Fig. 2c), the intensity of IFN-γ expression was enhanced by treatment with fibrin functionalized with FNIII 9-10 + FNIII 11-EDA (P<0.05) (Fig. 2d).
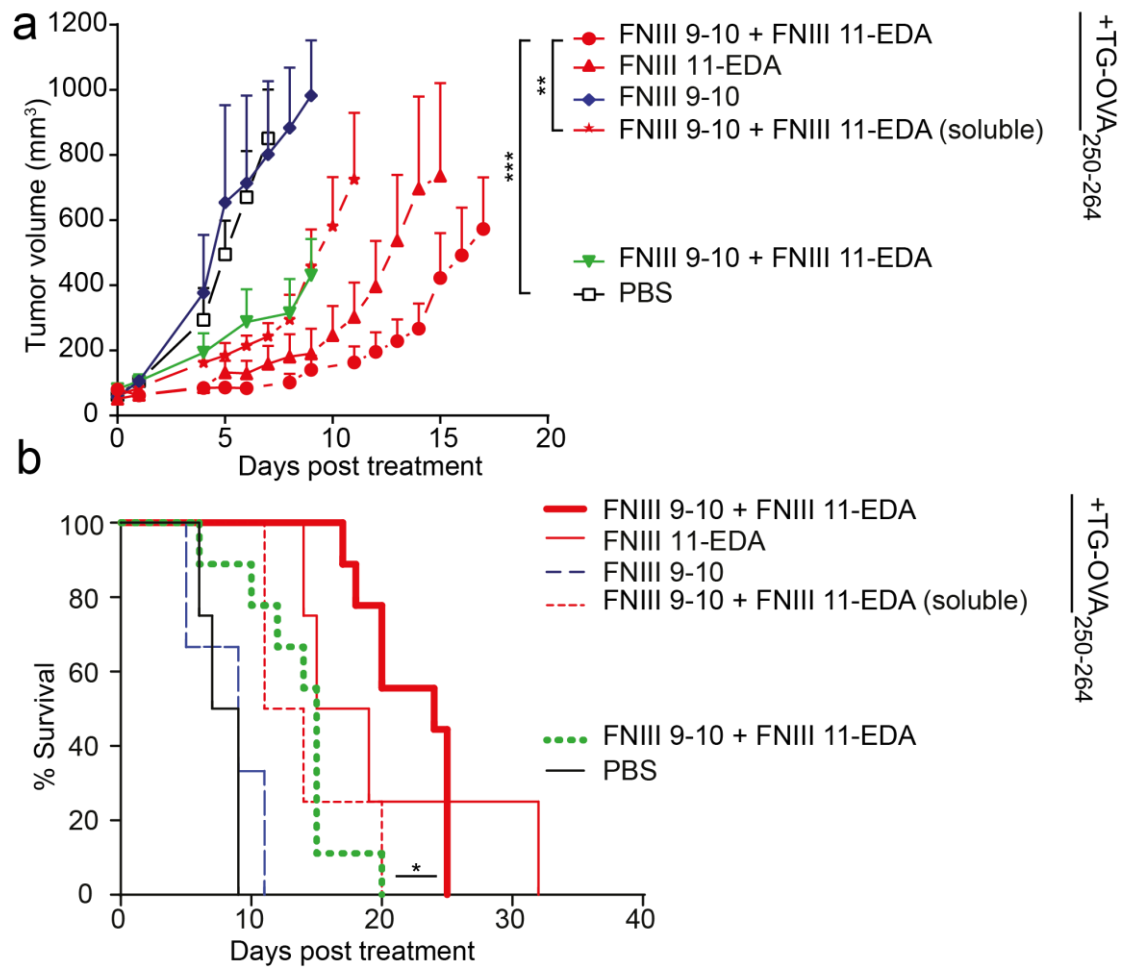
Fig. 3. Single implantation of fibrin matrices functionalized with FNIII 9-10 + FNIII 11-EDA in E.G7-OVA tumor bearing mice reduces tumor growth rate. C57BL/6J mice were injected s.c. with 10^6 E.G7-OVA cells on the back. When tumors reached 50 ± 5 mm^3, the ability of fibrin-binding FNIII EDA-containing FN fragments to induce a functional CD8$^+$ T cell response was tested by treating mice with fibrin matrices functionalized with various matrix formulations implanted s.c. or with soluble formulations injected i.d. Animals were sacrificed either when the tumor reached 1000 mm^3 or for humane reasons. (a, b) Tumor growth was significantly delayed in animals vaccinated using a fibrin matrix functionalized with FNIII 11-EDA ± FNIII 9-10 (each with an N-terminal TG domain) + TG-OVA$_{250-264}$ both in terms of tumor volume (a) and animal survival (b). TG-OVA$_{250-264}$-free matrices also proved slightly effective in delaying tumor growth (a) and extending animal survival (b). Growth curves were stopped when the second animal of the corresponding group died, the value corresponding to the first animal which died was kept as a constant until the curve was stopped. Growth curves represent mean ± SEM; Kaplan-Meier survival-curves (n = 4-9) from two independent experiments. *P < 0.05; **P < 0.01; ***P < 0.001.

2.3.5 Fibrin matrices functionalized with FNIII 11-EDA ± FNIII 9-10 mediate functional cytotoxic T lymphocyte responses in the E.G7-OVA tumor model

To explore the extent to which FNIII 11-EDA-generated $CD8^+$ T cells were capable of cell killing, i.e. function as cytotoxic T lymphocytes (CTLs), we employed a thymoma tumor model in which the cells express the xenoantigen OVA (E.G7-OVA). Tumor cells were injected subcutaneously (s.c.) in the back, and resulting tumors were allowed to reach a volume of 50 mm^3. At that point, a fibrin matrix containing the FN fragments of interest and TG-OVA$_{250–264}$ was implanted at a distant site at the level of the shoulder girdle close to the brachial lymph nodes or soluble OVA$_{257-264}$ controls were injected i.d. in the four footpads, and delays in tumor growth were measured. Soluble controls were injected i.d. in the four footpads.

When the fibrin matrix was implanted only once, strong delays in tumor growth were observed with treatments comprising FNIII 11-EDA, especially in conjunction with FNIII 9-10 (Fig. 3a). Omission of FNIII 11-EDA from the fibrin matrix resulted in no delay of tumor growth. Although the TG-OVA$_{250–264}$ peptide-free FNIII-EDA-containing matrix slightly reduced the tumor growth, the absence of antigen significantly reduced the response, demonstrating that the response is not mainly based on a general upregulation of immunity but is rather specific to the antigen co-incorporated in the fibrin matrix. Moreover, FNIII 9-10 + FNIII 11-EDA was not as effective when administered not bound to fibrin matrix, demonstrating functionality in the matrix-immobilized form. The Kaplan-Meier survival curves shown in Fig. 3b illustrate the

benefits of co-delivery of FNIII 9-10 and FNIII 11-EDA with the tumor cell-specific peptide epitope. Although all tumors eventually reached 1000 mm^3, the substantial delay in approaching this volume induced by a fibrin matrix with FNIII 11-EDA, especially in conjunction with FNIII 9-10, clearly indicates induction of functional CTL responses.

In the experiments described above, a single administration of a functionalized fibrin matrix was performed and the fibrin was slowly resorbed, whereas physiologically the FNIII EDA-containing FN proteolytic fragments would be present chronically. Thus, to further explore the ability of its chronic presence to induce CTL activity, we administered the functional fibrin matrices weekly after the tumors reached 50 mm^3. In this model also, tumor growth was significantly delayed in animals treated with fibrin matrices functionalized with FNIII 11-EDA ± FNIII 9-10 + TG-OVA$_{250-264}$ both in terms of tumor volume (Fig. 4a) and survival (Fig. 4b). Furthermore, none of the mice treated with PBS or with fibrin matrices lacking either FNIII 11-EDA or TG-OVA$_{250-264}$ survived more than 21 days post treatment, whereas half of the mice treated with fibrin matrices functionalized with FNIII 11-EDA + TG-OVA$_{250-264}$ ± FNIII 9-10 survived longer than 21 days and 20% even showed complete regression of the tumor, as shown in survival curves (Fig. 4b) and the individual growth curves (Fig. 4c). The efficacy of multiple injections of the soluble formulation was not assessed here as that approach already proved to be significantly less effective than functionalized fibrin matrix forms with a single administration. In this model of chronic exposure, co-treatment with FNIII 9-10 and FNIII 11-EDA yielded stronger CTL responses than mono-treatment with FNIII 11-EDA, both with the TG-OVA$_{250-264}$ peptide antigen comprising the OVA$_{257-264}$ epitope.
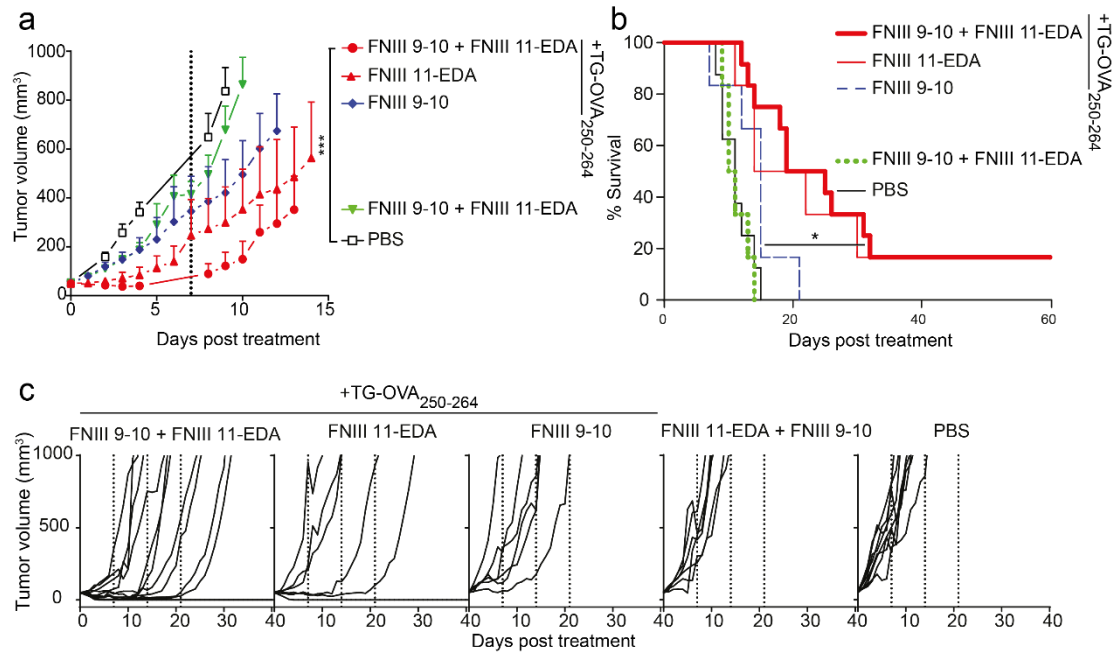
Fig. 4. Multiple implantations of fibrin matrices functionalized with FNIII 11-EDA ± FNIII 9-10 reduces E.G7-OVA tumor growth rate and in cases mediates regression. C57BL/6J mice were injected s.c. with 10^6 E.G7-OVA cells on the back. When tumors reached 50 ± 5 mm^3, mice were treated weekly (day 0 and dashed lines) for three weeks with fibrin matrices functionalized with various formulations implanted s.c. Mice were sacrificed when the tumor reached 1000 mm^3 or for humane reasons. Tumor growth was significantly delayed in animals treated using a fibrin matrix functionalized with FNIII 11-EDA ± FNIII 9-10 (each with an N-terminal TG domain) + TG-OVA$_{257-264}$ both in terms of tumor volume (a) and animal survival (b). Individual growth curves (c) show regression in some of the animals treated with fibrin gels functionalized with TG-OVA$_{250-264}$ and FNIII 11-EDA with or without FNIII 9-10 (each with an N-terminal TG domain). Growth curves were stopped when the second animal of the corresponding group died, the value corresponding to the first animal which died was kept as a constant until the curve was stopped. Growth curves represent mean ± SEM; Kaplan-Meier survival-curves (n = 6-12) from two independent experiments. *P < 0.05;***P < 0.001.

2.3.6 Fibrin matrices functionalized with FNIII 9-10 + FNIII 11-EDA mediate functional cytotoxic T lymphocyte responses in the B16-F10 tumor model with an endogenous antigen

In the experiments with E.G7-OVA cells, the surrogate tumor antigen OVA is a xenoantigen, not centrally tolerized in the mouse. To explore the activity of the FNIII 11-EDA domain to induce immunological responses versus a centrally tolerized antigen, we used the B16-F10 melanoma model. Fibrin matrices were functionalized with FNIII EDA-containing FN fragments and with the MHC I immunodominant epitope from tyrosinase-related protein-2 (TRP-2), namely TRP-2$_{180-188}$[38]. As with the OVA-derived epitope, we designed the TRP-2-derived epitope to contain a longer peptide sequence from TRP-2 for proteolytic processing of the antigen and an N-terminal TG sequence for immobilization in fibrin, namely TG-TRP-2$_{173-188}$. Mice were treated starting from the third day after tumor inoculation, when the tumors were palpable, and were further treated weekly for three weeks. Consistent with the results in the E.G7-OVA model, tumor growth was significantly delayed in animals treated with the fibrin matrix functionalized with FNIII 11-EDA + FNIII 9-10 + TG-TRP-2$_{173-188}$, as shown by the individual (Fig. 5a) and aggregate (Fig. 5b) growth curves, as well as the Kaplan-Meier survival curves (Fig. 5c). As in the experiments with the E.G7-OVA cells, the combination of the antigen with either FNIII 11-EDA or FNIII 11-EDA + FNIII 9-10 yielded similar results; only the latter, which proved slightly more effective at reducing the initial tumor volume, was retained for testing against the aggressive B16-F10 model.

The B16-F10 melanoma model is known as an immune suppressive model, owing in part to the infiltration of monocytic myeloid-derived suppressor cells (MO-MDSCs) in the tumor as well as their proliferation in the spleen[39,40]. Therefore, we examined MO-MDSC numbers in the spleens of the B16-F10-bearing mice. Mice receiving the fibrin matrices containing TG-TRP-$2_{173-188}$ but no FNIII fragments showed the same number of splenic MO-MDSCs compared to untreated mice or mice treated with fibrin matrices functionalized with FNIII 11-EDA + FNIII 9-10 without TG-TRP-$2_{173-188}$. However, mice treated with fibrin matrices functionalized with FNIII 11-EDA + FNIII 9-10 + TG-TRP-$2_{173-188}$ showed a substantial reduction in the number of splenic MO-MDSCs, demonstrating the ability of the FNIII 11-EDA domain to induce local (delay of tumor growth) and systemic (reduction in splenic MO-MDSC numbers) immune responses to an endogenous antigen, here the melanocyte-specific antigen TRP-2.
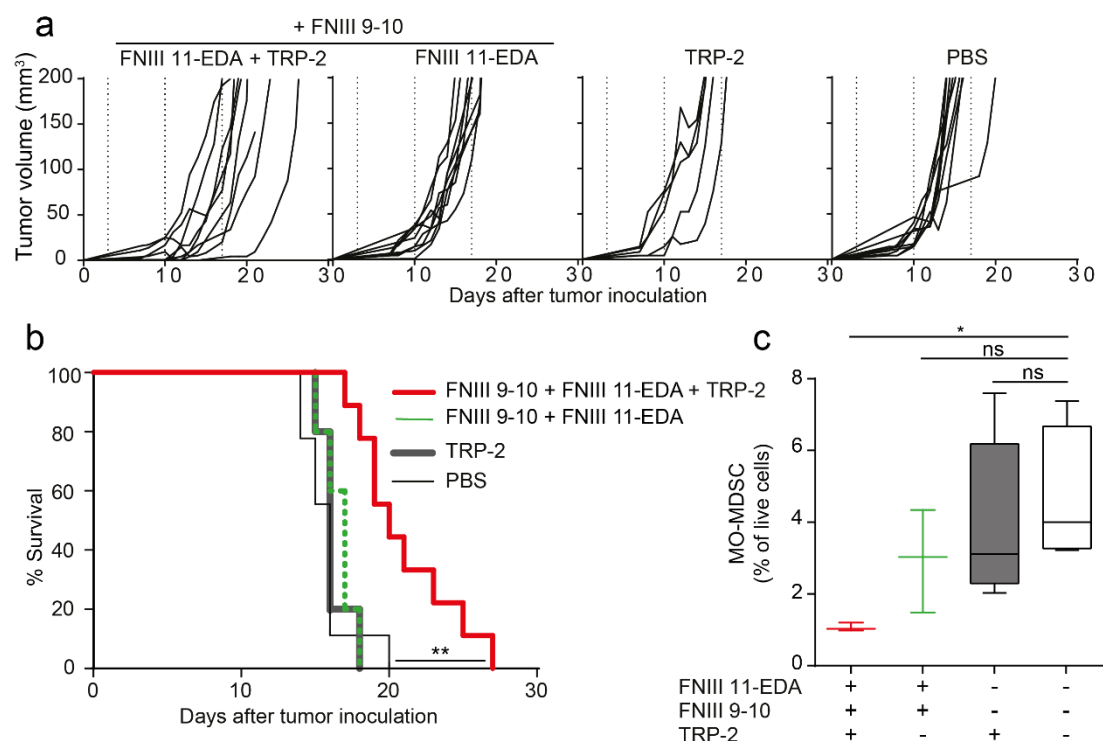
Fig. 5. Multiple implantations of fibrin matrices functionalized with FNIII 9-10 + FNIII 11-EDA reduces B16-F10 melanoma tumor growth rate and modulates anti-tumor immune suppression. C57BL/6J mice were injected s.c. with 2.5 x 10^5 B16-F10

cells on the back on day 0. On day 3, mice were treated weekly (dashed lines) for three weeks with fibrin gels functionalized with various formulations implanted s.c. Animal were sacrificed either when the tumor reached 200 mm^3 or for humane reasons. Individual growth curves (a) and survival curves (b) show that tumor growth was significantly delayed in animals treated with fibrin matrices functionalized with FNIII 11-EDA + FNIII 9-10 (each with an N-terminal TG domain) + TG-TRP-2$_{173-188}$, comprising the MHC-I immunodominant peptide epitope from the melanocyte-specific protein TRP-2 (TRP-2$_{180-188}$). (c) The percentage of monocytic myeloid-derived suppressor cells (MO-MDSC, flow-cytometry gated as being CD11b$^+$CD11c$^-$MHC-II$^-$Ly6C^{hi}Ly6G$^-$) in the spleen was significantly reduced in the mice treated with the fibrin gel containing and FNIII 9-10 + FNIII 11-EDA (each with an N-terminal TG domain) + TG-TRP-2$_{173-188}$ compared to the naïve control. Graphs show Kaplan-Meier survival-curves (n = 6-12) from two independent experiments. Box plots represent median ± 95% confidence interval (n = 3-5). *P < 0.05; **P < 0.01.

2.4 Discussion

Although roles of FN in processes such as embryogenesis and wound healing have been described[41,42], FN's interaction with the immune system is not well understood. The FNIII EDA domain, present in a splice variant of FN, which is found in sites of transient inflammation as in tissue damage[4–6] and of chronic inflammation such as psoriatic lesions[10–12] and scleroderma lesions[15], has been shown to agonize TLR4[14]. In the case of scleroderma, for example, agonization of TLR4 was shown to drive a cycle of fibrosis, leading to further FNIII EDA-containing FN expression, increasing TLR4 agonization and promoting continued fibrosis[15]; as such, TLR4 agonization via FNIII EDA is central to the pathophysiology of the disease. Moreover, because of its ability to activate TLR4, FNIII EDA has been explored in cancer vaccinology, utilizing FNIII EDA-antigen fusion proteins as DC-targeting adjuvants to induce anti-tumor CTLs[28,30,31]. In this work, at least part of the effect of the FNIII EDA domain has been attributed to

targeting the antigen for DC uptake through binding to TLR4[28,30]. Nevertheless, FNIII EDA showed anti-tumor potency only in combination with other TLR ligands.

In our study, we first sought to explore the dependence of FNIII EDA's agonization of TLR4 on its intramolecular context, addressing roles played by the N-terminally neighboring FNIII 11 domain and FNIII 9-10 domain, which binds cell-surface integrins $\alpha_5\beta_1$ and $\alpha_v\beta_3$[1,16,17,43], and by the C-terminally neighboring domain FNIII 12-13-14, which binds heparin and heparan sulfate[19] and growth factors[21]. Moreover, we hypothesized that the agonization of TLR4 by FNIII EDA could be cryptic, because some of the physiological mechanisms involving FN have been shown to be carried out by cryptic sites[44–47] requiring conformational modification or proteolytic cleavage to exert their functions, including stimulation of MMP expression by FNIII EDA[24]. Thus, we were also motivated to search for proteases that might enhance FNIII EDA activity.

We expressed a family of FN fragments (Fig. 1a) comprising the FNIII EDA repeat with various N-terminal and C-terminal extensions, so as to include FNIII 9-10, FNIII 11, and FNIII 12-13-14. Then, we characterized the ability of these recombinant FN fragments to agonize TLR4, activate DCs, stimulate CD8^{+} T cell expansion, and induce functional CTLs, where functionality was judged by cytotoxicity in a tumor vaccine model. Our *in vitro* results show that extension of the FNIII EDA domain to the N-terminus enhances its ability to agonize TLR4 (Fig. 1b, c) and induce inflammatory cytokine expression from DCs (Fig. 1d, e). This phenomenon was not sensitive to the details of the FNIII domain to the N-terminus, as extensions with FNIII 11, FNIII 9-10, and FNIII 9-10-11 yielded equivalent results (Fig. 1b, e). Thus, we conclude that co-binding of integrins $\alpha_5\beta_1$ and $\alpha_v\beta_3$ is likely not involved in the effect. Rather, the

observed 4-5 fold enhancement of TLR4-agonization activity may be due to structural stabilization of the FNIII EDA repeat, which, like other FNIII domains, is not stabilized by disulfide bonding. It is noteworthy that agonization of TLR4 by N-terminally extended FNIII EDA is very potent, comparable to that achieved by the prototypical microbial TLR4 agonist LPS (Fig.1b), yet without the cytotoxicity that is accompanied by high doses of LPS, which leads to lower NF-κB signaling[48] (Fig. 1b). Furthermore, the protein construct tested here were stable at concentration, showing no aggregation.

The possibility that our fragments could be contaminated with LPS was excluded by conducting these experiments in the presence of polymyxin B, which binds and inactivates LPS[49,50]; moreover, the expression and purification protocol for FNIII EDA (observed to be a poor agonist) and FNIII 11-EDA, FNIII 9-10-EDA, and FNIII 9-10-11 EDA (good agonists) were very similar. Finally, LPS endotoxin levels were tested in all the recombinant FN fragments and were found to be below 0.2 EU/μg in each.

Considering the C-terminal context of FNIII EDA, the existence of a protease substrate was suggested between the FNIII EDA and FNIII 12 domains using a bioinformatic analysis[32], specifically at the C-terminal end of FNIII EDA (position 87 of 94 total). Experimentally, elastase 2 (neutrophil elastase) was observed to cleave between FNIII EDA and FNIII 12 (Fig. 1f), and cleavage was shown to enhance TLR4 agonization compared to the intact control (Fig. 1g). Returning to the observation of the role of FNIII EDA and TLR4 in lesions such as in psoriasis[10–12] and scleroderma[15], which are characterized by neutrophil infiltration[51,52], it may be that neutrophil-derived elastase-2-mediated proteolysis of FN to potentiate a cryptic TLR4-agonizing site is involved in the pathophysiological mechanism.

Although FN is present in the serum, its main biological activities are carried out in immobilized form as a component of the ECM. Thus, we also sought to investigate FNIII EDA's immunological activity when immobilized in a matrix. As previously shown by our laboratory, recombinant proteins bearing an enzymatic substrate for the coagulation transglutaminase Factor XIIIa can be covalently incorporated into fibrin matrices[53], a method that has proven to be an efficient delivery method for integrin ligands[37] and growth factors in the context of tissue repair[20,22,37]. To determine whether FNIII EDA would induce similar reactions while presented in a more natural environment, we produced ECM-mimicking fibrin matrices functionalized with FNIII EDA-containing FN fragments and with the MHC I immunodominant peptide from OVA as a model antigen. In a first experiment aiming to test antigen-specific CD8$^+$ T cell expansion, exposure to fibrin matrices functionalized with FNIII 11-EDA and TG-OVA$_{250-264}$ induced expansion (Fig. 2b) with more intense IFN-γ production upon re-stimulation with antigen (Fig. 2d). Interestingly, the effect of the engineered matrix was comparable to that achieved by administration of OVA$_{257-264}$ (which does not require antigen processing) adjuvanted with LPS (Fig. 2d).

Surprisingly, fibrin matrices functionalized with FNIII 9-10-EDA induced significantly lower responses than matrices functionalized with both FNIII 11-EDA and FNIII 9-10. Such a difference may be due to FNIII 9-10-EDA's tendency to precipitate at the concentrations used for the preparation of the fibrin matrices. These results show that FNIII EDA-rich ECM analogs can enhance a pre-established immune response at the level of antigen-specific CD8$^+$ T cell expansion.

Because FNIII EDA has been shown to induce cellular immune responses including activation of CD8^{+} T cell responses, the domain in soluble form[26–31] has been explored extensively as a cancer vaccine adjuvant in mouse models including when antigens are fused to it[28,30,31], although most potently in combination with other TLR agonists[28,31]. Notably, when FNIII EDA-antigen fusions have been used as cancer vaccines, in conjugation with other TLR agonists, FNIII EDA has been used without N-terminal extension and as a soluble protein (i.e. not linked to the ECM)[28,30,31]. Here, we employed tumor cell-killing assays to characterize the functionality of ECM-bound FNIII EDA's effect upon CD8^{+} T cells to act as CTLs. Two models were utilized, one with a xenogeneic model tumor antigen, OVA (the E.G7-OVA thymoma model; Fig. 3 and 4), where the antigen is not centrally tolerized, and one with an endogenous tumor antigen TRP-2 (B16-F10 melanoma; Fig. 5), in which central tolerance must be overcome. The B16F10 melanoma model progresses very quickly, and as such the rate of tumor growth may outpace the rate of the adaptive immune response. In both models, administration of matrix-bound antigen (TG-OVA$_{250-264}$ or TG-TRP-2$_{173-188}$) with matrix-bound FNIII 11-EDA induced substantial delays in tumor growth, without any additional TLR agonists. Furthermore, while the addition of FNIII 9-10 did not improve the survival time of the mice, it nonetheless helped reduce the average tumor volume. Moreover, in the case of the E.G7-OVA model with repeated matrix implantation, complete tumor remission was observed in some instances (Fig. 4), however it is not known if the eventual escape in other animals from immune killing occurs via a *bona fide* immunological mechanism or due to selective pressure of vaccination toward antigenic selection leading to elimination of the OVA-encoding plasmid[54,55].

To demonstrate that a prolonged presence of the FNIII EDA domain bound to the fibrin matrix was beneficial, the same molecules in soluble form were injected i.d (Fig. 3). This control route was chosen, because it allows for an efficient delivery of the vaccine to the same skin-draining lymph node as the tumor (in addition to other non-affected lymph nodes) and thus maximizes the effect via a high percentage of targeted APCs being in contact with both the tumor antigens and the vaccine[56]. However, i.d. injection was much less effective in delaying tumor growth (Fig.3) compared to the fibrin matrix, clearly demonstrating that matrix binding of FNIII EDA fragment is beneficial. Furthermore, we judged the role of the inflammation from the surgical implantation of the matrix as being negligible, as FNIII-11-EDA-free matrices failed to provide protection against the tumor despite the presence of TG-OVA$_{250-264}$ (Fig.3). Thus, using two tumor models, one with an exogenous model antigen and one with an endogenous antigen, N-terminally-extended FNIII EDA without C-terminal extension with the native FNIII 12-13-14 domain was shown to induce potent immunity as characterized by the cytotoxic functionality of induced CTLs when the FN domains were co-administered in a matrix with antigen. Moreover, the ability to kill the syngeneic melanoma demonstrates the ability to induce functional autoimmunity.

Furthermore, in addition to exploring the ability of FNIII EDA to modulate immunity at the site of its presence, we explored effects in the spleen. The B16-F10 model is known to be immune suppressive through induction of MO-MDSCs, which traffic between the tumor and the spleen[57]. Administration of fibrin matrixes presenting FNIII 11-EDA, FNIII 9-10 and TG-TRP2$_{173-188}$ resulted in a substantial diminution of the frequency of MO-MDSCs in the spleen, demonstrating an ability to alter this immune suppressive mechanism (Fig. 5c).

In conclusion, these results bring insight into the immunological function of the FNIII EDA-containing FN splice variant *in vivo*. We revealed that the TLR4 agonizing potential of FNIII EDA is cryptic in FN, becoming exposed by cleavage between FNIII EDA and FNIII 12 by the neutrophil elastase 2. Lacking the C-terminal FNIII 12-13-14 domain, TLR4 agonization was potentiated up to 5 fold. Moreover, by using two tumor growth models, we demonstrated that induction of CTL responses to a xeno- and an auto-antigen by FNIII EDA activity is enhanced when the domain is bound to an ECM analog. Therefore, because the FNIII EDA-containing splice variant is expressed in sites of chronic inflammation, autoimmunity, and in many tumors[10–12], this ECM protein may contribute to the pathology and as well to an anti-tumoral benefit to the immune microenvironment by agonizing TLR4 especially after elastase-2-mediated proteolysis. In addition, delivering ECM-bound FNIII EDA fragments in combination with antigens could be an attractive option for anti-tumoral immunotherapies.

2.5 Methods

2.5.1 Recombinant proteins.

All FN fragments were engineered to bear at their N-terminus the coagulation transglutaminase Factor XIIIa peptide substrate NQEQVSPL (TG) and were cloned in a pET-22b (+) (Novagen) plasmid between the restriction sites NdeI and NotI. This plasmid contains a 6xHis-tag being added at the 3′ end of the inserted genes. *E. coli* BL21DE3 were transformed and used for protein production. The recombinant proteins were purified using a HIStrap column (GE Healthcare) and washed using 0.1

% Triton X-100 in PBS for LPS removal and an ATP solution (2 mM ATP, 50 mM Tris-HCl, 10 mM $MgSO_4$, pH 7.4) for DnaK removal. An imidazole (1 M) buffer was used for elution. The proteins were then stored in TBS at -80°C. Endotoxin levels were tested by Quantitative Chromogenic Limulus Amebocyte Lysate and were below 0.2 EU/μg.

2.5.2 Reagents.

Ultrapure LPS Escherichia coli 0111:B4 was purchased from InvivoGen. Low endotoxin grade OVA (<0.01 EU/μg protein) was used for immunization (Hyglos). MHC-I H-2Kb immunodominant peptides $OVA_{257-264}$ (SIINFEKL) and $TRP-2_{180-188}$ (SVYDFFVWL) were ordered from GenScript with the TG-sequence at their N-termini followed with N-terminal extension from the native protein OVA (SGLEQLE) [36] allowing proteolytic processing to liberate the epitopes (NQEQVSPLSGLEQLESIINFEKL, NQEQVSPLSGLEQLESVYDFFVWL). PE-labeled $H-2Kb/OVA_{257-264}$ pentamer was purchased from ProImmune. Pentamer staining was performed according to the manufacturer's instructions.

2.5.3 Western blotting.

FNIII 9-10-EDA-12-13-14 was first incubated with elastase 2 (Merck) at a 50:1 ratio for 3 h at 37°C in PBS. SDS-PAGE (12% polyacrylamide gels) was then performed, followed by transfer to a nitrocellulose membrane. The membrane was then incubated either with an HRP-conjugated anti-6xHis (abcam) or with an anti-FNIII EDA (abcam,

IST-9) antibody followed by an HRP-conjugated goat anti-mouse IgG1 secondary antibody (SouthernBiotech). After incubation, the blot was processed with SuperSignal West Pico Chemiluminescent Substrate (Pierce).

2.5.4 *In vitro* stimulation of bone marrow-derived dendritic cells.

Murine bone marrow-derived DCs were generated as described elsewhere[58]. On day 8, cells were plated at a density of 5×10^5 cells/well in 96-well plates and incubated overnight with 0.5 µM of recombinant proteins pre-incubated with 10 µg/ml of polymixin B to block interactions with any potentially contaminating LPS. Cytokines released in the supernatant were measured by ELISA (eBioscience).

2.5.5 *In vitro* stimulation of HEK-Blue TLR4 cells

HEK-Blue TLR4 LPS Detection Kit (Invivogen) containing HEK293 cells are engineered to express TLR4, MD2 and CD14 as well as a secreted embryonic alkaline phosphatase (SEAP) reporter gene controlled by an NF-κB-inducible promoter. HEK-Blue TLR4 cells were plated at a density of 10^4 cells/well in 48-well plates and were cultured for 48 h until they were 80% confluent. They were then incubated overnight with 0.5 µM of recombinant proteins pre-incubated with 10 µg/ml of polymixin B. All protein solutions and an elastase 2 control were incubated 3 h at 37°C before stimulation. FNIII 9-10-EDA-12-13-14 + elastase 2 was prepared in a 50:1 ratio. After incubation, the supernatant was diluted 1:10 in HEKBlue Detection Medium (Invivogen)

and the expression of SEAP was measured by light absorption at 620 nm. Cell culture medium was DMEM + 10% FBS and assay medium was DMEM + 2 % FBS.

2.5.6 *In vitro* stimulation of THP1-Blue cells.

THP1-Blue cells (Invivogen) are human THP-1 monocyte cell line engineered to express an NF-κB-inducible SEAP reporter construct. THP1-Blue cells were plated at a density of 5 x 10^5 cells/well in 96-well plates and incubated overnight with two-fold serial dilutions of recombinant proteins pre-incubated with 10 μg/ml of polymixin B or LPS ranging from 0.012 μM to 12.5 μM and 0.06 ng/μl to 30 ng/μl, respectively. After incubation, the supernatant was diluted 1:10 in HEKBlue Detection Medium (Invivogen) and the expression of SEAP was measured by light absorption at 620 nm. Cell culture medium was RPMI 1640 (2 mM L-glutamine, 1.5 g/L sodium bicarbonate, 4.5 g/L glucose, 10 mM HEPES and 1.0 mM sodium pyruvate) with 10% heat inactivated FBS supplemented with 100 μg/ml of Zeocin and assay medium was RPMI 1640 + 2 % FBS.

2.5.7 Mice and tumor cells.

C57BL/6J mice (aged 7–8 wk) were purchased from Harlan Laboratories and kept under pathogen-free conditions at the animal facility of Ecole Polytechnique Fédérale de Lausanne. All experiments were performed in accordance with Swiss law and with approval from the Cantonal Veterinary Office of Canton de Vaud, Switzerland. E.G7-OVA thymoma cells (i.e., EL4 cells (a thymoma line) expressing OVA as a surrogate tumor antigen, ATCC TIB-39) were obtained from American Type Culture Collection

(ATCC) and grown in RPMI medium 1640 (Invitrogen) supplemented with 10% heat-inactivated FBS, 1 mM sodium pyruvate, 30 mM Hepes, 50 µM 2-mercaptoethanol, and 0.4 mg/mL G418 antibiotic (Sigma). B16-F10 (ATCC CRL-2539) melanoma cells were obtained from American Type Culture Collection (ATCC) and were maintained in DMEM supplemented with 10% (vol/vol) FBS and penicillin/streptomycin/amphotericin B.

2.5.8 Preparation of functionalized fibrin matrices.

Fibrin matrices (150 µL) were formed by mixing a fibrinogen solution with a thrombin solution of equal volume in 1.5 mL Eppendorf tubes. The fibrin solution contained 16 mg/mL fibrinogen (plasminogen-, von Willebrand factor- and FN-depleted; Enzyme Research Laboratories) in HEPES buffer (20 mM HEPES, 150 mM NaCl, pH 7.4). The thrombin solution contained, 2 U/mL human thrombin (Sigma–Aldrich), 5 nmol of TG-OVA$_{250\text{-}264}$ and/or 5 nmol of FNIII 11-EDA or FNIII 9-10-EDA, and 5 mM Ca^{2+} in HEPES buffer.

2.5.9 Stimulation of antigen-specific CD8$^+$ response.

C57BL/6J mice were immunized by injection in the four footpads with a total dose of 50 µg OVA and 20 µg LPS on day 0. On day 14, fibrin gels functionalized with 5 nmol of TG-OVA$_{250\text{-}264}$ and 5 nmol of FNIII 11-EDA or FNIII 9-10-EDA were implanted s.c. on the back at the level of the shoulder girdle; alternatively mice were injected i.d. with 5 nmol of OVA$_{257\text{-}264}$ and 50 µg of LPS or plain PBS. On day 19 mice were sacrificed and the spleen was harvested.

2.5.10 Single-cell preparation and *ex vivo* antigen-specific cell restimulation.

Splenocytes were obtained by squeezing the spleen with a razor blade and disrupting the cell aggregates on a cell sieve, washing thoroughly, and lysing the red blood cells. For $CD8^+$ T cell antigen-specific restimulation and intracellular cytokine staining, immune cells were cultured at 37°C for 6 h in the presence of 1 µg/mL $OVA_{257-264}$ peptide. All cells were cultured in IMDM medium supplemented with 10% FBS and 1% penicillin/streptomycin (all from Invitrogen).

2.5.11 Flow cytometry and ELISA.

Before antibody staining for flow cytometry, all cells were labeled with live/dead fixable cell viability reagent in PBS (Invitrogen). For surface staining, cells were incubated for 15 min with the antibodies diluted in HBSS (Invitrogen)/0.5% BSA (PAA Laboratories). For antigen specificity, cells were stained with a SIINFEKL:H2Kb MHC I pentamer (ProImmune). For intracellular cytokine staining, cells were fixed in 2% paraformaldehyde solution, washed with 0.5% saponin (Sigma-Aldrich) in HBSS/0.5% BSA solution, and incubated with the antibodies diluted in saponin solution for 30 min. After washing, cells were resuspended in HBSS/0.5% BSA solution for analysis. Samples were acquired on CyAn ADP Analyzer (Beckman Coulter) and data were analyzed with FlowJo software (Tree Star). The antibodies anti-mouse CD11c, CD62L, B220, CD44 and IFN-γ were purchased from BioLegend; anti-mouse $CD3_ε$, CD8, CD11b, Ly6c, Ly6g, TNF-α and MHC-II antibodies were purchased from eBioscience (San Diego, CA, USA).

Ready-SET-go! ELISA kits for cytokine detection were purchased from eBioscience and used according to manufacturer's instructions.

2.5.12 Tumor growth assays.

Tumor cells were implanted s.c. in the back at the level of the junction between the thoracic and lumbar vertebrae of C57BL/6J mice with inoculation of 10^6 E.G7-OVA cells or 2.5×10^5 B16-F10 cells in 30 µL PBS (Invitrogen). The mice were then treated once (E.G7-OVA) or weekly for three weeks (E.G7-OVA and B16-F10) when their tumor reached 50 mm^3 (E.G7-OVA) or when the tumor became visible (B16-F10). Fibrin gels (150 µl total, fibrinogen (8 mg/ml)) were functionalized with 5 nmol of FNIII domain recombinant proteins and with or without 5 nmol of MHC I immunodominant peptide bound to the fibrin, as described above. Tumors were measured 5 times per week and volumes were calculated as ellipsoids based on three orthogonal measures. Animal were killed either when the tumor reached 200 mm^3 (B16-F10) or 1000 mm^3 (E.G7-OVA) or for humane reasons such as tumor necrosis, excessive loss of weight or evident isolation from the other animals.

2.5.13 Statistical Analyses

Statistical analyses were performed using Analysis of Variance (ANOVA) and Bonferonni posttest using GraphPad Prism.

2.6 Supporting Information
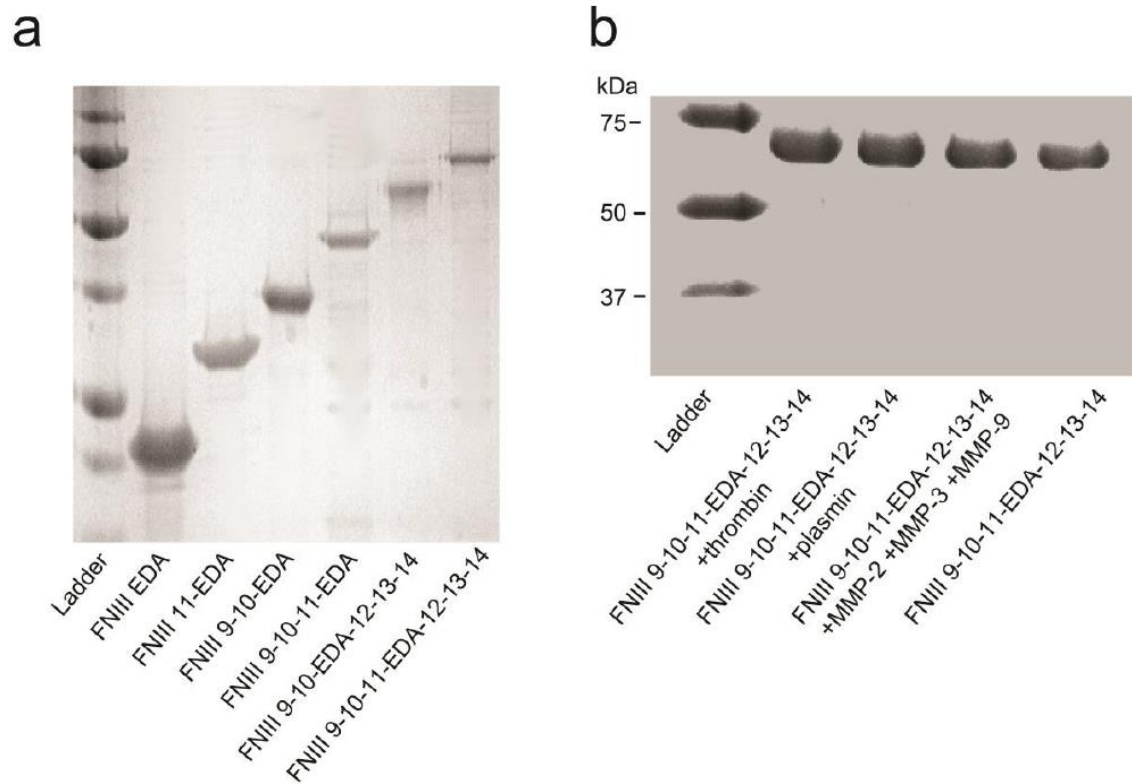
Fig. S1 (a) SDS-PAGE analysis of the 6 different FNIII EDA-containing FN fragments produced. (b) SDS-PAGE of FNIII 9-10-EDA-12-13-14 with or without prior incubation with thrombin or plasmin or a cocktail of MMP-2, MMP-3 and MMP-9

2.7 References

1.   Pankov, R. & Yamada, K. M. Fibronectin at a glance. *J. Cell Sci.* **115,** 3861–3863 (2002).

2.   ffrench-Constant, C. Alternative splicing of fibronectin--many different proteins but few different functions. *Exp. Cell Res.* **221,** 261–71 (1995).

3.   ffrench-Constant, C. & Hynes, R. O. Alternative splicing of fibronectin is temporally and spatially regulated in the chicken embryo. *Development* **106,** 375–88 (1989).

4.   Jarnagin, W. R., Rockey, D. C., Koteliansky, V. E., Wang, S. S. & Bissell, D. M. Expression of variant fibronectins in wound healing: cellular source and biological activity of the EIIIA segment in rat hepatic fibrogenesis. *J. Cell Biol.* **127,** 2037–48 (1994).

5.   Liao, Y. F., Gotwals, P. J., Koteliansky, V. E., Sheppard, D. & Van De Water, L. The EIIIA segment of fibronectin is a ligand for integrins alpha 9beta 1 and alpha 4beta 1 providing a novel mechanism for regulating cell adhesion by alternative splicing. *J. Biol. Chem.* **277,** 14467–74 (2002).

6.   ffrench-Constant, C., Van de Water, L., Dvorak, H. F. & Hynes, R. O. Reappearance of an embryonic pattern of fibronectin splicing during wound healing in the adult rat. *J. Cell Biol.* **109,** 903–14 (1989).

7.   Rybak, J. N., Roesli, C., Kaspar, M., Villa, A. & Neri, D. The extra-domain A of fibronectin is a vascular marker of solid tumors and metastases. *Cancer Res.* **67,** 10948–57 (2007).

8.   Villa, A. *et al.* A high-affinity human monoclonal antibody specific to the alternatively spliced EDA domain of fibronectin efficiently targets tumor neo-vasculature in vivo. *Int. J. Cancer* **122,** 2405–13 (2008).

9.   Borsi, L., Castellani, P., Allemanni, G., Neri, D. & Zardi, L. Preparation of phage antibodies to the ED-A domain of human fibronectin. *Exp. Cell Res.* **240,** 244–51 (1998).

10.   McFadden, J. P., Baker, B. S., Powles, A. V. & Fry, L. Psoriasis and extra domain A fibronectin loops. *Br. J. Dermatol.* **163,** 5–11 (2010).

11.   McFadden, J. P., Baker, B. S., Powles, A. V. & Fry, L. Psoriasis and streptococci: postscript regarding extra domain A fibronectin. *Br. J. Dermatol.* **161,** 706–7 (2009).

12.   McFadden, J., Fry, L., Powles, A. V. & Kimber, I. Concepts in psoriasis: psoriasis and the extracellular matrix. *Br. J. Dermatol.* **167,** 980–6 (2012).

13.   Astrof, S., Crowley, D. & Hynes, R. O. Multiple cardiovascular defects caused by the absence of alternatively spliced segments of fibronectin. *Dev. Biol.* **311,** 11–24 (2007).

14.   Okamura, Y. *et al.* The extra domain A of fibronectin activates Toll-like receptor 4. *J. Biol. Chem.* **276,** 10229–33 (2001).

15.   Bhattacharyya, S. *et al.* FibronectinEDA promotes chronic cutaneous fibrosis through Toll-like receptor signaling. *Sci. Transl. Med.* **6,** 232ra50 (2014).

16.   Charo, I. F., Nannizzi, L., Smith, J. W. & Cheresh, D. A. The vitronectin receptor alpha v beta 3 binds fibronectin and acts in concert with alpha 5 beta 1 in promoting cellular attachment and spreading on fibronectin. *J. Cell Biol.* **111,** 2795–800 (1990).

17.   Redick, S. D., Settles, D. L., Briscoe, G. & Erickson, H. P. Defining fibronectin's cell adhesion synergy site by site-directed mutagenesis. *J. Cell Biol.* **149,** 521–7 (2000).

18.   Ohashi, T. & Erickson, H. P. Domain unfolding plays a role in superfibronectin formation. *J. Biol. Chem.* **280,** 39143–51 (2005).

19.   Mostafavi-Pour, Z., Askari, J. A., Whittard, J. D. & Humphries, M. J. Identification of a novel heparin-binding site in the alternatively spliced IIICS region of fibronectin: roles of integrins and proteoglycans in cell adhesion to fibronectin splice variants. *Matrix Biol.* **20,** 63–73 (2001).

20.   Martino, M. M. & Hubbell, J. A. The 12th-14th type III repeats of fibronectin function as a highly promiscuous growth factor-binding domain. *FASEB J.* **24,** 4711–21 (2010).

21.   Wijelath, E. S. *et al.* Heparin-II domain of fibronectin is a vascular endothelial growth factor-binding domain: enhancement of VEGF biological activity by a singular growth factor/matrix protein synergism. *Circ. Res.* **99,** 853–60 (2006).

22.   Martino, M. M. *et al.* Engineering the growth factor microenvironment with fibronectin domains to promote wound and bone tissue healing. *Sci. Transl. Med.* **3,** 100ra89 (2011).

23.   Lin, F. *et al.* Fibronectin growth factor-binding domains are required for fibroblast survival. *J. Invest. Dermatol.* **131,** 84–98 (2011).

24.   Saito, S. *et al.* The fibronectin extra domain A activates matrix metalloproteinase gene expression by an interleukin-1-dependent mechanism. *J. Biol. Chem.* **274,** 30756–63 (1999).

25. Sekiguchi, K. & Hakomori, S. Functional domain structure of fibronectin. *Proc. Natl. Acad. Sci. U. S. A.* **77,** 2661–5 (1980).

26. Arribillaga, L. *et al.* A fusion protein between streptavidin and the endogenous TLR4 ligand EDA targets biotinylated antigens to dendritic cells and induces T cell responses in vivo. *Biomed Res. Int.* **2013,** 864720 (2013).

27. Mansilla, C. *et al.* Immunization against hepatitis C virus with a fusion protein containing the extra domain A from fibronectin and the hepatitis C virus NS3 protein. *J. Hepatol.* **51,** 520–7 (2009).

28. Mansilla, C. *et al.* Eradication of large tumors expressing human papillomavirus E7 protein by therapeutic vaccination with E7 fused to the extra domain a from fibronectin. *Int. J. Cancer* **131,** 641–51 (2012).

29. San Román, B. *et al.* The extradomain A of fibronectin (EDA) combined with poly(I:C) enhances the immune response to HIV-1 p24 protein and the protection against recombinant Listeria monocytogenes-Gag infection in the mouse model. *Vaccine* **30,** 2564–9 (2012).

30. Lasarte, J. J. *et al.* The extra domain A from fibronectin targets antigens to TLR4-expressing cells and induces cytotoxic T cell responses in vivo. *J. Immunol.* **178,** 748–56 (2007).

31. Rudilla, F. *et al.* Combination of a TLR4 ligand and anaphylatoxin C5a for the induction of antigen-specific cytotoxic T cell responses. *Vaccine* **30,** 2848–58 (2012).

32. Song, J. *et al.* PROSPER: an integrated feature-based tool for predicting protease substrate cleavage sites. *PLoS One* **7,** e50300 (2012).

33. Lipford, G. B., Bauer, S., Wagner, H. & Heeg, K. In vivo CTL induction with point-substituted ovalbumin peptides: immunogenicity correlates with peptide-induced MHC class I stability. *Vaccine* **13,** 313–20 (1995).

34. Ali, O. a, Emerich, D., Dranoff, G. & Mooney, D. J. In situ regulation of DC subsets and T cells mediates tumor regression in mice. *Sci. Transl. Med.* **1,** 8ra19 (2009).

35. Schense, J. C. & Hubbell, J. A. Cross-linking exogenous bifunctional peptides into fibrin gels with factor XIIIa. *Bioconjug. Chem.* **10,** 75–81 (1999).

36. Craiu, A., Akopian, T., Goldberg, A. & Rock, K. L. Two distinct proteolytic processes in the generation of a major histocompatibility complex class I-presented peptide. *Proc. Natl. Acad. Sci. U. S. A.* **94,** 10850–5 (1997).

37. Martino, M. M. *et al.* Controlling integrin specificity and stem cell differentiation in 2D and 3D environments through regulation of fibronectin domain stability. *Biomaterials* **30,** 1089–97 (2009).

38. Parkhurst, M. R. *et al.* Identification of a shared HLA-A*0201-restricted T-cell epitope from the melanoma antigen tyrosinase-related protein 2 (TRP2). *Cancer Res.* **58,** 4895–901 (1998).

39. Gabrilovich, D. I. & Nagaraj, S. Myeloid-derived suppressor cells as regulators of the immune system. *Nat. Rev. Immunol.* **9,** 162–74 (2009).

40. Dolcetti, L. *et al.* Myeloid-derived suppressor cell role in tumor-related inflammation. *Cancer Lett.* **267,** 216–25 (2008).

41. George, E. L., Georges-Labouesse, E. N., Patel-King, R. S., Rayburn, H. & Hynes, R. O. Defects in mesoderm, neural tube and vascular development in mouse embryos lacking fibronectin. *Development* **119,** 1079–91 (1993).

42. Valenick, L. V., Hsia, H. C. & Schwarzbauer, J. E. Fibronectin fragmentation promotes alpha4beta1 integrin-mediated contraction of a fibrin-fibronectin provisional matrix. *Exp. Cell Res.* **309,** 48–55 (2005).

43. Plow, E. F., Haas, T. A., Zhang, L., Loftus, J. & Smith, J. W. Ligand binding to integrins. *J. Biol. Chem.* **275,** 21785–8 (2000).

44. Zhong, C. *et al.* Rho-mediated contractility exposes a cryptic site in fibronectin and induces fibronectin matrix assembly. *J. Cell Biol.* **141,** 539–51 (1998).

45. Vogel, V. & Sheetz, M. Local force and geometry sensing regulate cell functions. *Nat. Rev. Mol. Cell Biol.* **7,** 265–75 (2006).

46. Davis, G. E., Bayless, K. J., Davis, M. J. & Meininger, G. A. Regulation of tissue injury responses by the exposure of matricryptic sites within extracellular matrix molecules. *Am. J. Pathol.* **156,** 1489–98 (2000).

47. Shinde, A. V. *et al.* Identification of the peptide sequences within the EIIIA (EDA) segment of fibronectin that mediate integrin alpha9beta1-dependent cellular activities. *J. Biol. Chem.* **283,** 2858–70 (2008).

48. Xaus, J. *et al.* LPS induces apoptosis in macrophages mostly through the autocrine production of TNF-alpha. *Blood* **95,** 3823–31 (2000).

49. Baldwin, G. *et al.* Effect of polymyxin B on experimental shock from meningococcal and Escherichia coli endotoxins. *J. Infect. Dis.* **164,** 542–9 (1991).

50. Karplus, T. E., Ulevitch, R. J. & Wilson, C. B. A new method for reduction of endotoxin contamination from protein solutions. *J. Immunol. Methods* **105,** 211–20 (1987).

51. Toichi, E., Tachibana, T. & Furukawa, F. Rapid improvement of psoriasis vulgaris during drug-induced agranulocytosis. *J. Am. Acad. Dermatol.* **43,** 391–5 (2000).

52.   Wetzel, A. *et al.* Increased neutrophil adherence in psoriasis: role of the human endothelial cell receptor Thy-1 (CD90). *J. Invest. Dermatol.* **126,** 441–52 (2006).

53.   Schense, J. C., Bloch, J., Aebischer, P. & Hubbell, J. A. Enzymatic incorporation of bioactive peptides into fibrin matrices enhances neurite extension. *Nat. Biotechnol.* **18,** 415–9 (2000).

54.   Beaudette, T. T. *et al.* In vivo studies on the effect of co-encapsulation of CpG DNA and antigen in acid-degradable microparticle vaccines. *Mol. Pharm.* **6,** 1160–9 (2010).

55.   Breckpot, K. *et al.* Lentivirally transduced dendritic cells as a tool for cancer immunotherapy. *J. Gene Med.* **5,** 654–67 (2003).

56.   Jeanbart, L. *et al.* Enhancing efficacy of anticancer vaccines by targeted delivery to tumor-draining lymph nodes. *Cancer Immunol. Res.* **2,** 436–47 (2014).

57.   Lindau, D., Gielen, P., Kroesen, M., Wesseling, P. & Adema, G. J. The immunosuppressive tumour network: myeloid-derived suppressor cells, regulatory T cells and natural killer T cells. *Immunology* **138,** 105–15 (2013).

58.   Lutz, M. B. *et al.* An advanced culture method for generating large quantities of highly pure dendritic cells from mouse bone marrow. *J. Immunol. Methods* **223,** 77–92 (1999).

Chapter 3

TLR4-9 agonists fibronectin EDA and CpG synergize to enhance antigen-specific Th1 and cytotoxic responses

Adapted from the original manuscript

Julier, Z., de Titta, A., Grimm, A.J., Simeoni, E., Swartz M.A., & Hubbell, J.A.

3.1 Abstract

Safe and effective subunit vaccines require adjuvants with a correct balance between strong activation of the immune system and low toxicity for the patient. Here we hypothesize that combination of CpG, a bacterial TLR9 agonist, with the endogenous TLR4 agonist extra domain A type III repeat of fibronectin (FNIII EDA), which has shown the ability to induce cytotoxic CD8$^+$ T cell responses in a non-toxic manner, would synergize to induce an efficient immune response while keeping the dose of the toxic CpG low. Here, we show that the combination of both adjuvants synergistically activates dendritic cells *in vitro,* induces a potent immune response sufficient to slow tumor growth in a murine tumor model and eradicates circulating hepatitis B virus in a transgenic HBV mouse model.

3.2 Introduction

The success of vaccines over the last decades is undeniable, however several infectious diseases are still missing an effective vaccine, such as human immunodeficiency virus, malaria, and chronic hepatitis B, and a general approach to therapeutic cancer vaccination is still lacking. Subunit vaccines, employing purified protein antigens rather than intact pathogens, require the addition of adjuvants for enhanced immunogenicity[1]. The first compound used as an adjuvant, which is still widely used in human vaccination, is alum. Alum-based adjuvants have been shown to be efficient in inducing T helper (Th)2 responses[2], leading to strong antibody secretion. Importantly, alum lacks the ability to induce potent cellular, Th1-biased responses, an important axis for fighting intracellular pathogens and cancer[3]. While adjuvants that are more potent than alum in inducing cell-mediated immunity have been developed, their application in clinic has been hindered by their toxicity and the systemic and local side effects they induce[4].

Hence, the development of safe and effective vaccines with fewer side effects remains a strong need[5] and requires the development of a new generation of adjuvants with a correct balance between activating the immune system toward a balanced Th1 and Th2 response, while maintaining low toxicity for the patient.

Toll-like receptors (TLRs) are a preferential target for the development of novel adjuvants for improved vaccination strategies, as many of them induce adaptive cellular immunity, which is central for eliminating a wide variety of pathogens and fighting cancer[6–9]. Activating ligands have been identified for most of the 13 known

human TLRs, most of them stemming from bacterial or viral origins, but endogenous agonists have also been identified[9]. Among the various TLR ligands currently tested in clinical trials as adjuvants for vaccines, the TLR9 agonist unmethylated CpG oligodeoxynucleotide has been shown to induce potent B cell humoral responses and most importantly induce the maturation of DCs and the subsequent secretion of Th1-biasing cytokines such as IL-12p70, IL-6 and TNF-α. Although reasonably safe at low dose[10,11], increasing the dose of CpG when the targeted disease requires a stronger response has been associated with risks of toxic shock[12].

Recent studies on the use of the endogenous TLR4 agonist extra domain A type III repeat of fibronectin (FNIII EDA) as an adjuvant showed its ability to induce cytotoxic CD8$^+$ T cell responses in a non-toxic manner in murine models[13–15]. Furthermore, our laboratory recently showed that the immunological activity of FNIII EDA was dependent of its molecular context and identified a more potent form of FNIII EDA N-terminally extended with the 11th type III repeat of FN (FNIII 11-EDA)[13].

Although single TLR targeting strategies have shown promising results[11], some combinations of TLR-agonists are known to synergize, notably by their co-activation of the MyD88 and TRIF intracellular pathways, and induce responses that are greater than the sum of their individual effects[16–20]. Not just the strength, but most importantly the quality of the response induced by combined TLRs agonists has been increased[20]. As the signaling crosstalk of TLR4 and TLR9, which signal though MyD88 and TRIF for the former and MyD88 only for the later, has been shown to amplify the inflammatory response in mice[21], we thus hypothesized that a combined administration of FNIII 11-EDA and CpG could synergize and activate immune cells more efficiently than either

alone. This effect might allow a reduction of the total dose of adjuvant needed to induce an efficient immune response, thus lowering the inherent toxicity of CpG.

Here, we first describe the synergistic pro-inflammatory cytokine secretion by dendritic cells (DCs) *in vitro* in response to the combination of FNIII 11-EDA and CpG. When injected in mice, ovalbumin (OVA) as a model antigen adjuvanted with combined half-doses of FNIII 11-EDA and CpG enhanced Th1 response and inflammatory cytokine secretion, both in CD4$^+$ and in CD8$^+$ T cells, compared to full doses of either CpG or FNIII 11-EDA. In addition, the proportion of antigen-specific CD8$^+$ T cells was also marginally increased. Using an E.G7-OVA T cell lymphoma tumor model expressing the xeno-antigen OVA, we validated the synergistic effect of the combination of the two TLR ligands FNIII 11-EDA and CpG on the generation of functional cytotoxic T lymphocytes (CTLs) through the limitation of tumor growth and enhanced survival.

Next, we sought to explore the ability of this TLR-agonist combination to break immune tolerance in a chronic hepatitis B transgenic mouse model expressing an hepatitis B virus (HBV) transgene (HBV-Tg mice)[22,23], which makes the mice tolerant to the hepatitis B protein antigens. We show that immunization with the hepatitis B surface antigen (HBsAg), adjuvanted with a combination of half doses of CpG and FNIII 11-EDA, was able to trigger an efficient Th1 immune response both in the spleen and the liver, a subsequent higher rate of HBsAg seroconversion, and more efficient clearance, highlighting a better Th1 cytokine secretion profile compared to full doses of the individual ligands.

3.3 Results

3.3.1 FNIII 11-EDA and CpG activate DCs in a synergistic manner

To determine whether FNIII 11-EDA and CpG were able to synergistically activate DCs, binomial combinations of both adjuvants were tested *in vitro* (Fig. 1) and the activation of DCs was evaluated by quantifying the production of the pro-inflammatory cytokines IL-12p70, IL-6 and TNF-α by ELISA. Although FNIII 11-EDA or CpG alone induced only mild activation of DCs at the doses tested (up to 2 μM each CpG and FNIII 11-EDA), their combination led to a synergistic increase in the production of IL-12p70 (Fig. 1a), IL-6 (Fig. 1b), and TNF-α (Fig. 1c). Indeed, the combination of both TLR agonists resulted in more than twice the expected theoretical amount of cytokine secreted for most concentration combinations tested.
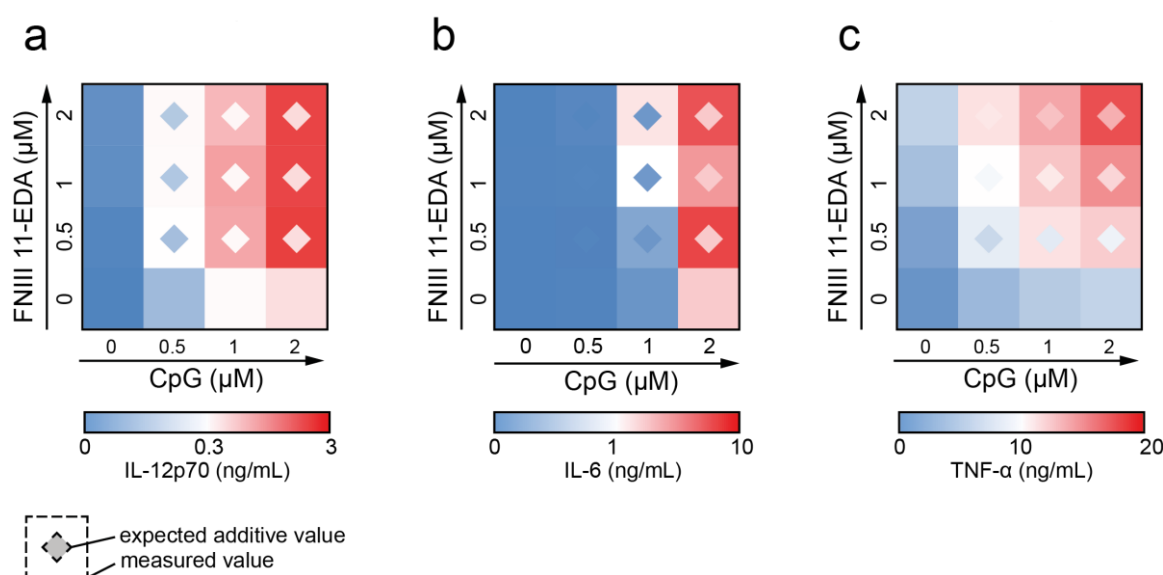
Figure 1. CpG and FNIII 11-EDA show synergistic activation of dendritic cells and stimulate strong IL-12p70, IL-6 and TNF-α production. *In vitro,* DCs secreted higher amounts of IL-12p70 (a) and IL-6 (b) TNF-α (c) when stimulated overnight with binary combination of FNIII 11-EDA and CpG (main squares) than the expected theoretical sum of both separated ligands (diamonds, sum of each individual ligand cytokine

secretion). Data shows ELISA readouts of measured from two independent experiments and expected cytokine concentration as heat maps; color scales are indicated.

3.3.2 Intradermal co-immunization with FNIII 11-EDA and CpG induces potent Th1 response and increases cytotoxic activity of antigen-specific CD8^{+} T cells

After observing that the two TLR agonists FNIII 11-EDA and CpG led to a synergistic activation of DCs *in vitro*, we proceeded to evaluate their ability to synergize towards mounting a potent antigen-specific response *in vivo* in an OVA prime-boost vaccination mouse model. Mice were immunized by intradermal injections with the model xeno-antigen OVA co-delivered with FNIII 11-EDA and/or with CpG on days 0 and 14 (Fig. 2a). To assess the potential synergy, effects of 5 nmol FNIII 11-EDA or 40 µg CpG were compared to the effect of the combination of half-doses of both TLR agonists together.

Both vaccinating with full-dose CpG and with the combination of both adjuvants at half-doses induced significant levels of SIINFEKL-MHCI-specific pentamers^{+} CD8^{+} T cells (SIINFEKL being the MHCI binding immunodominant peptide of OVA), while a full dose of FNIII 11-EDA had no observable effect. Combination of both adjuvants induced marginally higher levels of OVA-specific CD8^{+} T cells compared to CpG alone (Fig. 2b) and significantly higher frequency of IFN-γ^{+} TNF-α^{+} CD4^{+} T cells following *ex vivo* restimulation with OVA (Fig. 2c). Moreover, after restimulation of splenocytes with the SIINFEKL peptide (Fig. 2d,e), the CD8^{+} T cell population induced by the simultaneous administration of both adjuvants at the half doses showed a significantly enhanced

effector phenotype as shown by the higher frequency of IFN-γ producing CD8$^+$ T cells both in the total population of CD8$^+$ T cells (Fig. 2d) and degranulating LAMP1$^+$CD8$^+$ T cells (Fig. 2e). The half dose of CpG used in combination with half-dose of FNIII 11-EDA was also able to achieve a comparable level of production of IFN-γ by splenocytes restimulated for 3 days with OVA to that obtained with a full dose of CpG (Fig. 2f).
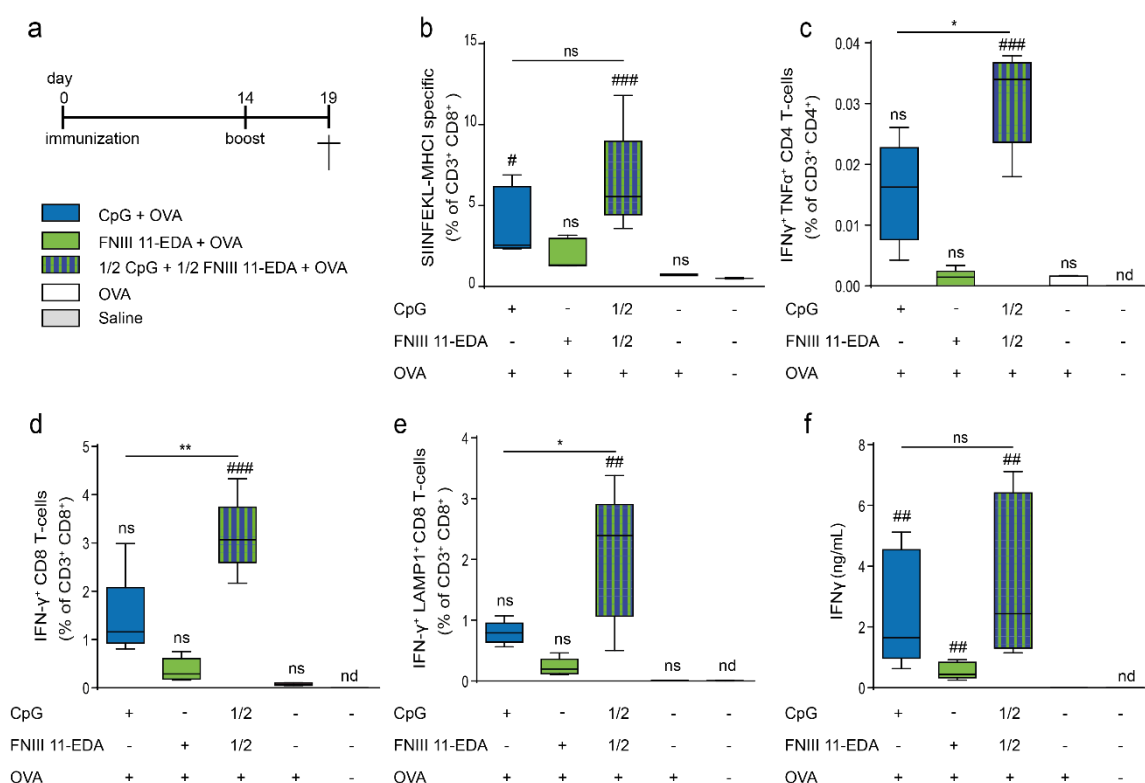
Figure 2. FNIII 11-EDA and CpG are effective at inducing antigen-specific CD8$^+$ T cell and Th1 responses. (a) Immunization schedule. C57BL/6J mice were immunized by intradermal injection in the four footpads with 50 μg of OVA adjuvanted with 40 μg of CpG or 5 nmol of FNIII 11-EDA or 20 μg of CpG plus 2.5 nmol of FNIII 11-EDA on day 0. On day 14, mice were injected with the same formulations as on day 0. On day 19, mice were sacrificed and the spleens were harvested. (b) Injection of 50 μg of OVA adjuvanted with combined 20 μg of CpG and 2.5 nmol of FNIII 11-EDA induced levels of SIINFEKL-MHC-I-specific CD8$^+$ T cells in the spleen comparable to that induced of 50 μg of OVA adjuvanted with 40 μg of CpG. (c) Frequency of IFN-γ$^+$TNF-α$^+$ CD4$^+$ splenocytes after 6 h *ex vivo* restimulation with OVA were evaluated by flow cytometry. The proportion of IFN-γ$^+$ TNF-α$^+$ CD4$^+$ T cells was also significantly improved by simultaneous injections of half doses of CpG and FNIII 11-EDA compared to full doses of each adjuvant alone. (d,e) Frequencies of IFN-γ$^+$ and IFN-γ$^+$ LAMP1$^+$ CD8$^+$ splenocytes after 6 h ex vivo restimulation with SIINFEKL were evaluated by flow cytometry. The frequency of IFN-γ producing CD8$^+$ T cells was significantly improved

(d) by simultaneous injections of half doses of CpG and FNIII 11-EDA compared to full doses of each adjuvant alone. (e) Similarly, the frequency of IFN-γ$^+$ LAMP1$^+$ CD8$^+$ T cells was significantly higher when both adjuvants were used. (f) IFN-γ production from splenocytes restimulated for 3 days *ex vivo* with OVA was evaluated by ELISA. Here, injection of half-doses of both adjuvants only marginally improved the production of IFN-γ compared to a full dose of CpG. Box plots represent means ± 95% confidence interval (n = 5). *, # P < 0.05; **, ## P < 0.01; ### P<0.001; ns, not significant; #, ##, ###, comparison to naïve group.

3.3.3 Injections of OVA adjuvanted with CpG plus FNIII 11-EDA mediate regression of E.G7-OVA tumor through functional cytotoxic T lymphocyte response

To determine the level of functionality of CD8$^+$ T cells generated after immunization with antigen combined with CpG and FNIII 11-EDA, the E.G7-OVA T cell lymphoma tumor model expressing OVA as a surrogate antigen was used. Tumor cells were injected subcutaneously (s.c.) in the back of mice and tumors were let grow until reaching a volume of 50 ± 5 mm^3, at which point treatments with OVA alone, OVA adjuvanted with CpG and/or FNIII 11-EDA, or saline were initiated and a second treatment dose injected 6 days later. Similarly to the previous experiment, OVA was injected with either 40 µg of CpG, 5 nmol of FNIII 11-EDA or both adjuvants combined at half-doses to assess synergistic activation. OVA was also injected with a half dose of CpG in the absence of FNIII 11-EDA to explore the extent to which response in the combined adjuvant group might be due to CpG alone. Tumor sizes were followed daily and used as an indication for CD8$^+$ T cell functionality.

Tumor regression was observed both in response to OVA combined with full-dose CpG and half-doses of combined CpG + FNIII 11-EDA as shown on average (Fig.

3a) and individual (Fig. 3b) tumor growth curves. Both groups temporarily showed examples of complete tumor regression, although this was more common when both adjuvants were co-administered. Tumor growth resumed faster when CpG at the full dose was used alone, whereas in mice treated with the combination of CpG and FNIII 11-EDA even at the half dose the treatment exerted control over tumor growth for a longer period of time. Only 2 out of 10 animals vaccinated with CpG alone survived longer than 25 days, while 7 out of 9 animals treated with CpG and FNIII 11-EDA even at the half dose survived longer than 30 days, with complete tumor remission in 3 out of 9 cases as shown by the Kaplan-Meier survival curves (Fig. 3c). OVA alone or supplemented with full-dose FNIII 11-EDA had only a mild effect on tumor growth. In support of the synergistic effect of FNIII 11-EDA and CpG, vaccination with OVA with the half-dose of CpG without co-administration of FNIII 11-EDA also had only a mild effect on tumor growth.
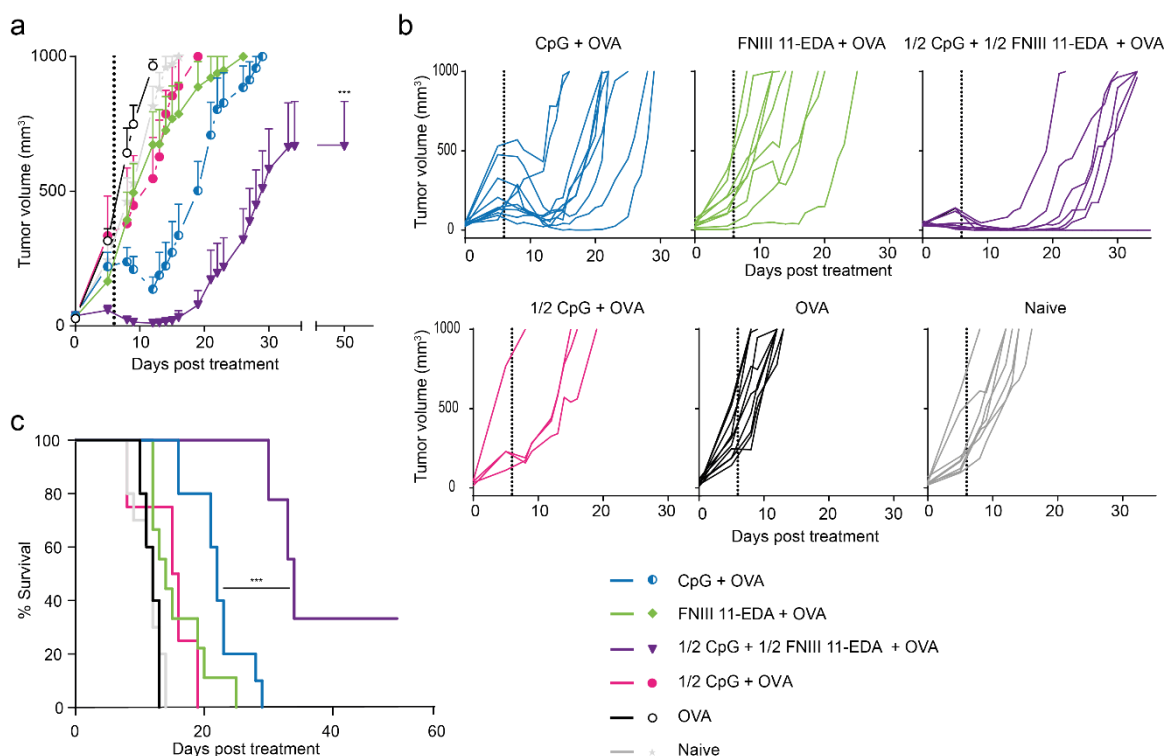
Figure 3. Multiple injections of OVA adjuvanted with both CpG and FNIII 11-EDA mediate regression of E.G7-OVA tumors. C57BL/6J mice were injected s.c. with 10^6 E.G7-OVA cells on the back. Mice were then treated with OVA or OVA adjuvanted either with combined half doses of CpG and FNIII 11-EDA or with full doses of each adjuvant alone or with a half dose of CpG without FNIII 11-EDA when their tumor reached 50 ± 5 mm^3 and received a second injection of the treatment 6 days later. Mice were sacrificed when the tumor reached 1000 mm^3 or for humane reasons. Tumor regression and growth delay were significantly improved in animals treated with combined adjuvants both in terms of tumor volume (a) and animal survival (b). Individual growth curves (c) show regression in most of the animals treated with both adjuvants although in most of them tumor growth eventually resumed. The values corresponding to the animal which died were kept as a constant until the curves were stopped. Growth curves represent mean ± SEM; Kaplan-Meier survival-curves (n = 4-10) from two independent experiments. *** P<0.001.

3.3.4 Co-immunization with HBsAg adjuvanted with FNIII 11-EDA and CpG leads to strong Th1 cytokine secretion and HBsAg seroconversion

To explore the ability of the CpG plus FNIII 11-EDA to break immune tolerance, we employed a HBV-Tg mouse model tolerant to the hepatitis B protein antigens and expressing the HBV in the liver and kidney[22]. Mice were vaccinated on day 0 and 14 by i.d. injection of HBsAg alone, HBsAg supplemented with CpG and/or FNIII 11-EDA, or saline as control. Mice were sacrificed on day 19 and blood, liver and spleen was harvested for *ex vivo* restimulation, ELISA and determination of viral load (Fig. 4a). To assess synergistic activation of the immune system in response to the TLR agonists, effects of 80 µg of CpG or 10 nmol of FNIII 11-EDA were compared to the half-dose of both adjuvants combined. Here the dose of each adjuvant was doubled compared to tumor experiment, as preliminary experiments with this model showed that relatively high doses were required.

After restimulation of splenocytes for 6 h with HBsAg *ex vivo* (Fig. 2b,c), a significant increase in the frequency of Th1 cytokine-secreting CD4$^+$ T cells was observed in response to co-vaccination with CpG and FNIII 11-EDA at the half dose (Fig. 4b) compared to CpG or FNIII 11-EDA alone at the full dose. However, the frequency of CD8$^+$ T cell secreting IFN-γ was higher when CpG was used as the only adjuvant (Fig. 4c). *Ex vivo* restimulation of liver cells with HBsAg for 6 h showed that vaccination with both adjuvants combined also increased the frequency of Th1 cytokine-secreting CD4$^+$ T cells compared to CpG alone, although FNIII 11-EDA alone unexpectedly showed a comparably high frequency (Fig. S1b). No difference in IFN-γ-secreting CD8$^+$ T cells populations in the liver was observed between the different treated groups (Fig. S1c). Co-immunization with CpG and FNIII 11-EDA slightly increased the level of production of IFN-γ by splenocytes (Fig. 4d) and liver cells (Fig. S1d) after restimulation for 3 days with HBsAg, although in most cases high variability prevented to reach statistical significance between groups.

We then evaluated the level of circulating HBsAg in the blood sampled at day 19, which is an indication of the elimination of virally-produced HBsAg by elicited antibodies secreted by the vaccine formulation, and of a limitation of the replication of the virus. Here all three treatment formulations, i.e. full-dose FNIII 11-EDA, full-dose CpG and combined half-doses of each adjuvant, significantly reduced the amount of circulating HBsAg in blood (Fig. 4e). The combination of half doses of each adjuvant significantly improved the elimination of the virally-produced protein compared to full-doses of each adjuvant alone. It is noteworthy that a half-dose of CpG without the addition of FNIII 11-EDA was not sufficient to achieve significant reduction of the amount of circulating HBsAg (Fig. S1e), demonstrating the synergistic response. Finally,

endpoint titers of anti-HBsAg IgGs were all significantly higher than control in all groups. The combination of CpG and FNIII 11-EDA yielded significantly higher titers than the other responding groups, while naïve mice showed no detectable level of anti-HBsAg antibodies (Fig. 4f).
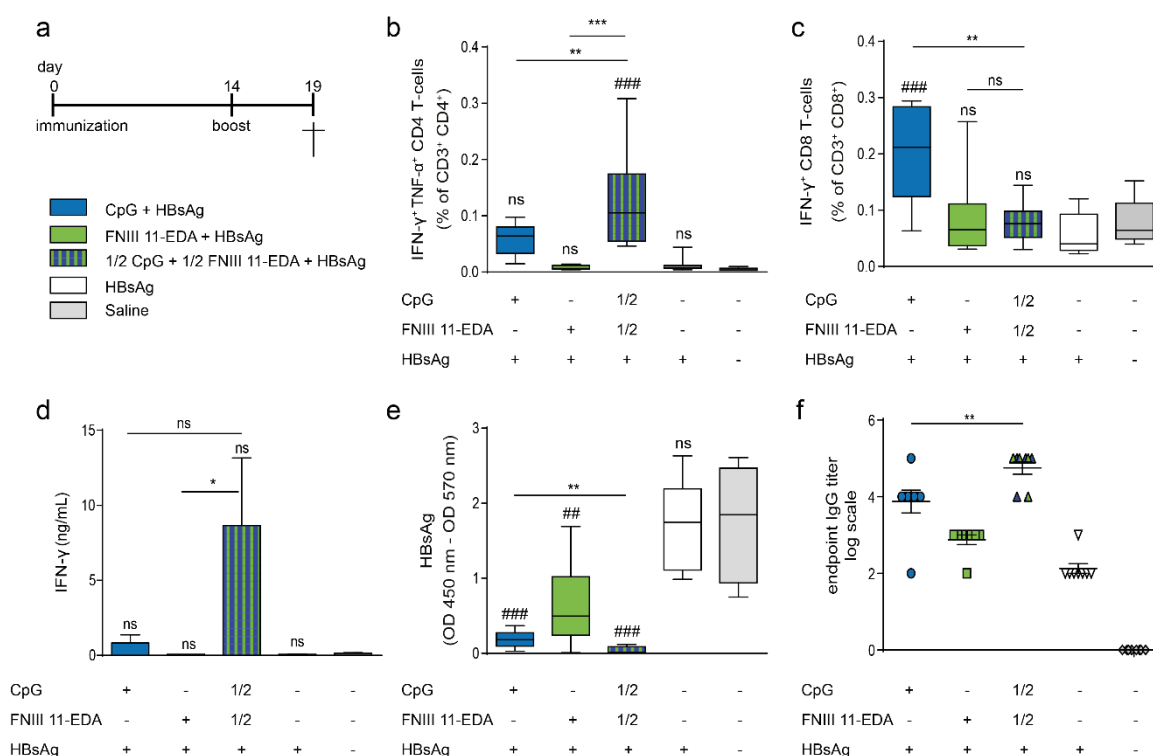
Figure 4. Co-injection of HBsAg adjuvanted with the two TLR agonists CpG and FNIII 11-EDA leads to enhanced production of inflammatory cytokines by T cells and HBsAg seroconversion. (a) Immunization schedule. HBV-Tg mice were immunized by intradermal injection in the four footpads with 10 µg HBsAg adjuvanted with 80 µg of CpG or 10 nmol of FNIII 11-EDA or 40 µg of CpG and 5 nmol of FNIII 11-EDA on day 0 and day 14. On day 19 mice were sacrificed and spleens, livers and blood were collected. (b,c) Frequency of IFN-γ$^+$TNF-α$^+$ splenocytes restimulated for 6 h *ex vivo* with HBsAg were evaluated by flow cytometry. The proportion of CD4$^+$ T cells producing IFN-γ and TNF-α was significantly improved by co-injection of half doses of both TLR agonists although a full dose of CpG alone yielded a higher amount of IFN-γ$^+$ CD8$^+$ T cells. (d) Magnitude of IFN-γ production from splenocytes restimulated *ex vivo* for 3 days with HBsAg were evaluated by ELISA; injection of half-doses of both adjuvants only marginally improved the production of IFN-γ compared to a full dose of CpG. (e) The concentration of HBsAg in the blood, as determined by ELISA (optical density), was significantly reduced in mice receiving the combinations of both adjuvants although all treatments were able to reduce the HBsAg concentration to some extent. (f) Endpoint titers of anti-HBsAg IgGs were all significantly higher than control in all groups. The combination of CpG and FNIII 11-EDA yielded the highest

titers of the responding groups. Naïve mice had no detectable level of anti-HBsAg IgGs. Box plots represent means ± 95% confidence interval (n = 8) from two independent experiments. *P < 0.05; **P < 0.01; ns, not significant; ##, ###, comparison to naïve group.

3.4 Discussion

Although the benefits of adjuvants towards improved vaccination safety and efficacy are indisputable, the perfect balance between activation of the immune system and side effects remains somewhat elusive. A possible strategy to achieve this desired balance would be the optimization of TLR agonist-based adjuvants[24]. In that regard, exploiting the ability of given pairs of TLR agonists to synergize to induce a stronger immune responses[18,20] would allow reduction of the amount of the adjuvant used in the vaccine. The TLR9 ligand CpG has proven to be an effective adjuvant[10] although safety issues arise when used at high doses[12]. The TLR4 agonist FNIII EDA and its variant FNIII 11-EDA, although not as strong as CpG, have nonetheless showed their ability to induce functional CD8$^+$ T cell responses without toxicity[13–15]. As co-activation of TLR4 and TLR9 has proved to be a promising immunotherapy strategy[21,25], we thus hypothesized that the combination of FNIII 11-EDA and CpG would induce an enhanced immune response while allowing the dose of the exogenous CpG to be kept at a low level.

In this study, we first wanted to verify the ability of CpG and FNIII 11-EDA to activate DCs in a synergistic manner (Fig. 1). Our results indeed show that activation of DCs was greatly enhanced in response to the co-stimulation with both adjuvants compared to stimulation with each of them separately, as shown by the secretion of

IL-12p70 (Fig. 1a), IL-6 (Fig. 1b) and TNF-α (Fig. 1c). The measured cytokines levels were frequently at least twice as high as sum of the values obtained by each TLR agonist alone, with near to 10-fold increases being observed for some combinations. These results are interesting as TLR synergies have been reported to rely heavily on activation of the TRIF and MyD88 pathways[17]. Although FNIII EDA constructs induce the production of TNF-α[13], which expression is strictly MyD88-dependent[26], the ability of FNIII 11-EDA to synergize with a TLR9 ligand indicate that the TRIF pathway is also probably activated. This suggests that FNIII 11-EDA signals through both TRIF and MyD88 and would have the potential to synergize with most TLR ligand[19].

To determine whether CpG and FNIII 11-EDA would synergize *in vivo* and induce an enhanced antigen-specific CD8$^+$ T cell response, we used OVA as a model antigen in a vaccination study. Effects of immunization with OVA alone, OVA adjuvanted with either full-dose CpG, full-dose of FNIII 11-EDA or combined half-doses of both adjuvants were compared (Fig. 2). Interestingly, combination of half doses of CpG and FNIII 11-EDA was able to induce a comparable amount of antigen-specific CD8$^+$ T cells to that obtained with a complete dose of CpG (Fig. 2b), while also leading to a higher quality response, as shown by the enhanced effector phenotype observed (Fig. 2c-e). Moreover it is especially remarkable that after *ex vivo* restimulation, the Th1-cytokine expression profile of CD4$^+$ T cells (Fig. 2c) induced by the combined half-doses was more than two-fold higher than the sum of the average frequency obtained with full doses of each adjuvant alone. A similar observation can be made on the average frequency of IFN-γ expressing-CD8$^+$ T cells (Fig. 2d,e) although these differences were much attenuated when observing secretion of IFN-γ from the total splenocytes population after 3 days of restimulation (Fig. 2f). These results show that the *in vitro*

observations of synergy between CpG and FNIII 11-EDA can be translated *in vivo* to induce a stronger or at least equivalent immune response while reducing the dose of CpG.

Both CpG and FNIII 11-EDA have shown separately their ability to induce efficient cellular immune responses in cell-killing assays[13,27]. Here we used the E.G7-OVA T cell lymphoma model to assess their ability to synergize to induce an effective anti-tumor CD8+ T cell response (Fig. 3). In this experiment, full doses of each adjuvant used separately were again compared to combined half-doses of both in their ability to control the growth of pre-established tumors. The half-dose of CpG without FNIII 11-EDA and full-dose FNIII 11-EDA used alone only slightly slowed tumor growth. Full dose CpG alone induced tumor regression, however growth resumed in all animals and none of them survived longer than 29 days. The majority of mice treated with both adjuvants together, however, lived longer than 33 days with one-third showing complete remission. It is also noteworthy that the tumor of more than half of the animals treated with both adjuvants temporarily regressed to undetectable levels before resuming growth, whereas only one out of ten tumors treated with CpG alone regressed to that level. It is possible that tumor escape in these animals was due to selective pressure leading to the appearance of OVA-free tumors cells[28]. In addition, it would be of interest to determine if increasing the number of injections would lead to complete remission of mice in the group treated with both adjuvants, as animals in these studies were treated only twice.

To demonstrate whether the cellular response induced by this synergy was sufficiently strong to overcome immune tolerance, we used HBV-Tg mice, which

express HBV and in which HBsAg, among others, is tolerized[22,23]. Here the total dose of each adjuvant was doubled compared to previous experiments, although the 2:1 ratio was conserved for single versus dual adjuvant comparison. In this model, the combination of CpG and FNIII 11-EDA enhanced the Th1 profile of the immune response both in the spleen and in the liver (Fig. 4b, S1b) compared to CpG, even though the frequency of expressing IFN-γ CD8^{+} T cells was unexpectedly significantly lower than that induced by CpG alone. However, such expression of IFN-γ was seemingly not antigen-specific, as unstimulated splenocytes showed similar results. Nevertheless, an antigen specific response was achieved as shown by the significantly reduced level of circulating HBsAg in the blood in mice treated with both adjuvants together compared to those treated with a single adjuvant (Fig. 4e). The fact that complete seroconversion was not achieved can be explain by the fact that HBV is replicated from an integrated transgene, which cannot be eliminated[23]. It is also interesting to note that a half dose of CpG used without FNIII 11-EDA was not sufficient to induce a significant reduction of the level of circulating HBsAg as shown in figure S1. Recent studies have demonstrated that the use of a second antigen, namely hepatitis B core antigen (HBcAg) was leading to stronger responses due to B cells help[29]. This strategy could further enhance our formulations.

Together these results clearly show that CpG and FNIII 11-EDA have the ability to synergize to break T cell tolerance and induce an enhanced antigen specific response. It is important that these improved effects were obtained while lowering the total dose of the foreign agent CpG, opening the door to the development of potent immunotherapies with fewer side effects and improved safety.

3.5 Methods

3.5.1 Reagents

Chemicals were obtained from Sigma-Aldrich. Low endotoxin grade OVA (<0.01 EU/µg protein) was used for immunization (Hyglos). PE-labeled H-2Kb/SIINFEKL pentamer was purchased from ProImmune. Pentamer staining was performed according to the manufacturer's instructions. CpG type-B 1826 oligonucleotide (5'-TCCATGACGTTCCTGACGTT-3') was purchased from Microsynth AG, and HBsAg from Prospec-Tany TechnoGene Ltd.

3.5.2 Recombinant proteins

FNIII 11-EDA fragment was cloned in a pET-22b (+) (Novagen) plasmid between the restriction sites NdeI and NotI. This plasmid contains a 6xHis-tag being added at the 3' end of the inserted genes. *E. coli* BL21DE3 were transformed and used for protein production. The recombinant proteins were purified using a HIStrap column (GE Healthcare) and washed using 0.1 % Triton X-100 in PBS for LPS removal and an ATP solution (2 mM ATP, 50 mM Tris-HCl, 10 mM $MgSO_4$, pH 7.4) for DnaK removal. An imidazole (1 M) buffer was used for elution. The proteins were then stored in tris-buffered saline (TBS) at -80 °C. Endotoxin levels were tested by Quantitative Chromogenic Limulus Amebocyte Lysate and were below 0.2 EU/µg.

3.5.3 *In vitro* stimulation of bone marrow-derived dendritic cells

Murine bone marrow-derived DCs were generated as described elsewhere[58]. On day 8, cells were plated at a density of 5×10^5 cells/well in DMEM supplemented with 10 % foetal bovine serum (FBS) and 1 % penicillin/streptomycin (PS) in 96-well plates. DCs were incubated for 6 h with 0, 0.5, 1 or 2 µM of CpG and/or recombinant FNIII 11-EDA. To block interactions with any potentially contaminating LPS, FNIII 11-EDA was pre-incubated with 10 µg/ml of polymixin B. Cytokines released in the supernatant were measured by ELISA (eBioscience).

3.5.4 Flow cytometry and ELISA

Blood was collected from the tail vein, and serum was separated by centrifugation and stored at -20 °C. Viable cells were detected by LIVE/DEAD (L/D) Fixable Aqua stain (Invitrogen) and the following antibodies were used for surface and intracellular staining: CD3ε Pacific Blue, CD4 FITC, CD8 APC-Cy7, IFN-γ APC, LAMP1 PE, TNF-α PE (eBioscience). For staining of blood, splenocytes, and liver cells, cells were exposed for 5 min at RT to 0.155 M NH_4Cl to lyse erythrocytes. The following staining steps were performed on ice. Cells were washed with PBS, stained for 15 min with Aqua L/D stain, resuspended in PBS with 2 % FBS for surface staining for 15 min and finally fixed for 15 min in PBS + 2 % PFA. IFN-γ intracellular staining was performed in PBS + 2 % FBS supplemented with 0.5 % Saponin. For antigen specificity, cells were stained with a SIINFEKL:H2Kb MHC-I pentamer (ProImmune). Flow cytometry measurements were performed using a CyAn ADP Analyzer (Beckman Coulter). Detection of HBsAg

and IFN-γ were performed using an HBsAg ELISA kit (AMS biotechnology, Abingdon, UK) and a Ready-Set-Go ELISA Kit (eBioscience), respectivel according to the manufacturers protocol.

3.5.5 Mice

C57BL/6J mice (aged 7-8 wk) were purchased from Harlan Laboratories (France). Chi 1.3.32 (line 1.3.32, on a C57BL/6J background) mice (HBV-Tg, aged 7-10 wk) replicating a 1.3 equivalent complete HBV genome were kindly provided by Dr. Didier Trono (Ecole Polytechnique Fédérale de Lausanne, EPFL)[22]. These mice replicate the virus at high levels in the liver and kidneys. As well, the levels of circulating HBsAg and viral particles in the serum of these mice are comparable to chronically infected humans. Both types of mice were kept under pathogen-free conditions at the animal facility of EPFL. All experiments were performed in accordance with Swiss law and with approval from the Cantonal Veterinary Office of Canton de Vaud, Switzerland.

3.5.6 *In vivo* antigen-specific T cell response

C57BL/6J mice were immunized by intradermal injection in the four footpads with a total dose of 50 µg OVA adjuvanted with 40 µg of CpG (referred to as full-dose CpG) or 5 nmol of FNIII 11-EDA (referred to as full-dose FNIII 11-EDA) or 20 µg of CpG and 2.5 nmol of FNIII 11-EDA combined on day 0 and day 14. On day 19 mice were

sacrificed and the spleen harvested for *ex vivo* restimulation and flow cytometry staining.

3.5.7 *Ex vivo* antigen-specific cell restimulation

Liver immune cells were isolated from hepatocytes by low speed spins, and debris were removed using a 37.5 % Percoll® (GE Healthcare) gradient. Splenocytes and liver cells were exposed for 5 min at RT to 0.155 M NH_4Cl to lyse erythrocytes. For antigen-specific restimulation, immune cells were cultured *in vitro* at 37 °C for 6 h in the presence of 40 µg/mL of HBsAg or 100 µg/mL of OVA in supplemented with 10 % FBS and 1 % PS (all from Invitrogen). After 3 h of *in vitro* restimulation, Brefeldin-A (5 µg/mL) was added and intracellular cytokine production was assessed by flow cytometry. Antigen-specific restimulation was also carried out over 3 days for measurement of secreted cytokines by ELISA.

3.5.8 Tumor growth assays

Tumor cells were implanted s.c. in the back at the level of the junction between the thoracic and lumbar vertebrae of C57BL/6J mice with inoculation of 10^6 E.G7-OVA cells in 30 µL PBS (Invitrogen). The mice were then treated when their tumor reached 50 ± 5 mm^3 and received a second injection of the treatment 6 days later. Mice were immunized by injection in the four footpads with a total dose of 50 µg OVA adjuvanted with 40 µg of CpG (referred to as full-dose CPG) or 5 nmol of FNIII 11-EDA (referred to

as full-dose FNIII 11-EDA) or 20 µg of CpG and 2.5 nmol of FNIII 11-EDA or 20 µg of CpG alone withoutFNIII 11-EDA. Tumors were measured 5 times per week and volumes were calculated as ellipsoids based on three orthogonal measures. Animal were killed when the tumor reached 1000 mm^3 or for humane reasons such as tumor necrosis, excessive loss of weight or evident isolation from the other animals in accordance with Swiss regulations.

3.5.9 Immunization of HBV-Tg mice

All experiments carried out with HBV-Tg mice were performed in P2 and P3 biosafety levels. Intradermal immunizations of mice were performed in the four footpads. Vaccine contained 10 µg HBsAg in 100 µl PBS adjuvanted with 80 µg of CpG (referred to as full-dose CpG) or 10 nmol of FNIII 11-EDA (referred as full-dose CpG) or 40 µg of CpG and 5 nmol of FNIII 11-EDA. Mice were immunized twice, on days 0 and 14. Mice were sacrificed on day 19 and blood, liver and spleen collected for *ex vivo* restimulation and flow cytometric analysis.

3.5.10 Data Analysis

All flow cytometry data were analyzed using FlowJo (TreeStar Inc.). Graphing and statistical analyses of worked-up data were performed using GraphPad Prism v.5. 1-way ANOVA with Bonferroni post-test was used for interpreting flow cytometry and ELISA data (***$P < 0.001$; **$P < 0.01$; *$P < 0.05$).

3.6 Supporting Information
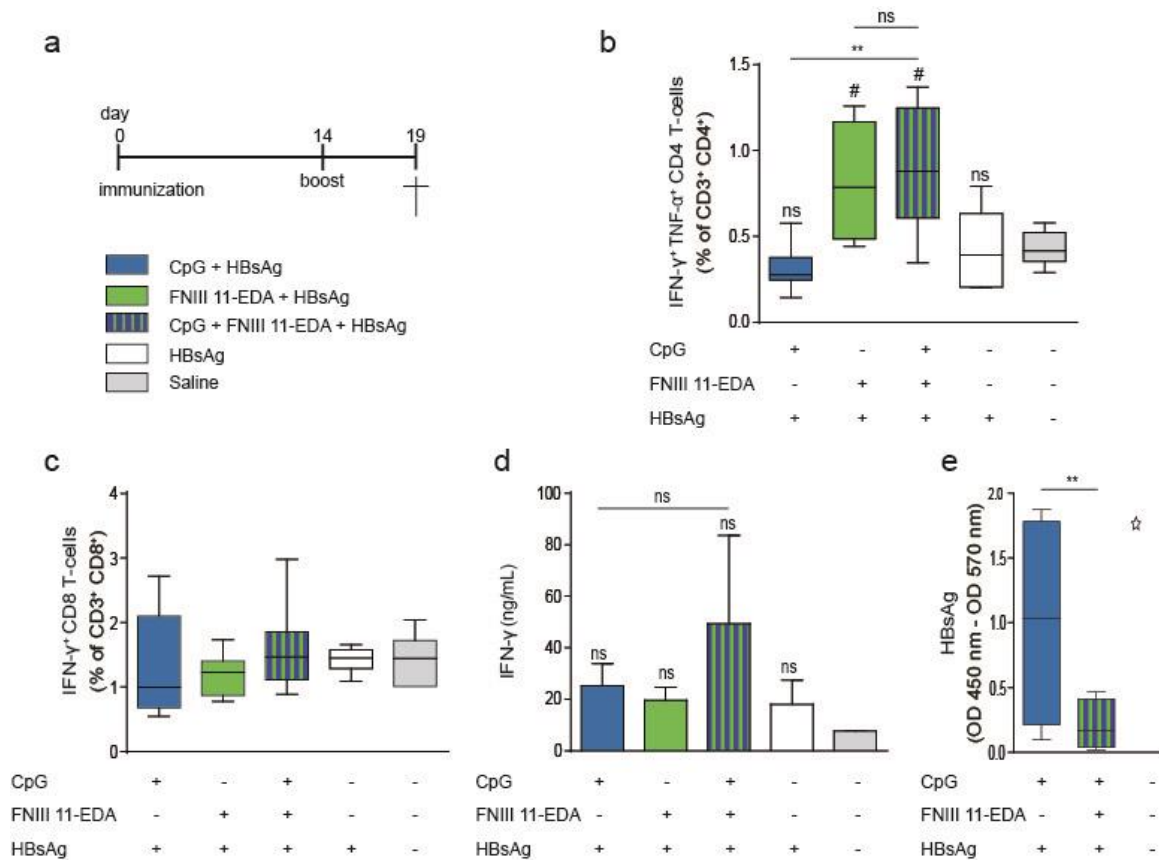
Figure S1. (a) Immunization schedule. HBV-Tg mice were immunized by intradermal injection in the four footpads with 10 μg HBsAg adjuvanted with 80 μg of CpG or 10 nmol of FNIII 11-EDA or 40 μg of CpG and 5 nmol of FNIII 11-EDA on day 0 and day 14. On day 19, mice were sacrificed and spleens, livers and blood were collected. (b) Frequencies of IFN-γ$^+$TNF-α$^+$ CD4$^+$ T cells from liver restimulated *ex vivo* for 6 h with HBsAg were evaluated by flow cytometry. Here the proportion of CD4$^+$ T cells producing IFN-γ and TNF-α was significantly improved by co-injection of half doses of both TLR agonists compared to a full dose of CpG alone although a full dose of FNIII 11-EDA yielded a comparable frequency of IFN-γ$^+$TNF-α$^+$ CD4$^+$ T cells. (c) Frequencies of IFN-γ$^+$ CD8$^+$ T cells restimulated for 6 h *ex vivo* with HBsAg were evaluated by flow cytometry (d) Magnitudes of IFN-γ production from liver T cells restimulated *ex vivo* for 3 days with HBsAg were evaluated by ELISA; injection of half-doses of both adjuvants only marginally improved the production of IFN-γ compared to a full dose of CpG. (e) A separate experiment where mice were vaccinated following the same schedule but with only 40 μg of CpG or 20 μg of CpG and 2.5 nmol of FNIII 11-EDA shows that 40 μg of CpG alone is not sufficient to achieve a HBsAg seroconversion. Box plots represent means ± 95% confidence interval (n = 8). *P < 0.05; **P < 0.01; ns, not significant; ##, ###, comparison to naïve group.

3.7 References

1. Brito, L. A. & O'Hagan, D. T. Designing and building the next generation of improved vaccine adjuvants. *J. Control. Release* **190,** 563–579 (2014).

2. Petrovsky, N. & Aguilar, J. C. Vaccine adjuvants: Current state and future trends. *Immunol. Cell Biol.* **82,** 488–496 (2004).

3. Marrack, P., McKee, A. S. & Munks, M. W. Towards an understanding of the adjuvant action of aluminium. *Nat. Rev. Immunol.* **9,** 287–293 (2009).

4. Batista-Duharte, A., Portuondo, D., Carlos, I. Z. & Pérez, O. An approach to local immunotoxicity induced by adjuvanted vaccines. *Int. Immunopharmacol.* **17,** 526–536 (2013).

5. Harandi, A. M., Medaglini, D. & Shattock, R. J. Vaccine adjuvants: A priority for vaccine research. *Vaccine* **28,** 2363–2366 (2010).

6. Wilson-Welder, J. H. *et al.* Vaccine adjuvants: Current challenges and future approaches. *J. Pharm. Sci.* **98,** 1278–1316 (2009).

7. Tagliabue, A. & Rappuoli, R. Vaccine adjuvants: the dream becomes real. *Hum. Vaccin.* **4,** 347–9 (2008).

8. Iwasaki, A. & Medzhitov, R. Toll-like receptor control of the adaptive immune responses. *Nat. Immunol.* **5,** 987–95 (2004).

9. De Nardo, D. Toll-like receptors: Activation, signalling and transcriptional modulation. *Cytokine* **74,** 181–189 (2015).

10. Krieg, A. M. CpG still rocks! Update on an accidental drug. *Nucleic Acid Ther.* **22,** 77–89 (2012).

11. de Titta, A. *et al.* Nanoparticle conjugation of CpG enhances adjuvancy for cellular immunity and memory recall at low dose. *Proc. Natl. Acad. Sci. U. S. A.* **110,** 19902–7 (2013).

12. Bode, C., Zhao, G., Steinhagen, F., Kinjo, T. & Klinman, D. M. CpG DNA as a vaccine adjuvant. *Expert Rev. Vaccines* **10,** 499–511 (2011).

13. Julier, Z., Martino, M. M., de Titta, A., Jeanbart, L. & Hubbell, J. A. The TLR4 Agonist Fibronectin Extra Domain A is Cryptic, Exposed by Elastase-2; use in a fibrin matrix cancer vaccine. *Sci. Rep.* **5,** 8569 (2015).

14. Lasarte, J. J. *et al.* The extra domain A from fibronectin targets antigens to TLR4-expressing cells and induces cytotoxic T cell responses in vivo. *J. Immunol.* **178,** 748–56 (2007).

15. Mansilla, C. *et al.* Immunization against hepatitis C virus with a fusion protein containing the extra domain A from fibronectin and the hepatitis C virus NS3 protein. *J. Hepatol.* **51,** 520–7 (2009).

16. Zhu, Q. *et al.* Toll-like receptor ligands synergize through distinct dendritic cell pathways to induce T cell responses: implications for vaccines. *Proc. Natl. Acad. Sci. U. S. A.* **105,** 16260–16265 (2008).

17. Bagchi, A. *et al.* MyD88-dependent and MyD88-independent pathways in synergy, priming, and tolerance between TLR agonists. *J. Immunol.* **178,** 1164–1171 (2007).

18. Napolitani, G., Rinaldi, A., Bertoni, F., Sallusto, F. & Lanzavecchia, A. Selected Toll-like receptor agonist combinations synergistically trigger a T helper type 1-polarizing program in dendritic cells. *Nat. Immunol.* **6,** 769–76 (2005).

19. Garcia-Cordero, J. L., Nembrini, C., Stano, A., Hubbell, J. A & Maerkl, S. J. A high-throughput nanoimmunoassay chip applied to large-scale vaccine adjuvant screening. *Integr. Biol.* **5,** 650–8 (2013).

20. Zhu, Q. *et al.* Using 3 TLR ligands as a combination adjuvant induces qualitative changes in T cell responses needed for antiviral protection in mice. *J. Clin. Invest.* **120,** 607–616 (2010).

21. De Nardo, D., De Nardo, C. M., Nguyen, T., Hamilton, J. A & Scholz, G. M. Signaling crosstalk during sequential TLR4 and TLR9 activation amplifies the inflammatory response of mouse macrophages. *J. Immunol.* **183,** 8110–8118 (2009).

22. Guidotti, L. G., Matzke, B., Schaller, H. & Chisari, F. V. High-level hepatitis B virus replication in transgenic mice. *J. Virol.* **69,** 6158–69 (1995).

23. Dembek, C. & Protzer, U. Mouse models for therapeutic vaccination against hepatitis B virus. *Med. Microbiol. Immunol.* **204,** 95–102 (2015).

24. Dunne, A., Marshall, N. A. & Mills, K. H. G. TLR based therapeutics. *Curr. Opin. Pharmacol.* **11,** 404–411 (2011).

25. Raman, V. S. *et al.* Applying TLR synergy in immunotherapy: implications in cutaneous leishmaniasis. *J. Immunol.* **185,** 1701–10 (2010).

26. Lin, X., Kong, J., Wu, Q., Yang, Y. & Ji, P. Effect of TLR4/MyD88 signaling pathway on expression of IL-1β and TNF-α in synovial fibroblasts from

temporomandibular joint exposed to lipopolysaccharide. *Mediators Inflamm.* **2015,** 329405 (2015).

27. Ali, O. A., Huebsch, N., Cao, L., Dranoff, G. & Mooney, D. J. Infection-mimicking materials to program dendritic cells in situ. *Nat. Mater.* **8,** 151–158 (2009).

28. Beaudette, T. T. *et al.* In vivo studies on the effect of co-encapsulation of CpG DNA and antigen in acid-degradable microparticle vaccines. *Mol. Pharm.* **6,** 1160–9 (2010).

29. Buchmann, P. *et al.* A novel therapeutic hepatitis B vaccine induces cellular and humoral immune responses and breaks tolerance in hepatitis B virus (HBV) transgenic mice. *Vaccine* **31,** 1197–1203 (2013).

Chapter 4

**The Extra Domain A of Fibronectin acts
as a growth factor-binding domain;
impairs wound healing**

4.1 Abstract

Fibronectin (FN) is an essential multidomain protein of the extracellular matrix (ECM) essential for numerous ECM-dependent processes. A splice variant of FN, the FN type III repeat extra domain A (FNIII EDA) still shows some functions that are not yet fully elucidated. Here, by screening a variety of growth factors (GF) and cytokines, we showed that FNIII EDA and its variant FNIII 11-EDA have the ability to bind certain signaling molecules, with PDGF-AA showing the strongest affinity. We then tested the ability of the FNIII 11-EDA-PDGF-AA complex to modulate fibroblasts proliferations and differentiation, suggesting a potential mild synergy between the two proteins. Finally, using a skin wound model, we explored how fibrin matrices functionalized with FNIII 11-EDA-containing FN fragments influence tissue repair outcome.

4.2 Introduction

Fibronectin (FN) is an essential component of the extracellular matrix (ECM). This multidomain glycoprotein is crucial in numerous ECM-dependent processes such as cell adhesion, migration, growth, and differentiation[1], with certain functions depending on the presence of the alternatively spliced type III repeat extra domain A (FNIII EDA). This alternatively spliced isoform of FN which is expressed during embryogenesis[2,3], within tumors[4,5], at sites of chronic inflammation[6–8] or in response to tissue damages[9,10], is known to bind integrins $\alpha 9\beta 1$, $\alpha 4\beta 1$ and $\alpha 4\beta 7$[10–12] and agonize Toll-like receptor 4 (TLR4)[13,14], however some functions of FNIII EDA are not yet fully elucidated.

Previous researches from our laboratory showed that FN binding could modulate the activity of GFs[15] and cytokines[16]. Interestingly, FNIII 12-13-14, which has been shown to have the ability to modulate the effects of vascular endothelial growth factor-A (VEGF-A) and platelet-derived growth factor (PDGF)-BB and bone morphogenetic protein-2 (BMP-2)[15], is the C-terminal neighboring domain of FNIII EDA (Fig. 1). Furthermore in addition to be FNIII EDA's expression sites, wounds and inflammation microenvironments[17] rich in GFs and cytokines, suggesting that FNIII EDA could modulate the activity of bound signaling proteins upon FN splicing. Moreover FNIII EDA is known to actively modulating the healing process[18] at sites of injury as skin wound healing in FNIII EDA$^{-/-}$ mice was shown to be abnormal[19], however its precise role within the healing process remains poorly understood.
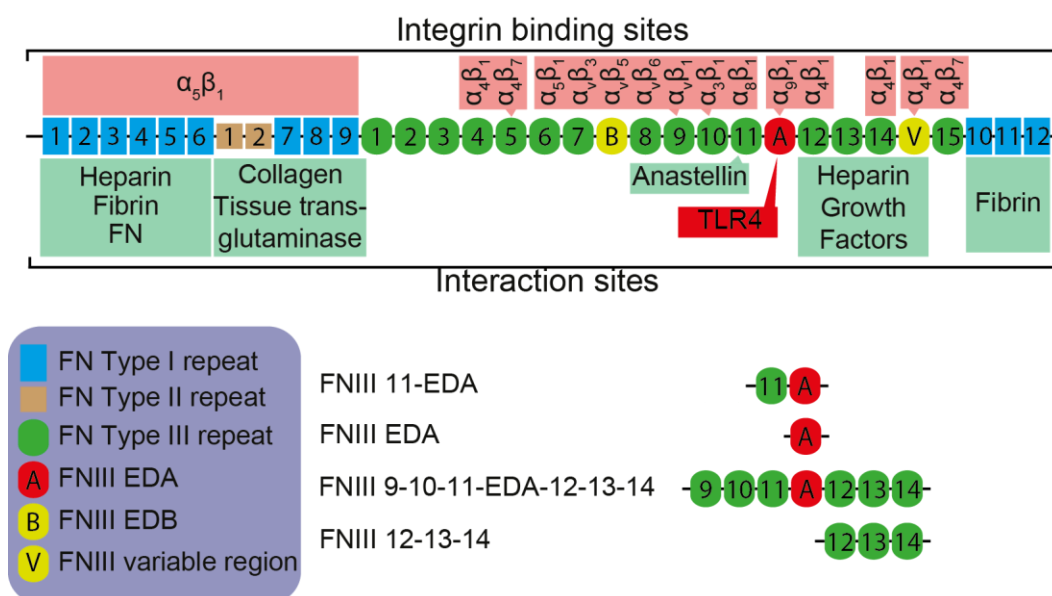
Fig. 1. Fibronectin structure. FNIII EDA-containing FN fragments produced and full length FN with some of its interaction sites displayed

Even though other domains of FN have been shown to bind growth factors (GF)[15,20] and cytokines[16] the ability of FNIII EDA to do so remains unexplored. Here we tested the binding of a wide library of GFs and cytokines to FNIII EDA. In order to represent more accurately the *in vivo* situation we also used a form of FNIII EDA N-terminally extended with the anastellin-binding[21] FNIII 11, FNIII 11-EDA, as FNIII EDA can be truncated at its C-terminus[22] (Chapter 2) but not at its N-terminus. Based on the results from the binding assays we then evaluated the ability of FNIII 11-EDA-GFs complexes to modulate fibroblasts proliferation and differentiation.

Finally, in order to better understand the role and function of FNIII EDA during tissue repair we used a skin wound model and treated the wounds with functionalized fibrin matrices creating a FNIII 11-EDA-rich microenvironment. As we showed in a previous study, the ability of FNIII EDA to agonize TLR4 is cryptic[22] and relies on a proteolytic cleavage by elastase 2 at its C-terminus to release its activity. We therefore

sought to understand whether any observed effect on the healing process would be dependent on the molecular context of FNIII EDA's position within the FN chain. Hence, we also tested the natural sequence FNIII 9-10-11-EDA-12-13-14 (Fig. 1) as well as the cleaved form FNIII 11-EDA + FNIII 12-13-14.

4.3 Results

4.3.1 Detection of GF and cytokines binding to FNIII 11-EDA

The capacity of FNIII 11-EDA to bind a wide panel of GFs and cytokines was assessed by ELISA (Fig. 2a). ELISA plates were coated with GFs and cytokines and incubated with FNIII 11-EDA. Bound FNIII 11-EDA was then detected with an anti-FNIII EDA antibody followed by an HRP-conjugated secondary antibody. Among all GFs and cytokines tested only placenta growth factor-2 (PlGF-2), PDGF-AA, PDGF-BB, stromal cell-derived factor-γ (CXCL12-γ or SDF-1 γ) and BMP-2 showed significant binding. PDGF-AA (A_{450nm} > 0.8) and CXCL12-γ (A_{450nm} > 0.6) in particular showed strong binding to FNIII 11-EDA. In order to verify that the observed binding was not due to FNIII 11 we repeated the experiment using FNIII EDA and tested its ability to bind PlGF-2, PDGF-AA, PDGF-BB, CXCL12-γ, BMP-2 and bovine serum albumin (BSA) as control. The binding observed in that case (Fig. 2b) was equivalent to the one observed with FNIII 11-EDA, thus confirming that the GFs and cytokines binding to FNIII 11-EDA does not depend on the presence of FNIII 11 domain.
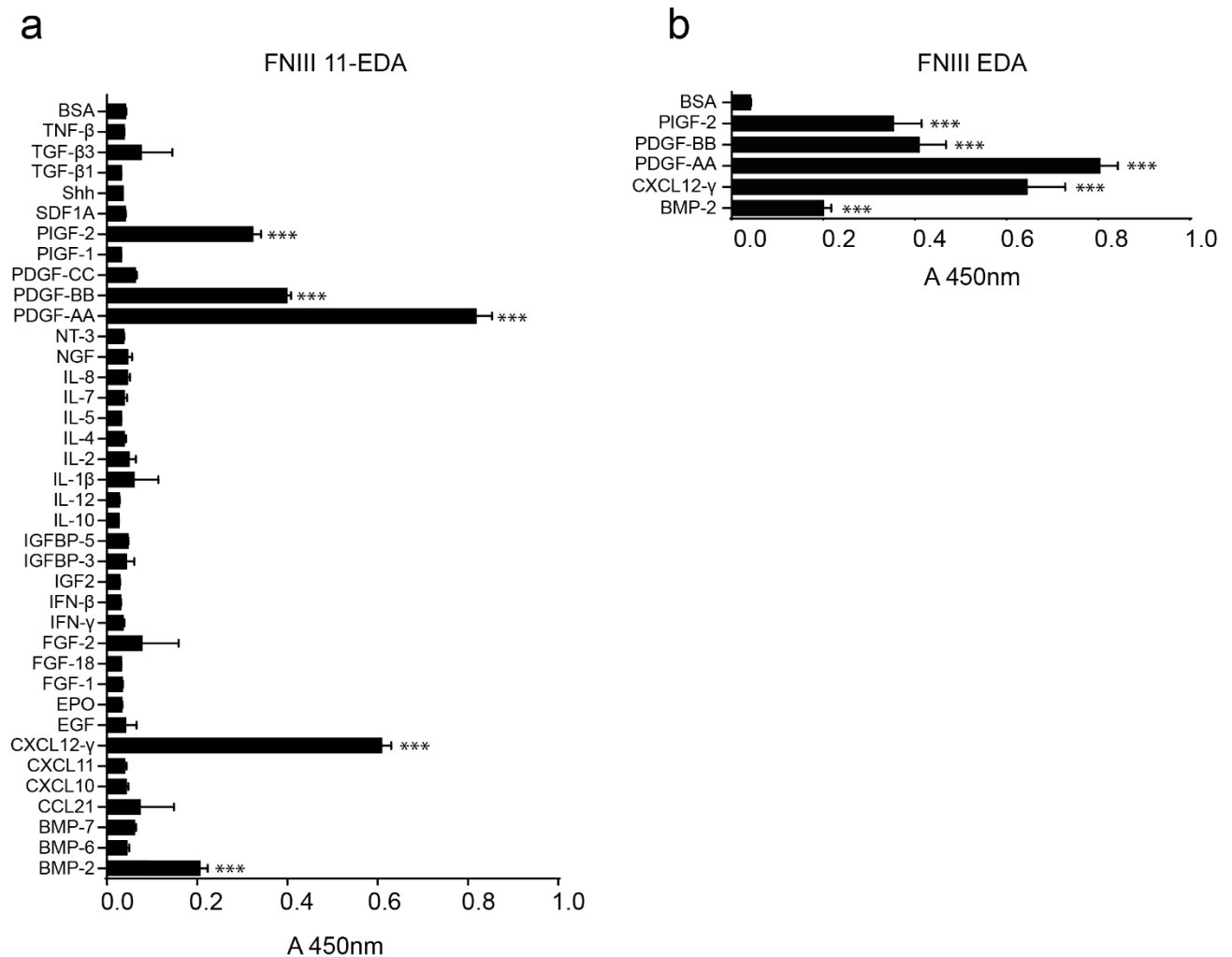
Fig. 2. Binding of GFs and cytokines to FNIII 11-EDA and FNIII EDA. (a) GF and cytokine binding to FNIII 11-EDA measured by ELISA. Only PlGF-2, PDGF-AA, PDGF-BB, CXCL12-γ and BMP-2 showed significant binding to FNIII 11-EDA. (b) Binding of BSA, PlGF-2, PDGF-AA, PDGF-BB, CXCL12-γ and BMP-2 to FNIII EDA measured by ELISA. Bars represent mean ± SEM (n=3) from two independent experiments. *** P< 0.001; comparison to BSA.

4.3.2 FNIII 11-EDA and PDGF-AA stimulate fibroblast proliferation and differentiation

We sought to understand whether the binding of PDGF-AA to FNIII 11-EDA could modulate its biological activity. PDGF-AA being known to stimulate fibroblast proliferation[23–25], we cultured 3T3 fibroblasts in normal media or in presence of FNIII 11-EDA or PDGF-AA or both and after 4 days cell proliferation was measured using alamarBlue (Fig. 3a) and cells were stained to assess differentiation by flow cytometry (Fig. 3b). Here FNIII 11-EDA alone did not stimulate fibroblast proliferation and PDGF-AA only marginally induced proliferation compared to the untreated control (Fig. 3a). However combination of both FNIII 11-EDA and PDGF-AA together significantly stimulated cell proliferation compared to the control although this effect was not statistically different to the one obtained using PDGF-AA alone (Fig. 3a). Furthermore, PDGF-AA and FNIII EDA have been reported to drive fibroblast differentiation to myofibroblasts[12,26], thus we observed whether the FNIII 11-EDA-PDGF-AA complex could enhance differentiation along with the proliferation. Differentiation of fibroblasts to myofibroblasts being characterized by expression of alpha-smooth muscle actin (α-SMA)[27], thus we stained the cells and measured their expression of α-SMA by flow cytometry (Fig. 3b). While only a marginal increase in α-SMA expression was observed upon stimulation with FNIII 11-EDA or PDGF-AA, the combination of both led to a significant increase in the expression of α-SMA compared to the untreated control group.
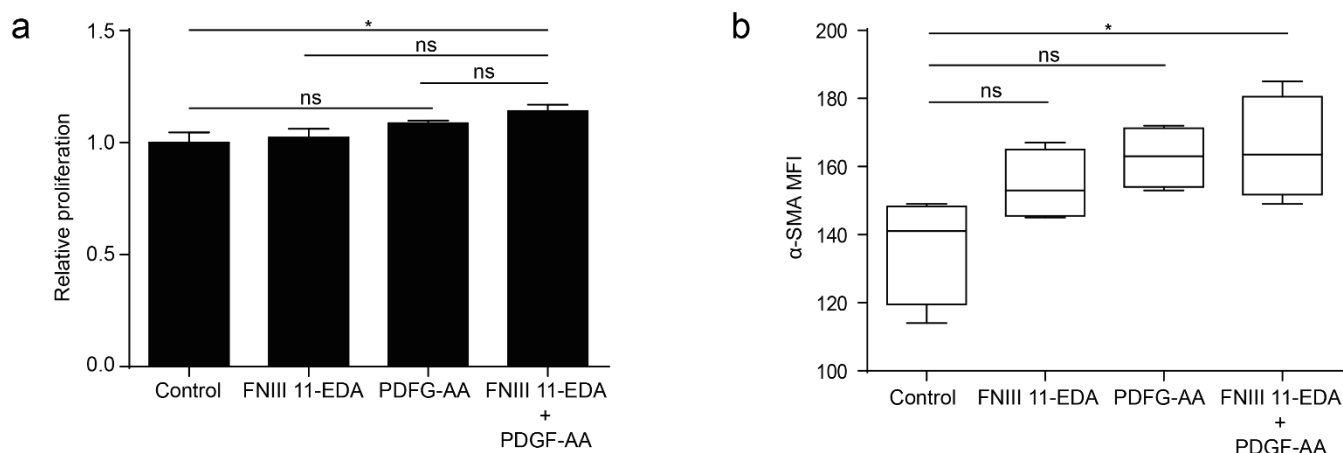
Fig. 3. FNIII 11-EDA and PDGF-AA induce fibroblast proliferation and differentiation. (a) Fibroblasts proliferation upon stimulation with FNIII 11-EDA and PDGF-AA. Fibroblasts were cultured in presence of FNIII 11-EDA or PDGF-AA or both. After 4 days cell proliferation was measured using alamarBlue. FNIII 11-EDA and PDGF-AA together significantly stimulated fibroblast proliferation. (b) Fibroblast differentiation to myofibroblasts upon stimulation with FNIII 11-EDA and PDGF-AA was evaluated by flow cytometry. Combination of FNIII 11-EDA and PDGF-AA induced differentiation of fibroblasts as shown by the mean fluorescence intensity (MFI) of α-SMA intracellular staining. Bars represent mean $\pm$ SEM. Box plots represent means $\pm$ 95% confidence interval (n = 4) from a single experiment. * P< 0.05; ns, not significant.

4.3.3 Fibrin matrices functionalized with FNIII 11-EDA-containing fibronectin fragments delay skin wound healing

We then explored whether the presence of FNIII 11-EDA at wound sites would influence the healing process and if this effect was dependent on the molecular context of FNIII 11-EDA. FNIII 11-EDA being naturally present in the ECM, we decided to incorporate the fragments bound in matrix to mimic the *in vivo* situation. Here, as a matrix model, we used a fibrin hydrogel with a volume of 80 μL and a concentration of 10 mg/mL of fibrinogen. To be incorporated in the matrix, the FN fragments were designed to contain a transglutaminase substrate sequence derived from α_2-plasmin inhibitor (NQEQVSPL, denoted herein TG) at the N-terminus. Therefore, the FN

102

fragments were covalently incorporated in the matrix through the transglutaminase activity of factor XIIIa during fibrin polymerization[28]. To determine whether the molecular context of FNIII 11-EDA could modulate its effect on wound closure, we also tested fibrin matrix compositions containing either FNIII 9-10-11-EDA-12-13-14 which is the natural FN chain within which FNIII EDA is located, or with FNIII 11-EDA and FNIII 12-13-14 as separate molecules, which occurs upon cleavage by elastase 2 secreted by neutrophils, releasing the immunological activity of FNIII 11-EDA[22]. In order to determine whether any observed effect by the matrices functionalized with FN fragments was due to TLR4 agonization, fibrin matrices loaded with an amount of LPS corresponding to the level of TLR4 activation by the dose FNIII 11-EDA[22] used in the other matrices were also tested.

Full-thickness back-skin wounds were treated with the fibrin matrices and wound histology was analyzed after 7 days. Interestingly wounds that received fibrin matrices containing any forms of FNIII 11-EDA all showed a delay in re-epithelization, reaching statistical significance in the case of FNIII 11-EDA + FNIII 12-13-14 (Fig. 4a). However, observation of the granulation tissue area showed statistical equivalence among all groups (Fig. 4b) although the matrices containing only fibrin induced slightly larger granulation area than any other group. Surprisingly fibrin matrices loaded with LPS yielded the smallest granulation area. Representative wound histology for all groups are shown in Fig. 4c.
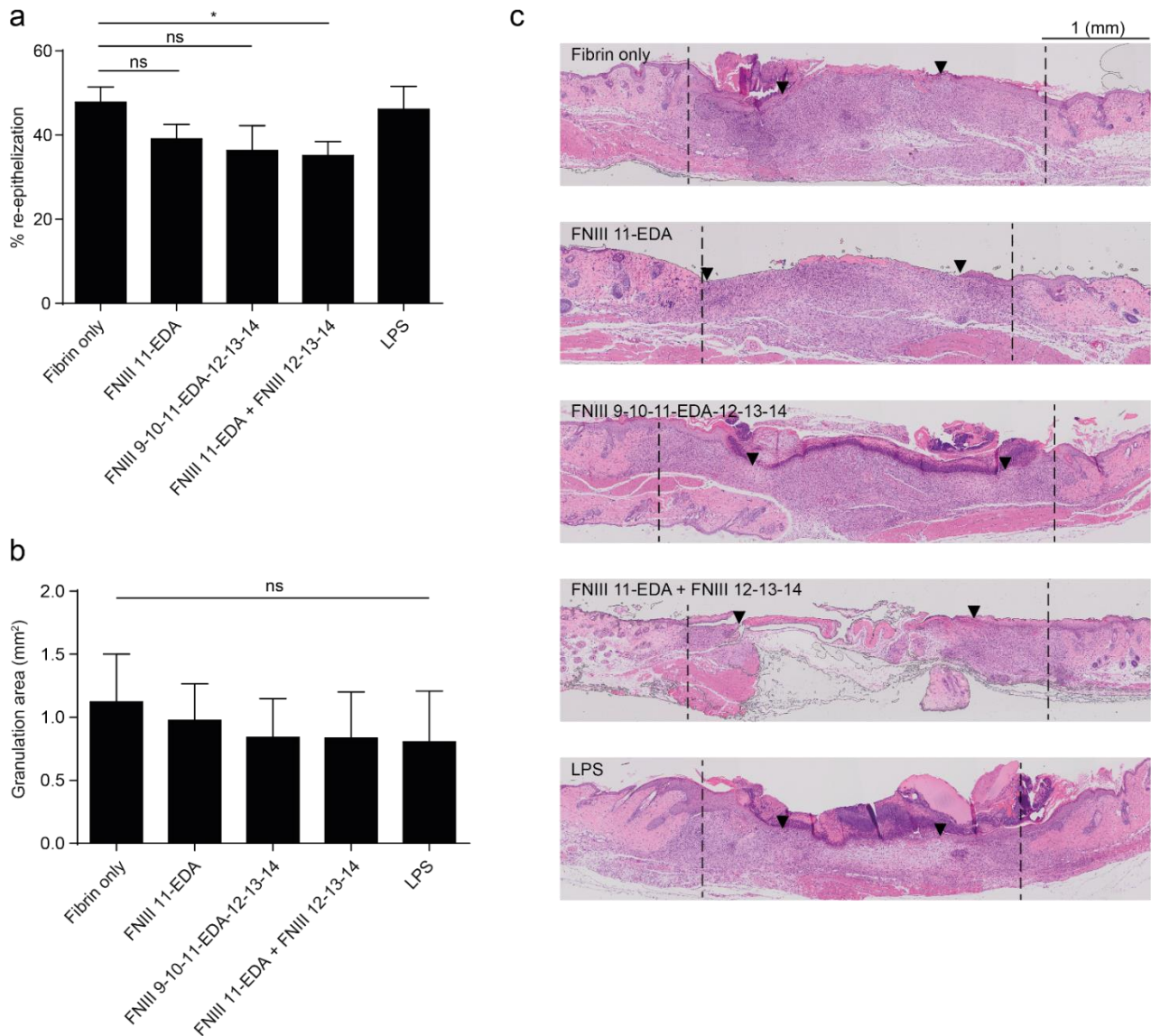
Fig. 4. Treatment of skin wounds with fibrin matrices functionalized with FNIII 11-EDA + FNIII 12-13-14 delays re-epithelization. Full-thickness back-skin wounds (6 mm in diameter) were treated with fibrin matrices functionalized with fibronectin fragments. After 7 days wound closure (a) and granulation tissue (b) formation were evaluated by histology. (c) Representative histology at 7 days (hematoxylin and eosin staining). Dashed lines indicate wound edges; black arrows indicate tips of the healing epithelium tongue. Bars represent mean ± SEM. (n = 4-6) from a single experiment. * P< 0.05; ns, not significant.

4.4 Discussion

Although expression of FNIII EDA is essential for embryonic development[29] some of its functions are not yet fully understood. A splice variant of FN, FNIII EDA is expressed during embryogenesis[2,3] and later upon tissue damages[9,10] or within tumors[4,5] and chronic inflammation[6–8] sites. Furthermore many recent studies regarding FNIII EDA explored its ability to agonize TLR4 and sustain inflammation[22,30] or drive fibrosis[31]. However, although the interactions between many domains of FN, including FNIII EDA's neighboring domain FNIII 12-13-14, and GFs and cytokines are well documented[15,16,20,32], the ability of FNIII EDA to bind signaling molecules remains mostly unexplored. FNIII EDA also actively modulates the healing process[18] at sites of injury as shown by abnormal skin wound healing in FNIII EDA$^{-/-}$ mice[19], however its precise role within the healing process remains poorly understood.

We showed in a previous study the cryptic nature of FNIII EDA[22], its ability to agonize TLR4 being enhanced upon cleavage of FN by elastase 2. In the same study we showed that although the C-terminus of FNIII EDA can be exposed by proteolysis, no evidence suggests that an N-terminally exposed FNIII EDA can occur *in vivo*. Furthermore, we showed that N-terminal extension of FNIII EDA with FNIII 11 is necessary in order to retain its full ability to agonize TLR4. For these reason FNIII 11-EDA was used in place of FNIII EDA in the present study.

Due to FNIII EDA's placement within the FN chain (Fig. 1) next to the GF-binding domain FNIII 12-13-14 in addition to its expression in GF- and cytokine-rich microenvironments[17], we hypothesized that FNIII EDA could bind and modulate the

activity of bound signaling proteins upon FN splicing. Here we tested the binding of multiple GFs and cytokines to FNIII 11-EDA (Fig. 2a) and FNIII EDA (Fig. 2b), with PlGF-2, PDGF-AA, PDGF-BB, CXCL12-γ and BMP-2 showing significant binding. Surprisingly, although the number of GFs binding FNIII 11-EDA is limited, these GFs come from three different families, the vascular endothelial growth factor (VEGF) family (PlGF-2), the PDGF family (PDGF-AA, PDGF-BB) and the transforming growth factor β (TGF-β) family (BMP-2). CXCL12-γ is a chemokine located in the heart and brain associated with chronic inflammation[33].

The strong binding to PDGF-AA is particularly intriguing. Indeed, although FN devoid of FNIII EDA already showed the ability to bind these four GFs, PDGF-AA showed the lowest affinity for FN[32]. We sought to investigate whether FNIII 11-EDA could modulate the activity of PDGF-AA on fibroblasts proliferation and differentiation to myofibroblasts. Although PDGF-AA is a known mitogen for fibroblast[23–25], it was not able in our case to stimulate a significant fibroblast proliferation *in vitro* on its own (Fig. 3a). The FNIII 11-EDA-PDGF-AA complex however did significantly stimulate fibroblast proliferation compared to the untreated control (Fig. 3a). Furthermore, when used alone both FNIII 11-EDA and PDGF-AA marginally induced fibroblast differentiation to myofibroblasts, whereas the FNIII 11-EDA-PDGF-AA complex was able to drive significant differentiation as shown by the increased expression of α-SMA (Fig. 3b). These results suggest that FNIII 11-EDA modulates the effect of PDGF-AA on fibroblast proliferation and differentiation, although the lack of statistical significance between the effect of PDGF-AA alone and the FNIII 11-EDA-PDGF-AA complex keeps the door open to the possibility that the observed effect could be merely the additive effect of FNIII 11-EDA and PDGF-AA. Furthermore, fibroblast 3T3 being relatively fast to

proliferate, slow growing primary fibroblasts might be a better option to repeat this experiment.

Interestingly, the PDGF-AA-driven fibroblast to myofibroblasts differentiation has been reported to be a promoter of wound closure[26]. Moreover lack of FNIII EDA leads to abnormal wound healing as shown in FNIII EDA^{-/-} mice[19], suggesting that FNIII EDA actively modulates the healing process[18] although its precise function during tissue repair remains unknown. Thus, in order to better characterize the effect of FNIII EDA on wound closure, we used a skin wound model in which wounds were treated with functionalized fibrin matrices creating a microenvironment rich in FNIII EDA-containing FN fragments. Here, in order to assess whether the any observed effect would be proteolysis-dependent[22], we compared fibrin matrices functionalized with FNIII 11-EDA to matrices functionalized with the longer natural sequence FNIII 9-10-11-EDA-12-13-14 or with the cleaved form FNIII 11-EDA and FNIII 12-13-14 on different molecules. Surprisingly after 7 days all FNIII EDA-containing fibrin matrices compositions impaired re-epithelization to some extent compared to matrices containing only fibrin (Fig. 4a,c) although this effect was greater with FNIII 11-EDA and FNIII 12-13-14 on separate molecules. Interestingly LPS-containing fibrin matrices did not influence re-epithelization, suggesting that that the effect observed with FNIII EDA-containing matrices is likely not due to TLR4 agonization. Moreover, all matrices compositions slightly reduced the granulation tissue area (Fig. 4b,c). These surprising results suggest that an FNIII 11-EDA-rich microenvironment impairs wound healing and that this effect is accentuated upon FN cleavage by elastase 2. However, these results should be interpreted with caution given that only one endpoint was used for the experiment. As FNIII EDA is induced by TGF-β1[34], which reaches maximum expression 72h post-

wounding[35], it would be also of interest to include different timepoints for the beginning of the treatments. Furthermore, the natural wound healing process involves the formation of fibrin-plasma fibronectin matrix immediately after injury[36], with FNIII EDA-containing fibronectin appearing only after 2 days. This could suggest that FNIII EDA would be beneficial to the healing process only when applied on the wound after a couple days.

In conclusion, we showed that FNIII EDA is yet another GF binding domain of FN, with an especially strong affinity for PDGF-AA. FNIII 11-EDA and PDGF-AA showed the ability to enhance fibroblasts proliferation and differentiation into myofibroblasts although more experiment are required to further investigate a potential synergy between these proteins. Fibrin matrices functionalized with variants of FNIII 11-EDA had surprisingly negative effect on wound closure, however here again more experiment will be required to precisely characterize how FNIII EDA affects tissue repair. In that regard, it would be of special interest to explore how PDGF-AA delivered in a FNIII 11-EDA-containing fibrin gel would influence wound healing.

4.5 Methods

4.5.1 Recombinant proteins

Fibronectin fragments were engineered to bear at their N-terminus the coagulation transglutaminase Factor XIIIa peptide substrate NQEQVSPL (TG) and were cloned in a pET-22b (+) (Novagen) plasmid between the restriction sites NdeI and NotI.

This plasmid contains a 6xHis-tag being added at the 3' end of the inserted genes. *E. coli* BL21DE3 were transformed and used for protein production. The recombinant proteins were purified using a HIStrap column (GE Healthcare) and washed using 0.1 % Triton X-100 in PBS for LPS removal and an ATP solution (2 mM ATP, 50 mM Tris-HCl, 10 mM MgSO4, pH 7.4) for DnaK removal. An imidazole (1 M) buffer was used for elution. The proteins were then stored in TBS pH 7.4 at -80°C. Endotoxin levels were tested by Quantitative Chromogenic Limulus Amebocyte Lysate and were below 0.2 EU/µg.

4.5.2 Growth factors and cytokines

All GFs were purchased in their mature forms, highly pure (> 95% pure), carrier free and lyophilized. PDGF-DD, and BMP-2 were purchased from R&D Systems. FGF-2 were purchased from Invitrogen. CCL21, CXCL10, CXCL11, CXCL12-γ, FGF-1, FGF-18, BMP-7, TGF-β1, TGF-β2, TGF-β3, EGF, IL-2, IL-4, IL-5, IL-7, IL-8, IL-10, IL-12, PDGF-AA, PDGF-AB, PDGFCC, PlGF-1, PlGF-2, IGF-2, NGF and NT-3 were purchased from PeproTech EC Ltd. Except TGF-β1, TGF-β2, TGF-β3, BMP-2, BMP-6 and BMP-7 that have been produced in eukaryotic cells, the other GFs were produced in *E. coli* and therefore were not glycosylated. All GFs were reconstituted and stored according to the provider's instructions, in order to regain full activity and no loss of protein.

4.5.3 Detection of GF and cytokine binding to FNIII 11-EDA

ELISA plates (Nunc MaxiSorp, Thermo Fisher Scientific) were coated with 50 nM GFs (in PBS, 1 h at 37°C) and blocked with 2 % bovine serum albumin (BSA) in phosphate buffer saline (PBS) with 0.05 % Tween 20 (PBS-T) for 1 h at RT. Then, wells were washed with PBS-T and further incubated with 10 nM of FNIII 11-EDA in PBS-T with 0.1 % BSA; 45 min at RT. After 3 washes with PBS-T, wells were incubated for 45 min at RT with anti-FNIII EDA (abcam, IST-9) antibody followed by an HRP-conjugated goat anti-mouse IgG1 secondary antibody (SouthernBiotech). After washes, antibody was detected with tetramethylbenzidine substrate by measurement of the absorbance at 450 nm.

4.5.4 Proliferation of fibroblasts

Swiss 3T3 fibroblasts were plated at 10^4 per well in 24-well plates containing DMEM medium with 10 % FBS and incubated for 4 days with 150 ng/mL FNIII 11-EDA or 100 ng/mL PDGF-AA or both. On day 4 alamarBlue (ThermoFisher scientific) was added to the media according to manufacturer's recommendations followed by incubation for 3 h. 100 µl of the media was then transferred to a 96-well plate and fibroblast proliferation was measured by light absorption at 570 nm.

4.5.5 Flow cytometry

Flow cytometry measurements were performed using a CyAn ADP Analyzer (Beckman Coulter) and data were analyzed using FlowJo software. Viable cells were

detected by LIVE/DEAD (L/D) Fixable Aqua stain (Invitrogen) and an anti- α-SMA FITC

(abcam) antibody was used for surface and intracellular staining. The following staining

steps were performed on ice. Cells were washed with PBS, stained for 15 min with Aqua

L/D stain, resuspended in PBS + 2 % FBS for surface staining for 15 min and finally fixed

for 15 min in PBS + 2 % PFA. Intracellular staining was performed in PBS + 2 % FBS

supplemented with 0.5 % saponin.

4.5.6 Skin wound model

C57BL/6 male mice were 10 to 12 weeks old at the beginning of the experiment.

Their backs were shaved and two full-thickness punch-biopsy wounds (6 mm in

diameter) were created in each mouse. Directly after, fibrin matrices (80 µl, 10 mg/ml

fibrinogen, 2 U/ml of thrombin, 4 U/ml of factor XIII, 5 mM CaCl2) empty or containing

1 nmol of FNIII 9-10-11-EDA-12-13-14 or FNIII 11-EDA with or without 1 nmol of FNIII

12-14 or 200 ng of LPS were polymerized on the wounds. The wounds were then

covered with adhesive film dressing (Hydrofilm, Hartmann). After 7 days, mice were

sacrificed and the wounds were harvested for histological analysis.

4.5.7 Histological analysis

An area of 8 mm in diameter, which includes the complete epithelial margins,

was excised. Wounds were cut on one edge and embedded. Histological analyses were

performed on serial sections (4µm paraffin sections) until reaching the central portion

of the wound. The extent of re-epithelialization and granulation tissue formation was measured by histomorphometric analysis of tissue sections (H&E stain) using ImageJ software. For analysis of re-epithelialization: the distance that the epithelium had traveled across the wound was measured; the muscle edges of the panniculus carnosus were used as indicator for the wound edges; re-epithelialization was calculated as the percentage of the distance of edges of the panniculus carnosus muscle. For granulation tissue quantification: the area covered by a highly cellular tissue was determined in order to obtain the area at the center of the wound.

4.5.8 Statistical Analysis

Statistical analysis were performed using 1-way analysis of variance (ANOVA) and Bonferonni posttest using GraphPad Prism v.5.

4.6 References

1. Pankov, R. & Yamada, K. M. Fibronectin at a glance. *J. Cell Sci.* **115,** 3861–3863 (2002).

2. ffrench-Constant, C. Alternative splicing of fibronectin--many different proteins but few different functions. *Exp. Cell Res.* **221,** 261–71 (1995).

3. ffrench-Constant, C. & Hynes, R. O. Alternative splicing of fibronectin is temporally and spatially regulated in the chicken embryo. *Development* **106,** 375–88 (1989).

4. Rybak, J. N., Roesli, C., Kaspar, M., Villa, A. & Neri, D. The extra-domain A of fibronectin is a vascular marker of solid tumors and metastases. *Cancer Res.* **67,** 10948–57 (2007).

5.   Villa, A. *et al.* A high-affinity human monoclonal antibody specific to the alternatively spliced EDA domain of fibronectin efficiently targets tumor neo-vasculature in vivo. *Int. J. Cancer* **122,** 2405–13 (2008).

6.   McFadden, J. P., Baker, B. S., Powles, A. V. & Fry, L. Psoriasis and extra domain A fibronectin loops. *Br. J. Dermatol.* **163,** 5–11 (2010).

7.   McFadden, J., Fry, L., Powles, A. V. & Kimber, I. Concepts in psoriasis: psoriasis and the extracellular matrix. *Br. J. Dermatol.* **167,** 980–6 (2012).

8.   McFadden, J. P., Baker, B. S., Powles, A. V. & Fry, L. Psoriasis and streptococci: postscript regarding extra domain A fibronectin. *Br. J. Dermatol.* **161,** 706–7 (2009).

9.   Jarnagin, W. R., Rockey, D. C., Koteliansky, V. E., Wang, S. S. & Bissell, D. M. Expression of variant fibronectins in wound healing: cellular source and biological activity of the EIIIA segment in rat hepatic fibrogenesis. *J. Cell Biol.* **127,** 2037–48 (1994).

10.   Liao, Y. F., Gotwals, P. J., Koteliansky, V. E., Sheppard, D. & Van De Water, L. The EIIIA segment of fibronectin is a ligand for integrins alpha 9beta 1 and alpha 4beta 1 providing a novel mechanism for regulating cell adhesion by alternative splicing. *J. Biol. Chem.* **277,** 14467–74 (2002).

11.   Shinde, A. V. *et al.* Identification of the peptide sequences within the EIIIA (EDA) segment of fibronectin that mediate integrin alpha9beta1-dependent cellular activities. *J. Biol. Chem.* **283,** 2858–70 (2008).

12.   Kohan, M., Muro, A. F., White, E. S. & Berkman, N. EDA-containing cellular fibronectin induces fibroblast differentiation through binding to alpha4beta7 integrin receptor and MAPK/Erk 1/2-dependent signaling. *FASEB J.* **24,** 4503–4512 (2010).

13.   Saito, S. *et al.* The fibronectin extra domain A activates matrix metalloproteinase gene expression by an interleukin-1-dependent mechanism. *J. Biol. Chem.* **274,** 30756–63 (1999).

14.   Okamura, Y. *et al.* The extra domain A of fibronectin activates Toll-like receptor 4. *J. Biol. Chem.* **276,** 10229–33 (2001).

15.   Martino, M. M. *et al.* Engineering the growth factor microenvironment with fibronectin domains to promote wound and bone tissue healing. *Sci. Transl. Med.* **3,** 100ra89 (2011).

16.   Tortelli, F., Pisano, M., Briquez, P. S., Martino, M. M. & Hubbell, J. A. Fibronectin Binding Modulates CXCL11 Activity and Facilitates Wound Healing. *PLoS One* **8,** 1–11 (2013).

17.   Barrientos, S., Stojadinovic, O., Golinko, M. S., Brem, H. & Tomic-Canic, M. Growth factors and cytokines in wound healing. *Wound Repair Regen.* **16,** 585–601 (2008).

18.   To, W. S. & Midwood, K. S. Plasma and cellular fibronectin: distinct and independent functions during tissue repair. *Fibrogenesis Tissue Repair* **4,** 21 (2011).

19.   Muro, A. F. *et al.* Regulated splicing of the fibronectin EDA exon is essential for proper skin wound healing and normal lifespan. *J. Cell Biol.* **162,** 149–60 (2003).

20.   Martino, M. M. & Hubbell, J. A. The 12th-14th type III repeats of fibronectin function as a highly promiscuous growth factor-binding domain. *FASEB J.* **24,** 4711–21 (2010).

21.   Ohashi, T. & Erickson, H. P. Domain unfolding plays a role in superfibronectin formation. *J. Biol. Chem.* **280,** 39143–51 (2005).

22.   Julier, Z., Martino, M. M., de Titta, A., Jeanbart, L. & Hubbell, J. A. The TLR4 Agonist Fibronectin Extra Domain A is Cryptic, Exposed by Elastase-2; use in a fibrin matrix cancer vaccine. *Sci. Rep.* **5,** 8569 (2015).

23.   Seikrit, C. *et al.* Biological responses to PDGF-AA versus PDGF-CC in renal fibroblasts. *Nephrol. Dial. Transplant.* **28,** 889–900 (2013).

24.   Bonner, J. C., Osornio-Vargas, A. R., Badgett, A. & Brody, A. R. Differential proliferation of rat lung fibroblasts induced by the platelet-derived growth factor-AA, -AB, and -BB isoforms secreted by rat alveolar macrophages. *Am. J. Respir. Cell Mol. Biol.* **5,** 539–547 (1991).

25.   Simm, A., Nestler, M. & Hoppe, V. PDGF-AA, a potent mitogen for cardiac fibroblasts from adult rats. *J. Mol. Cell. Cardiol.* **29,** 357–368 (1997).

26.   M, D. *et al.* An Essential Role for Senescent Cells in Optimal Wound Healing through Secretion of PDGF-AA. *Dev. Cell* **31,** 722–733 (2014).

27.   Serini, G. & Gabbiani, G. Mechanisms of myofibroblast activity and phenotypic modulation. *Exp. Cell Res.* **250,** 273–283 (1999).

28.   Schense, J. C. & Hubbell, J. A. Cross-linking exogenous bifunctional peptides into fibrin gels with factor XIIIa. *Bioconjug. Chem.* **10,** 75–81 (1999).

29.   Astrof, S., Crowley, D. & Hynes, R. O. Multiple cardiovascular defects caused by the absence of alternatively spliced segments of fibronectin. *Dev. Biol.* **311,** 11–24 (2007).

30.   Fullard, N. & O'Reilly, S. Role of innate immune system in systemic sclerosis. *Semin. Immunopathol.* **37,** 511–7 (2015).

31.   Bhattacharyya, S. *et al.* FibronectinEDA promotes chronic cutaneous fibrosis through Toll-like receptor signaling. *Sci. Transl. Med.* **6,** 232ra50 (2014).

32.   Martino, M. M. *et al.* Growth factors engineered for super-affinity to the extracellular matrix enhance tissue healing. *Science* **343,** 885–8 (2014).

33.   Janowski, M. Functional diversity of SDF-1 splicing variants. *Cell Adhes. Migr.* **3,** 243–249 (2009).

34.   Serini, G. *et al.* The fibronectin domain ED-A is crucial for myofibroblastic phenotype induction by transforming growth factor-β1. *J. Cell Biol.* **142,** 873–881 (1998).

35.   Bryan, D., Walker, K. B., Ferguson, M. & Thorpe, R. Cytokine gene expression in a murine wound healing model. *Cytokine* **31,** 429–38 (2005).

36.   Lenselink, E. a., 2013. Role of fibronectin in normal wound healing. Int. Wound J. 313–316. doi:10.1111/iwj.12109

Chapter 5

Conclusion

The extracellular matrix (ECM) protein fibronectin (FN) is a remarkably polyvalent molecule essential for processes such as cell adhesion, migration, growth, and differentiation[1]. Nevertheless, some functions of FN are not yet understood. The alternatively spliced type III repeat extra domain A (FNIII EDA) shows the ability to stimulate the immune system through agonization of Toll-like receptor 4 (TLR4)[2] and to modulate wound healing[3]. However, the exact physiological roles FNIII EDA carries out during these processes remain enigmatic.

In chapter 2 of this thesis we revealed that the TLR4 agonizing potential of FNIII EDA is cryptic, becoming exposed by proteolytic cleavage by elastase 2, secreted by neutrophils, between FNIII EDA and FNIII 12. Moreover, we showed that the ability of FNIII EDA to trigger an antigen-specific immune response is enhanced when it is delivered in an ECM-like microenvironment, which correlates with the observation that FNIII EDA is usually expressed in the cellular form of FN. Furthermore, FNIII EDA and TLR4 activation contribute to the progression of diseases characterized by neutrophil infiltration such as psoriasis[4] or scleroderma[5]. Thus, the creation of strong TLR4-agonizing microenvironment by neutrophil-derived elastase 2-mediated proteolysis of FN could be part of the underlying mechanism contributing to the progression of these pathologies. In addition, we showed, using two tumor growth models, the ability of ECM-bound FNIII EDA to induce a functional cytotoxic T lymphocyte response. Thus, these findings could contribute to the development of new anti-tumoral immunotherapy strategies, either by delivering ECM-bound FNIII EDA fragments in combination with antigens, or by inducing the elastase 2-dependent proteolysis of FN within the tumor, increasing the level of immunoactive FN.

In chapter 3 we demonstrated the ability of the N-terminally extended form of FNIII EDA, FNIII 11-EDA, to synergize with the TLR9 ligand CpG, leading to an enhanced activation of DCs. Interestingly, TLR synergies have been reported to rely heavily on simultaneous activation of the TRIF and MyD88 pathways[6]. TLR9 signals strictly through MyD88 while TLR4 can signal through both pathways. Thus, as FNIII EDA has previously been reported to signal through MyD88[7], this suggests that it also has the ability to activate the TRIF pathway. Moreover, this also suggests that FNIII EDA could have the capacity to synergize with many TLR ligands[8]. We then showed the ability of CpG and FNIII EDA to synergize *in vivo* using a tumor model and a chronic hepatitis B transgenic mouse model expressing a hepatitis B virus (HBV) transgene. Indeed, the combination of both TLR agonists displayed the ability to synergize to break T cell tolerance and induce an enhanced antigen specific response. These enhanced responses were achieved while lowering the total dose of CpG, thus lowering the risks of potential side effects. Hence, as multiple adjuvant therapies are required to achieve an efficient response against specific diseases[9,10], combination of CpG and FNIII EDA might lead to the development of potent immunotherapies with fewer side effects and improved safety. Based on this, a potential development could involve intratumoral deliveries of CpG along with elastase 2, as previously mentioned, as this would create a multiple-antigen multiple-adjuvant microenvironment. Although we showed in Chapter 2 that the efficacy of FNIII 11-EDA could be enhanced by a delivery in a fibrin matrix, the integration of CpG in such matrices represent a difficult challenge. Thus, in order to study the ability of FNIII 11-EDA and CpG to synergize with a minimum of variability, soluble formulations were chosen. However, future development should include the administration of both FNIII 11-EDA and CpG in an ECM analog.

Finally, in chapter 4 we revealed that FNIII EDA is a growth factor (GF) binding domain of FN. All GFs that tested positive for binding to FNIII EDA and FNIII 11-EDA were already known binders of FN[11], with PDGF-AA being the weakest one. However, here PDGF-AA displayed the strongest binding to FNIII EDA. We demonstrated that FNIII 11-EDA and PDGF-AA have together the ability to enhance fibroblasts proliferation and differentiation into myofibroblasts in comparison to PDGF-AA alone. However, as our results barely reached statistical significance, further investigation would be required to validate that point. PDGF-AA-driven fibroblast to myofibroblasts differentiation has been reported to promote tissue repair upon wound infiltration[12] while FNIII EDA$^{-/-}$ mice presented abnormal wound closure[3]. We thus hypothesized that fibrin gels functionalized with FNIII 11-EDA would accelerate wound healing through interaction with PDGF-AA and possibly other GFs. However, the FNIII 11-EDA-containing-ECM analogs surprisingly delayed wound closure. This effect is likely not due to the pro-inflammatory properties of FNIII 11-EDA as LPS-containing fibrin matrices did not influence re-epithelization. Furthermore, excessive GF sequestration rendering them unable to promote wound healing is also unlikely as fibrin gels containing the GF binding domain FNIII 12-13-14[13,14] are not reported to impair wound closure. Larger sample sizes and additional experiment end points, would be required to precisely characterize how FNIII EDA affects tissue repair.

In conclusion, this thesis brings insight into the immunological, and to some extent regenerative, functions of FNIII EDA. Moreover, the link we expose between elastase 2 secretion by neutrophils and TLR4 agonization might help to better understand the progression of diseases such as scleroderma and psoriasis.

Furthermore, our results can present interesting novel options for the development of

potent adjuvant formulations for immunotherapies with fewer side effects.

5.1 References

1. Pankov, R. & Yamada, K. M. Fibronectin at a glance. *J. Cell Sci.* **115,** 3861–3863 (2002).

2. Okamura, Y. *et al.* The extra domain A of fibronectin activates Toll-like receptor 4. *J. Biol. Chem.* **276,** 10229–33 (2001).

3. Muro, A. F. *et al.* Regulated splicing of the fibronectin EDA exon is essential for proper skin wound healing and normal lifespan. *J. Cell Biol.* **162,** 149–60 (2003).

4. McFadden, J. P., Baker, B. S., Powles, A. V. & Fry, L. Psoriasis and streptococci: postscript regarding extra domain A fibronectin. *Br. J. Dermatol.* **161,** 706–7 (2009).

5. Bhattacharyya, S. *et al.* FibronectinEDA promotes chronic cutaneous fibrosis through Toll-like receptor signaling. *Sci. Transl. Med.* **6,** 232ra50 (2014).

6. Bagchi, A. *et al.* MyD88-dependent and MyD88-independent pathways in synergy, priming, and tolerance between TLR agonists. *J. Immunol.* **178,** 1164–1171 (2007).

7. Mansilla, C. *et al.* Immunization against hepatitis C virus with a fusion protein containing the extra domain A from fibronectin and the hepatitis C virus NS3 protein. *J. Hepatol.* **51,** 520–7 (2009).

8. Garcia-Cordero, J. L., Nembrini, C., Stano, A., Hubbell, J. A. & Maerkl, S. J. A high-throughput nanoimmunoassay chip applied to large-scale vaccine adjuvant screening. *Integr. Biol. (Camb).* **5,** 650–8 (2013).

9. Melero, I. *et al.* Therapeutic vaccines for cancer: an overview of clinical trials. *Nat. Rev. Clin. Oncol.* **11,** 509–524 (2014).

10. Raman, V. S. *et al.* Applying TLR synergy in immunotherapy: implications in cutaneous leishmaniasis. *J. Immunol.* **185,** 1701–10 (2010).

11. Martino, M. M. *et al.* Growth factors engineered for super-affinity to the extracellular matrix enhance tissue healing. *Science* **343,** 885–8 (2014).

12. Demaria, M. *et al.* An Essential Role for Senescent Cells in Optimal Wound Healing through Secretion of PDGF-AA. *Dev. Cell* **31,** 722–733 (2014).

13. Martino, M. M. & Hubbell, J. A. The 12th-14th type III repeats of fibronectin function as a highly promiscuous growth factor-binding domain. *FASEB J.* **24,** 4711–21 (2010).

14. Martino, M. M. *et al.* Engineering the growth factor microenvironment with fibronectin domains to promote wound and bone tissue healing. *Sci. Transl. Med.* **3,** 100ra89 (2011).

Ziad Julier

Swiss, 03.09.1985

Passage de Montriond 3, 1006 Lausanne, Switzerland

Phone : +41 (0) 79 285 21 81, E-mail : ziad.julier@gmail.com

EDUCATION

PhD in Biotechnology & Bioengineering, EPFL, Switzerland   **2011 – 2015**

MSc in Biotechnology & Bioengineering, EPFL, Switzerland   **2008 – 2010**

BSc in Life Sciences & Technology, EPFL, Switzerland   **2004 – 2008**

RESEARCH EXPERIENCE

EPFL, Switzerland   **Apr. 2011 – Present**

Laboratory for Regenerative Medicine & Pharmacobiology

PhD Student

Supervision by Prof. Jeffrey A. Hubbell

Thesis work summary:

- Development of cancer vaccine based on functionalized fibrin matrices
- Characterization of the mechanisms involving the extra domain A of fibronectin (EDA) in the adaptive immune response.
- Development of cancer vaccine based on functionalized nanoparticles
- Development of Hepatitis B therapeutic vaccine based on functionalized nanoparticles and engineered forms of EDA
- Characterization of the role of EDA and the activation of TLR4 during regenerative processes

Université de Lausanne, Switzerland   **Sep. 2012 – Feb. 2013**

Centre pluridisciplinaire d'oncologie Clinique

Research Assistant

6 months civil service assignment – Characterization of Tie2-expressing monocytes phenotypes in breast cancer patients

EPFL, Switzerland   **Jan. 2011 – Mar. 2011**

Laboratory for Regenerative Medicine & Pharmacobiology

Research Assistant

In vivo evaluation of the ability of engineered forms of EDA to induce a $CD8^+$ T-cell response in mice

Université de Lausanne, Switzerland   **Oct. 2011 – Dec. 2011**

Department of Pharmacology and Toxicology

Research Assistant

Analysis of the co-expression of the neuropeptides CGRP and SP in dorsal root ganglion neurons using in situ hybridization

EPFL, Switzerland   **Aug. 2010 – Oct. 2010**
Laboratory for Regenerative Medicine & Pharmacobiology
Research Assistant
The immunological activity of EDA was modulated using protein engineering techniques

EPFL, Switzerland   **Sep. 2009 – Jul. 2010**
Laboratory for Regenerative Medicine & Pharmacobiology
Master Student
The immunological activity of different forms of the extra domain A of fibronectin (EDA) was evaluated *in vitro*

SKILLS PROFILE & LANGUAGES

General laboratory skills: Protein expression in bacteria, Cloning, Protein purification using FPLC, ELISA, Protein expression in mammalian cells, Flow cytometry, Mammalian cell culture, Magnetic cell sorting, In situ hybridization, IHC, work in P2 and P3 biosafety levels, preparation of polymeric nanocarriers
Mice handling skills: i.d, s.c, i.v and i.p injections, organs harvesting (including with P2 safety constraints), basic surgeries, management of breeding for transgenic lines, genotyping, tumor implantations, skin punches for wound healing models
Immunology related skills: Endotoxin detection assays, MHC Tetramer Technology, Adoptive transfer, Dendritic cells isolation, T cells isolation, Chemotaxis assay, T cells restimulation assays
Tissue Engineering related skills: Functionalization of biomaterials, cell culture in 3D matrices, protein engineering
Computer Skills: C, C++, Java, Perl, Latex, Python. Proficient with Linux and Windows (XP/7/8), Word, Excel, Prism, FlowJo
Languages: French (native), English (fluent), Italian (intermediate), Arabic (basic)

PUBLICATION LIST

Z. Julier, A. de Titta, A.J. Grimm, E. Simeoni, M.A. Swartz and J.A. Hubbell, "TLR4-9 agonists fibronectin EDA and CpG synergize to enhance antigen-specific Th1 and cytotoxic responses." *Submitted*

Z. Julier, M. M. Martino, A. de Titta, L. Jeanbart, and J. A. Hubbell, "The TLR4 Agonist Fibronectin Extra Domain A is Cryptic, Exposed by Elastase-2; use in a fibrin matrix cancer vaccine," Sci. Rep., vol. 5, p. 8569, 2015.

A. de Titta, M. Ballester, **Z. Julier**, C. Nembrini, L. Jeanbart, A. J. van der Vlies, M.A. Swartz, and J.A. Hubbell, "Nanoparticle conjugation of CpG enhances adjuvancy for cellular immunity and memory recall at low dose.," Proc. Natl. Acad. Sci. U. S. A., vol. 110, no. 49, pp. 19902–7, Dec. 2013.

INTERNATIONAL CONFERENCES

Biomedical Engineering Society (BMES) Annual Meeting, Oral Presentation   **Oct. 2014**
"Incorporation of The Extra Domain A of Fibronectin (EDA) in Fibrin Matrices Mediates Activation of DCs and T-cell-dependent Tumor Regression"

Max Planck Institute Science Day, Oral Presentation   **Oct. 2014**
"Materials and Protein Engineering Approaches for Modulating Immunity"

TEACHING EXPERIENCES

Co-supervisor for Antonio Jimenez on Bachelor Project   **Oct. 2014 – Jun. 2015**

Supervisor for Niklas Van Neyghem during summer internship   **Jun. 2012 – Sept. 2012**

Supervisor for Cynthia Marchand on Bachelor Project   **Feb. 2012 – Jun. 2012**

Teaching assistant for molecular biology class one day per week, **Oct. 2011 – Jun. 2012**
intended for 2nd year BS student

Supervisor for David Boyer during summer internship   **Jun. 2011 – Sept. 2011**

SOCIETY MEMBERSHIP

Club Francophone des Cellules Dendritiques   **Dec. 2011 – Present**
Dendritic cells society for researcher from French-speaking countries

OTHER EXPERIENCES

Halocline underwater experience, scuba apparel company, Switzerland   **May. 2015 – Present**
Co-founder

Beyond Barriers, diving school, Switzerland   **Aug. 2013 – Present**
Founder & PADI IDC staff instructor

F&J Consulting, construction industry, Switzerland   **Aug. 2005 – Feb. 2006**
Thermal Camera Operator

INTERESTS AND ACTIVITIES

- Scuba diving, wildlife, marine related subjects.
- Cooking
- Do-it-yourself projects such as diving equipment, mechanical and electrical devices, furniture
- Learning about science and other fields in general
- Basketball, played in Swiss league for 10 years